DIFFERENTIAL PHASE ACOUSTIC MICROSCOPE FOR MICRO-NDE

BIO-IMAGING RESEARCH, INC.

NASA Contractor Report 189617

DIFFERENTIAL PHASE ACOUSTIC MICROSCOPY FOR MICRO-NDE

D. D. Waters
T. L. Pusateri
S. R. Huang

BIO-IMAGING RESEARCH, INC.
Lincolnshire, Illinois

Contract NAS1-19099 SBIR Phase II
May 1992

National Aeronautics and
Space Administration

Langley Research Center
Hampton, Virginia 23665-5225

CONTENTS

List of Figures

List of Tables

ABSTRACT

A differential phase scanning acoustic microscope (DP-SAM) was developed, fabricated, and tested in this project. This includes the acoustic lens and transducers, driving and receiving electronics, scanning stage, scanning software, and display software. This DP-SAM can produce mechanically raster-scanned acoustic microscopic images of differential phase, differential amplitude, or amplitude of the time gated returned echoes of the samples. The differential phase and differential amplitude images provide better image contrast over the conventional amplitude images. A specially designed miniature dual beam lens was used to form two foci to obtain the differential phase and amplitude information of the echoes. High image resolution (1 μm) was achieved by applying high frequency (around 1 GHz) acoustic signals to the samples and placing two foci close to each other (1 μm). Tone burst was used in this system to obtain a good estimation of the phase differences between echoes from the two adjacent foci. The system can also be used to extract the V(z) acoustic signature. Since two acoustic beams and four receiving modes are available, there are 12 possible combinations to produce an image or a V(z) scan. This provides an unique feature of this system that none of the existing acoustic microscopic systems can provide for the micro NDE applications. The entire system, including the lens, electronics, and scanning control software, has made a competitive industrial product for nondestructive material inspection and evaluation and has attracted interest from existing acoustic microscope manufactures.

Subject Terms: Differential phase scanning acoustic microscopy, phase contrast ultrasonic microscopy, SAM, nondestructive evaluation, NDE, dual beam acoustic lens.

1. PROJECT SUMMARY

The Project, which is the subject of a Phase II SBIR proposal NASA SBIR 88-1-II entitled "Differential Phase Acoustic Microscopy for Micro-NDE"[1], extends the work which was undertaken during the Phase I of the project "Differential Phase Acoustic Microscopy" completed during 1988.

While demonstrating the proof of principle of the dual beam differential phase acoustic lens the work was only undertaken at an operating frequency of 50 MHz. Having achieved the desired objectives we embarked upon developing a lens which had the same fundamental physical characteristics as the previous lens but achieved a much higher spatial resolution due to a 20-fold increase in the operating frequency. The resulting 1 GHz lens is the subject of the following report.

Although prior work would enable us to design the electronic circuitry to adequately support the theoretical operating characteristics of the lens the mechanical requirements of the ancillary hardware and the lens itself proved to provide the greatest challenge throughout the duration of the project.

While all of the design for both the lens and the electronics was undertaken by this company, help with the fabrication of the lens and transducers was provide by Stanford University where equipment suitable for the sputtering of the transducers and the mounting on the substrate are readily available. Excessive cost eliminated the opportunity to buy or lease such equipment on this particular contract. It is equally true that the unavoidable need to work on the fabricated and mounted lens without tools similar to those more appropriate to the semiconductor industry may have been the cause of some difficulties experienced during integration and test of the lens system and the consequential need for rework on the device.

During the lens fabrication phase of the project, conducted off of the BIR site, it was possible to not only design and build the electronics which would be used to drive the lens but also to write the software which would enable us to scan the lens across a surface and build an image file from the collected data. The scanning control and the image display software are both the subject of this project report.

After overcoming all system functional problems which occurred at the early stage of this project, which were difficult to attribute to any specific feature of the lens or electronics, full integration of the lens system was completed on schedule. For example, dimensional analysis of the lens using an optical microscope identified regions of the transducer which could have been at variance with the specification and hence result in a performance difference from that originally defined; measurements of the electric impedance of the transducers showed great

deviation from the designed values and the 3-dB matching pads in the original design were removed and new impedance matching network was redesigned based on the measurements; poor vertical alignment of the lens in the holder resulting in a low output and hence poor signal-to-noise ratio created its own problems. All these problems of the system have been solved at the final stage of the system integration.

In theory the 1 GHz differential phase lens has a spatial resolution of approximately 1 μm (dictated by the distance between foci) and a topographic resolution of approximately 10-20 Å with the capability to penetrate about 1 μm below the surface of material (both being dictated by the operating frequency of the transducers and the phase noise of the electronics). In practice however, due to the difficulty of preparing a sample with the required precision, none of these parameters have been experimentally verified.

Scanning time for a material surface area of .25 mm^2 to 1 mm^2 range from approximately 11 minutes to 200 minutes depending on the required resolution. The process is automatic once the sequence has been initiated. The area of coverage can be adjusted for a number of discrete areas; the time for a complete scan is approximately proportional to the size of the selected area.

The developed scanning control and display software produces an image on the color display monitor as each line being scanned allowing the users to adjust the signals. Off-line pseudo coloring or gray scale re-mapping of the images are provided by the image display software in an attempt to enhance the visual representation of the materials topography and/or other characteristics. The palette can be changed to suit the operator or the application. Other image display features, including image zooming, pixel value re-scaling, and multiple image displaying, are also supported by the image display software.

As the designing, building, testing, and interfacing of the lens, electronics, scanning stages, and control software is completed, it has provided us with a very strong base from which to continue with Phase III of the project. The entire assembly, including the computer, provides the user with a high resolution self contained laboratory instrument acoustic microscope which, if considered through industrial design, could make a competitive product for industrial inspection. The lens alone is novel and has attracted interest from existing manufacturers of acoustic microscopes.

2. BACKGROUND

2.1 Prior Arts

The scanning acoustic microscope (SAM) invented by C. F. Quate[1-3] provides powerful techniques for high resolution NDE of materials[4]. In current commercial SAM systems, the amplitude of the received signal provides the image contrast. Previously we reported[5-8] a differential phase/amplitude SAMs, operating at low frequencies, which can utilize the phase or amplitude gradients received from the object for image contrast. The differential phase part of this system is the *acoustic counterpart of the Nomarski optical microscope*. It is particularly useful where high sensitivities are required and conventional amplitude acoustic microscopic imaging yields little or no image contrast. We undertook the development of such a microscope at an intermediate frequency of 50 MHz during Phase I and are in the process of finalizing the design of a microscope operating at an extended frequency of 1 GHz. Imaging of stress patterns in solids, ion-implanted semiconductors, titanium:titanium diffusion bonds, grains in solids, and composite materials are candidate applications for this system.

Imaging with phase information can be classified into two different categories:

(1) Use one probe beam and compare the phase of the received signal with that of the transmitter. Such a system can be operated both in continuous wave (CW) mode and in pulsed mode.[9-13] It suffers from the fact that any mechanical and/or thermal disturbance within the propagation path of the acoustic beam can lead to spurious variations in the signal that often overshadow the wanted signal from the object.

(2) From the argument given in (1) above, it is clear that in order to attain the highest phase stability one must derive a phase reference which has propagated through the same medium as the probing beam. This is the essential requirement for the differential phase technique and is the main theme for this proposal. Any thermal and/or mechanical disturbance common between the two beams is hence rejected, leading to an enhanced detection sensitivity.

2.2 Significance of the Current Design

Our proposal of differential phase techniques in scanning acoustic microscopy relies upon phase comparison between signals arriving from two adjacent regions of the object. At a given frequency, one would ideally want these two regions to be as close to each other as possible — a requirement of *two adjacent foci* — to maintain a high imaging resolution. It is this requirement that makes the operation of the proposed microscope similar to that of the Nomarski

optical microscope. The detection sensitivity in such a microscope is three to four orders of magnitude higher than that of conventional amplitude-contrast microscopes.

The basic elements of the proposed method are illustrated in Figure 1. The heart of the system is a dual-beam acoustic lens. The operation of this lens is very similar to the Nomarski optical objective. The back of the lens rod consists of two tilted surfaces. Using the geometrical acoustic ray tracing techniques, the tilt angles and the dimensions of the lens are designed so that the central ray from each transducer intersects the lens axis at the back focal plane. After these two central rays cross the lens-water interface they travel parallel to the axis, resulting in two adjacent foci. Off-center rays travel in parallel to the their corresponding central rays inside the lens and change the propagation direction at the lens-water interface and focus at the two foci. The two transducers mounted on the back surfaces of the lens are excited by two separate pulsers. The two echoes received are fed into a phase-sensitive detector (PSD). The first stage of the PSD is a limiting amplifier so that the output is not sensitive to amplitude variations. The delay between the received echoes is adjusted to be one quarter of the wave period. This ensures that the signals fed into the PSD are in phase quadrature, resulting in linearity and maximum sensitivity for the microscopic imaging.

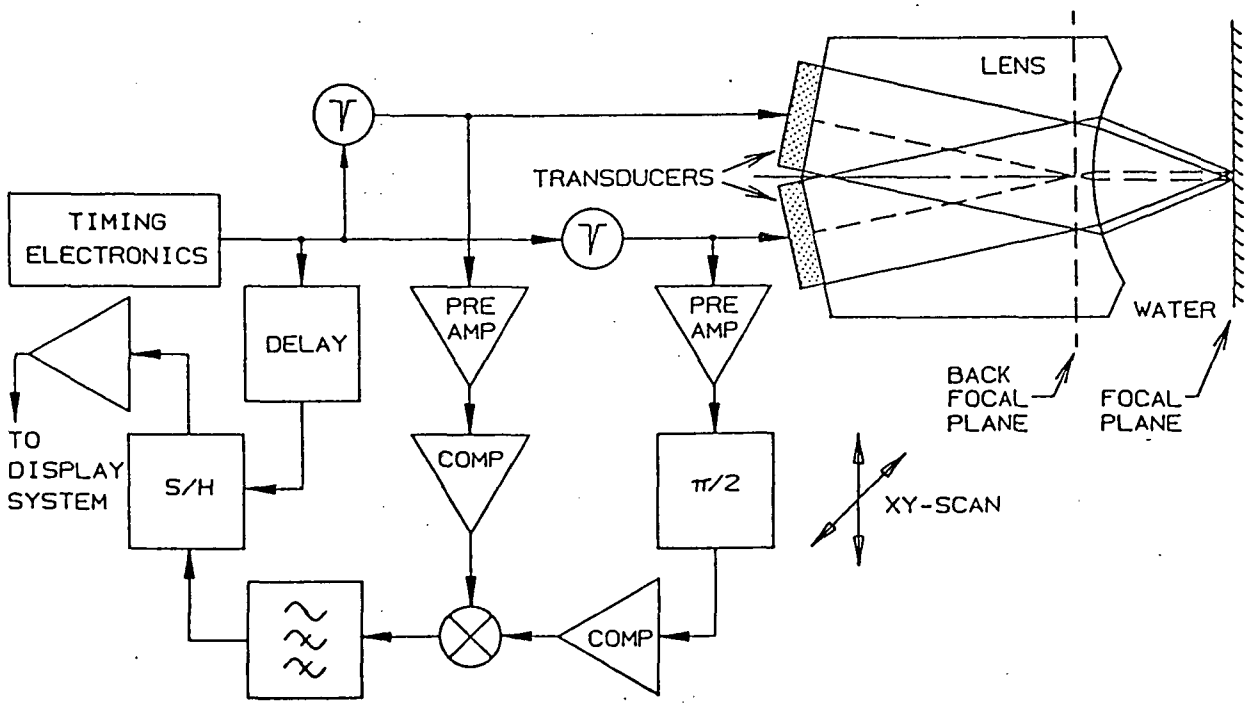

Figure 1. Block diagram for a general differential phase scanning acoustic microscopy system.

This technique has been previously demonstrated at 10 MHz.[5-8] At this frequency the lateral resolution for this dual-beam microscope is 150 μm (approximately one wavelength). It is important to state that in conventional systems the lateral resolution is determined by the F/number of the lens and the wavelength. In our dual-beam microscope the separation between the two focal spots plays the primary role in determining the lateral resolution. It is for this reason that the optimum lateral resolution of a dual-beam microscope is somewhat lower than that of a point focus single-beam microscope. From the experience with a 10 MHz microscope, we anticipate the lateral resolution for an optimized dual-beam lens to be one wavelength at the imaging frequency. In order to exploit the enhanced sensitivity of this microscope with higher *lateral resolution*, the operating frequency has to be increased.

2.3 Current Design

The current design of the differential phase lens is based entirely upon the results of the previous phase of the project with one major exception. The original aim, as laid down in the Phase I proposal, was to make the design transition from a 50 MHz lens to a 1 GHz lens in two stages, namely with an intermediate lens at 300 MHz. It was jointly agreed that this would not be a cost effective way to achieve the desired end result and that, based on the findings of Phase I, the design of a 1 GHz lens would be progressed.

The fabrication needs for the 1 GHz lens are significantly different from that of the 50 MHz, as can be seen from the dimensional detail given in Table 1. It was considered that this would be the area of work where the most unknowns exist and, as a consequence, most of the project emphasis would be placed.

3. DEVELOPMENT DETAIL

It is possible to categorize the work undertaken by this company, while pursuing this project, into five major groups. These are as follows:

- Define the physical characteristics of the **dual beam differential phase acoustic lens** and related transducers for operation at 1 GHz. Fabricate the lens and corresponding transducers.
- **Electrical and electronic design** of hardware necessary to stimulate the lens (transducers) and condition the returned signal in preparation for image generation;
- **Mechanical design** of the scanning stage, electronic enclosures, and lens holder;
- **Computer** and associated peripherals;
- Development of all the **software code** which will be used to control the scanning stage, take the data from the echo signal, and generate a visual representation of the acoustic response;

The following provides a detail discussion on each of the major categories listed.

3.1 Dual Beam Lens

3.1.1 *Geometric Design Characteristics*

The differential phase lens requires that there are two transducers accommodated in the same acoustic buffer rod and that the effective acoustic path length is identical resulting in two adjacent focal spots on the same plane.

As previously stated to attain the two adjacent focal spots, the lens geometry has to be designed so that the central ray from each transducer passes through the intersection point of the lens back focal plane and the lens axis, as shown in Figure 2. For a lens with radius R, the separation between the two spots is therefore given by:

$$\Delta x = 2F/n \tan\theta \qquad (1)$$

where n is the velocity ratio across the lens, $F \equiv nR/(n-1)$ is the paraxial focal length and θ is the tilt angle at the back of the lens. For a given value of Δx, the angle θ can be determined from equation (1). For a given θ, in order for the central ray to pass through the intersection point of the lens axis and the back focal plane, the full width (diameter) of the transducer w must be

$$w = 2(l - F/n) \sin\theta \tag{2}$$

where l is the rod length of the lens. It is at once clear that the smaller Δx, the smaller θ and, for a given transducer diameter and a given focal length, the longer the length of the lens rod. We therefore must aim for the largest R and smallest n to achieve an acceptable length. Also, it is seen that there is always an engineering compromise to be made between Δx and the length of the rod: the larger Δx, the smaller the length of the rod.

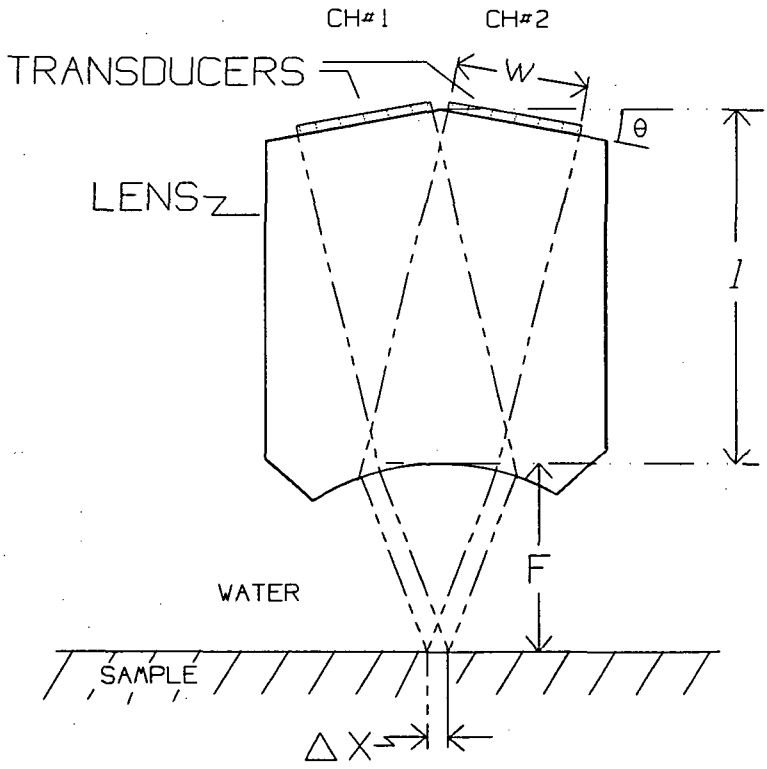

Figure 2. The geometric design parameters of the dual beam lens.

We chose fused quartz as the material for the 1 GHz surface imaging lenses, as it is isotropic and there are no problems with insonating the lens at angles other than normal. We aimed for a Δx of 1 μm for the 1 GHz lenses in Phase II. The lens parameters are given in Table 1. As a direct comparison the values used for both the 1 GHz (Phase II design) and 50 MHz (Phase I design) lenses are given. The detail of the 50 MHz lens performance can be found in the Phase I report.

Parameter	Value	
	50 MHz	**1 GHz**
Separation (Δx)	0.035 mm	1.07 μm
Lens radius (R)	2 mm	60 μm
Lens aperture (A)	3.6 mm	110 μm
Transducer diameter (w)	3.3 mm	150 μm
Rod length (l)	65 mm	2.886 mm
Velocity ratio (n)	3.9	3.93
Tilt angle (θ)	1.5°	1.5°
Opening angle (α)	64.2°	66.4°
Paraxial focal length (F)	2.7 mm	80.45 μm
Pulse width (T)	60 ns	30-50 ns

Table 1. Parameters for the 50 MHz and 1 GHz dual beam lenses.

It has been shown[3] that in order to perform subsurface imaging the following have to be satisfied:

(i) The focal length in water has to be large enough so that, when the lens is defocused for focusing into the interior of the object, the lens can physically clear the object surface.

(ii) The lens has to have an opening angle of about 10° - 15° in water so that when the beam enters the solid the effective angular aperture of the lens is in the range of 30° - 40°.

From our experience in subsurface imaging[3,4,14,15], in order to image subsurface planes in the range of 1 mm to 5 mm with nearly diffraction limited focal spots, the focal length

of the lens had to be in the range of 20 - 30 mm. Scaling these numbers down for the high resolution system developed in this project, in the search for a dual-beam lens design for subsurface applications, given that F or R is large, we have found that in order to maintain Δx to a reasonable value the length of the lens rod becomes prohibitively long. The lens design for a subsurface imaging lens, as given in the report for Phase I, clearly shows that to achieve the objectives the theoretical size of the buffer rod is unreasonably long, concluding that the design is really only practical for surface measurements or topography.

3.1.2 *Broadband Diffraction Analysis*

The geometrical acoustic design considerations provide a basis for elementary lens design. However, they fail to predict the field distribution in the vicinity of the focal plane. Of particular interest to us is the level of the sidelobes and the beamwidth near the focal plane. Therefore, broadband diffraction analysis and near field simulation techniques were used to verify the design criteria.

The analysis is limited to a two-dimensional case in the (x,z) coordinate system as shown in Figure 3. We assume that the ultrasound field can be represented by a scalar function $u(x,z)$ and we ignore the effects of reflection and mode conversion within the lens. It is assumed that the transducer acts as the source of a set of elementary sources located at (x_1,z_1) given by $x = z \cot\theta$. We also assume that the signal emitted from each elementary source has a Gaussian pulse shape in the form:

$$f(t) = e^{-(2t/T)} e^{j2\pi ft} \tag{3}$$

where T is the pulsewidth between the e^{-1} points. The field emitted from each elementary source on the transducer, in turn, acts as the source for secondary wavelets at the surface of the lens given by $(x-l-R)^2 + z^2 = R^2$. The wavefronts leaving (x_1,z_1) and arriving at (x_2,z_2) have undergone a delay of r_1/v_1, where v_1 is the velocity in the lens. Similarly, the wavefronts leaving the surface of the lens and arriving at the output location (x_3,z_3) will have suffered an additional delay of r_2/v_2, where v_2 is the velocity in the liquid. The field at the output plane is hence given by:

$$u(x_3,z_3) = \sum_{1}^{M} \sum_{1}^{N} \frac{f(t - r_1/v_1 - r_2/v_2)}{\sqrt{r_1 r_2}} \tag{4}$$

where M and N are the number of elementary source points on the lens and transducer respectively. We have:

$$r_1 = [(x_2-x_1)^2 + (z_2-z_1)^2]^{1/2}$$
$$r_2 = [(x_3-x_2)^2 + (z_3-z_2)^2]^{1/2} \quad (5)$$

Given equation (4), the field can be calculated at any distance from the lens.

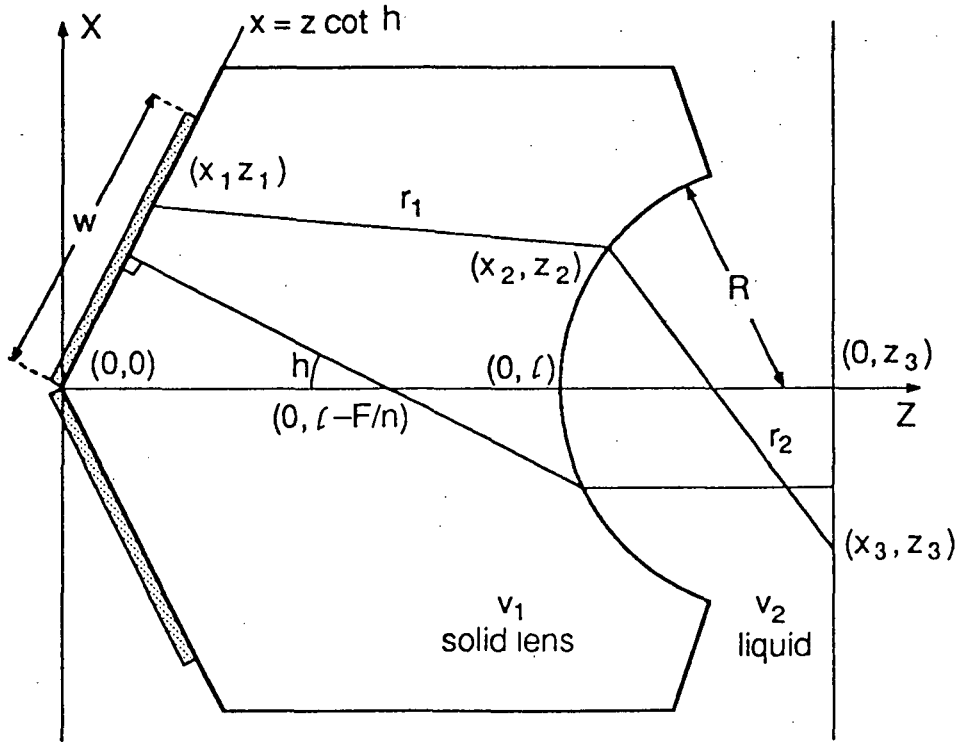

Figure 3. Dual beam lens geometry for broadband diffraction analysis.

3.1.3 *Near field Simulation*

For 1 GHz acoustic lenses, a material with a relatively low attenuation and high velocity such as sapphire is normally used to reduce the lens curvature and to overcome the effects of high attenuation at high frequencies.[2] However, sapphire is anisotropic and so unless the effects of anisotropy are known and taken into account in the lens design and fabrication, the two beam paths of the differential phase lens will be different and so accurate phase difference calculations will be very difficult. In the case of isotropic materials, such as fused quartz, this problem will not occur. However, the effect of the attenuation through the lens rod has to be taken into consideration.

At 1 GHz the consequential small size of the lens requires that a number of fabrication considerations will also have to be made, namely, whether the transducer is piezo-electric film or zinc oxide sputtered onto the tilted surface of the lens material, and if surfaces are formed using mechanical grinding techniques or chemically etched. The fabrication of such a lens is more in tune with the techniques employed by the semiconductor industry than that of the manufacturer of traditional acoustic lenses.

Table 1, which has been previously supplied, defines the physical properties of the lens produced. Since the fabrication technique cannot be guaranteed to exactly replicate the dimensions in Table 1, a computer near field simulation was developed which would enable us to quickly determine performance of any lens which deviated from the ideal.

This near field simulation is based upon the previous work by Tjotta and Tjotta (1980)[10]. They showed that for a disk transducer and small tilt angle, the field at the back focal plane for the near field case is given by:

$$U(x',y',z'=0) \equiv e^{jk_\ell(\zeta - x't)}\hat{U}(r') \tag{6}$$

where $\hat{U}(r')$ is circularly symmetric,
k_ℓ = longitudinal wavenumber in lens

$$r' = \sqrt{x'^2 + y'^2} \qquad \text{and}$$

$$\hat{U}(r') = \left[1+e^{ja^2k_\ell/(2\zeta)}\left[-1+2\int_0^{ak_\ell r'/(2\zeta)} J_1(2s)\, e^{j2\zeta s^2/(k_\ell a^2)}\, ds\right]\right] \tag{7}$$

If we then apply the thin lens approximation, namely that the transmission across the spherical lens surface is assumed to add only an additional phase shift to the wave,we obtain the field at the lens, which can then be propagated to produce the field at the focal plane using the Fourier transform (angular spectrum propagation) techniques.

Figure 4 shows the theoretical plot of the two beam profiles in the focal plane, based on the characteristics of the 1 GHz dual beam lens as defined in Table 1.

By observation of the simulation the simulated -10 dB beam width of each single beam was 3.3 μm and the simulated beam separation was 0.94 μm. All sidelobes, including the first sidelobe, are lower than -20 dB. The two beam overlap at -1 dB level. While the separation between the two beams is approximately correct, the performance would be better suited to differential phase measurements if the beams were marginally narrower, ie. less overlap.

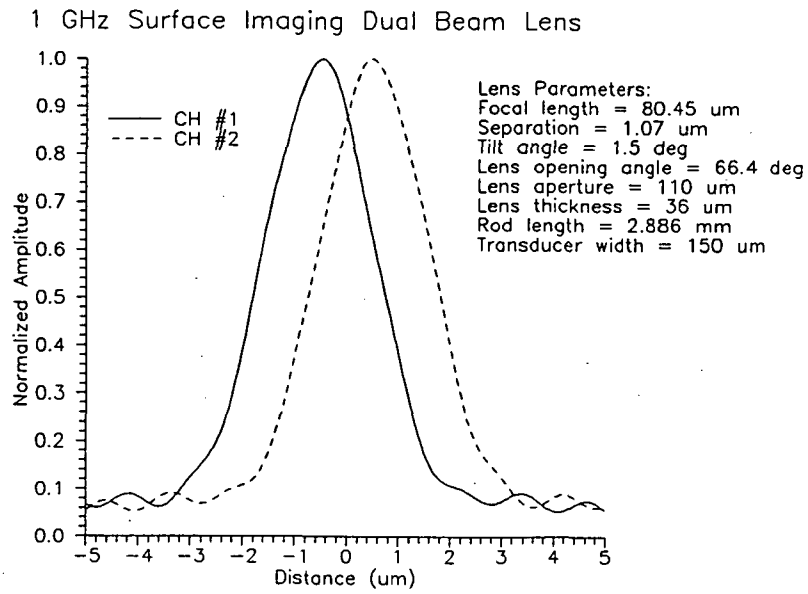

Figure 4. Beam profiles in the focal plane for both transducers.

3.1.4 *Lens and Transducer Fabrication*

Compared to a conventional acoustic lens, which has only single beam axes, the fabrication of the dual beam lens is difficult. The alignment between the transducers, the ridge of the buffer rod and the lens aperture is critical to the effective performance of the lens. At 1 GHz the tolerances are in the submicron range making fabrication a skilled process.

From previous work we have verified that the practical lens design corresponds with the theoretical design within certain limits which are mainly determined by the machining inaccuracies.

These tolerances, when considering the 50 MHz lens, are large in comparison to the magnitude of those tolerable with the 1 GHz lens design.

The definition of the form of the transducer(s) was an integral part of the lens design process. Both have parameters which are dependant. Having established the basis for the lens the process of fabricating the lens in the stated form was started. This activity was conducted almost entirely at Stanford University, under the direction of Professor Khuri-Yakub, where there are facilities and equipment more suited to the fabrication of the lens than are available at the BIR facility.

Figure 5 shows a schematic of the buffer rod with its "tent" shaped top opposite the lens. The diameter of the buffer rod is 0.25 in, and the total length is 2.886 mm. The lens itself is to have a radius of 60 μm and an aperture of 110 μm. The bevel of the two transducer planes is 1.5° with respect to the horizontal. All these parameters are as per the design criteria defined in Table 1. The bevel at the lens end of the buffer rod will be 10 degrees. This bevel angle is chosen to minimize multiple reflections in the rod.

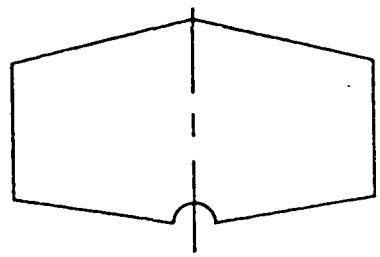

Figure 5. Cross section of quartz lens.

Figure 6 shows the quartz block from which the lenses were made. The first step in *creating* was to make the tent for the transducer surfaces starting from a 0.75" diameter quartz rod. The two ends of this block are polished parallel and flat in preparation for making the tilted transducer surfaces. The length of the rod is 2.886 mm which is the desired final length of the buffer rod. The block is next polished with a tilt angle of 1.5° in order to generate one of the transducer surfaces. The rod is then tilted through 3° in order to produce the opposite transducer surface plane. After this step the rod is cored and two 0.25" diameter pieces are made as shown in Figure 6.

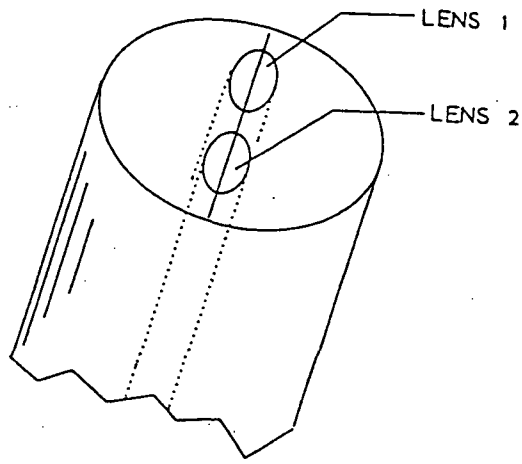

Figure 6. Placement of the two lenses on the quartz rod.

Once the large quartz rod is cored and the appropriate buffer rod of required diameter, length, and "tent" shape is available the lens is ground and polished. The major task here was to align the lens under the intersection of the transducer planes. Failure to achieve this would make the individual acoustic path lengths and the focal distance of each different and render the dual beam lens useless as a comparative instrument.

The quartz material being very brittle is hard to work with, especially in sizes suitable for the lens construction as defined. The first attempt at this process was unsuccessful; the rod fractured during an attempt to introduce the spherical shaped lens.

The transducers are formed on the roof of the lens as close to the ridge as is practically possible. (The assumption made during the design calculations for the lens, and also the simulations, is that the gap between the transducers is infinitely small).

Prior to forming the transducers a substrate of conductive material is deposited over the entire roof of the lens rod. The zinc oxide, ZnO, transducers are then singly sputtered on to the substrate area, the duration of the sputtering being used to determine the amount of deposition and hence the thickness of the device. For a given surface area the thickness will determine the operating resonance frequency of the transducer, in this case the desired frequency being 1 GHz. For an air backed transducer, that is one that does not have a matching layer, the resonant frequency is given as $c/2\Delta$, where c is the stiffened longitudinal speed of sound in ZnO and Δ is the thickness of the ZnO layer. Therefore, the ZnO layer thickness was estimated to be 3.15 μm for the transducers to be operating at 1 GHz. The variation in the speed of sound in ZnO used for the transducers is the approximated quantity.

Finally, a gold wire is bonded to the rear of each transducer.

The quartz rod lens was mounted in a brass housing designed to accommodate the lens. Two matching networks, one for each channel, are placed close to the lens housing on the lens housing supporting arm. For further details on the lens housing and matching networks see section 3.3.3.

3.2 Electrical/Electronic Design

Figure 7 is a block diagram of the electronics and acoustic system, including the lens and all the essential drive electronics. The following provides a description of the function of each module as bounded by the dotted lines on the drawing.

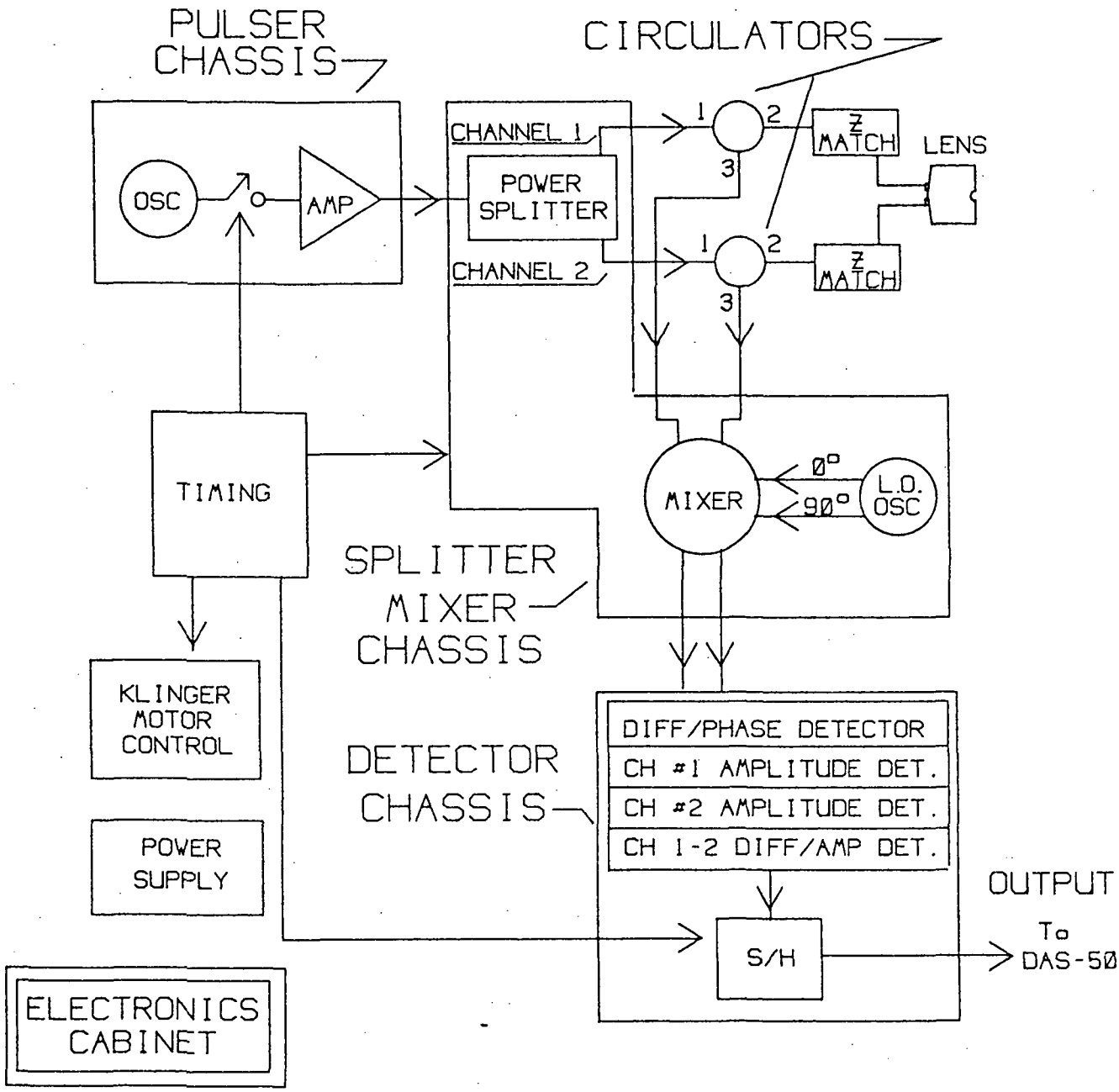

Figure 7. Block diagram for the electronic system.

A small cabinet contains all the electronics, besides the computer, that is needed to generate and process the signals needed to scan the lens across a sample and produce the image source data. This rack houses six major components:

1. Pulser chassis
2. Splitter/Mixer chassis
3. Detector chassis
4. Digital delay generator
5. Motor driver/controller
6. Power supply

The length of the cables connecting the drive to the mechanical scanner limits the distance between the cabinet and the scanner. (Short cables are a prudent choice when dealing with the 1 GHz high frequency signals being used in this unit).

The transmitting part of the unit is made up of the Pulser and Splitter. The receiver consists of the Mixer and Detector.

The details of all the electrical circuits and the mechanical configuration of the individual chassis are included in the Appendix.

An overall system block diagram is shown in Figure 8.

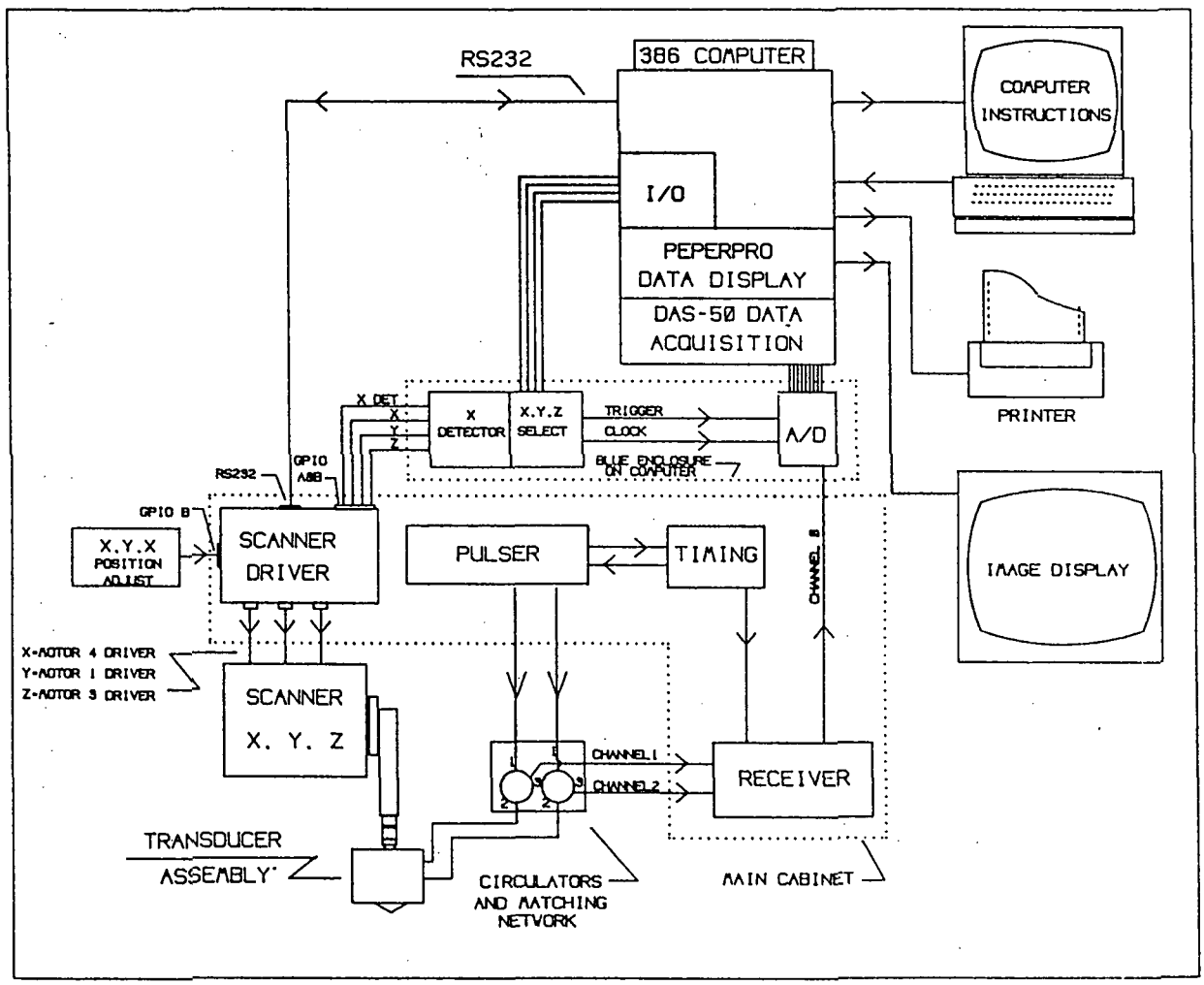

Figure 8. Overall block diagram of the microscope system.

3.2.1 *Pulser Chassis*

The Pulser chassis contains a 1 GHz YIG oscillator which produces a continuous 1 GHz signal. Three R.F. switches let only a specific number of cycles of the 1 GHz signal pass on to an R.F. amplifier thus producing a tone burst. This tone burst leaves the chassis and is passed on to the Splitter/Mixer chassis.

3.2.2 *Splitter*

The Splitter section of the Splitter/Mixer chassis divides the tone burst in to two channels of identical signals. These signals leave this chassis and go through two circulators, one for each channel.

The tone bursts are used to stimulate the transducers and thus produce two ultrasonic beams which impinge on the sample. An echo from the sample returns to the transducer; the received signal is directed by the circulator to the Mixer side of this chassis. The 1GHz echo is amplified and mixed down to 300 MHz.

The 300 MHz I.F. (intermediate frequency) was chosen for the following three reasons:

(i) better equipment is available for processing the signal at a lower frequency;

(ii) the equipment is less expensive at a lower frequency;

(iii) the system can be readily adapted to a variety of transducers at other frequencies by changing the YIG oscillators frequency in the Pulser and Splitter/Mixer chassis.

One of the resulting I.F. tone bursts is phase shifted by 90°. Both are then sent to the Detector chassis.

3.2.3 *Detector Chassis*

The Detector is designed to phase detect or provide amplitude detection on each channel. This provides three modes of scanning.

The phase detection, which is the unique purpose of this scanner, will deliver a scan sensitive to the phase relationship of one beam with respect to the other. The phase

information gathered is different and looks different than the traditional amplitude scan which only looks at amplitude variations of one channel.

Because both channels are available during an amplitude scan it is possible to produce scan data which is sensitive to the relative amplitude of both channels.

3.2.4 *Digital Delay Generator*

The Digital delay generator is the heart of the timing signal generation. This generator is operating at free-running mode to produce the gating signals for switching transmission and receiver switches. A repetition rate of 390 kHz is used to turn on the tone burst in the Pulser chassis. Gating signals also hold off the receiver during transmission thus avoiding the possibility of damage due to a large stimulus being placed on a necessarily sensitive input.

The range delay and gating signals for the sample/hold is also controlled by this Delay Generator. Gating controls are position by the operator in order to select the part of the returning echo that is to be used during image reconstruction.

3.2.5 *Klinger Motor Drives*

The Klinger motor drive and control gets *instructions* from the system computer on how far and how fast the motor units are to move the transducer during the scanning. A hand controller is attached to this unit and allows the control and positioning the transducer prior to scanning. This is a proprietary unit designed by Klinger.

3.2.6 *Power Supplies*

Modular linear d.c. power supplies inside the cabinet supplies +15V, -15V and +5V for the operation of the three chassis and incidental circuitry.

3.3 Mechanical Design

The major mechanical considerations of the system design were firstly, and the more obvious of the two, the scanning stages themselves, and secondly the design of the lens holder. Both are

described below. Outline drawings of the scanner stage and assembly are provided in the Appendix.

3.3.1 *Scanning Stage and Lens Support*

The mechanical assembly holding the sample sits on a thick aluminum plate table which floats on an air cushion provided by four small cycle innertubes. This simple air cushion is a popular method used to isolate the scanning table from outside vibrations.

Klinger Scientific equipment is used to make up the scanner's structure. The transducer is mounted to three motorized linear positioning devices held over the sample by a rigid structure. These motorized devices scan in the X and Y direction to make a two dimensional picture, and scan in a Z direction to focus and gather V(z) data.

The Klinger UT100.25CC DC motor driven stages are controlled by computer through the Klinger three axis DCS750.3ND controller.

This total mechanical assembly is 29" wide by 29" deep and 30" high and sits on any rigid work bench or table. This table should sit on a concrete floor away from rotating machines or other devices that causes mechanical vibration.

3.3.2 *Sample Handling*

The sample to be scanned must have a highly polished surface as the focal length of the lens is only 80 μm. A holder has been provided, with opposing screws which acts much like a small vice to hold a sample up to 1.8" in diameter and over .25" high. The vice can be replaced with just a flat surface for scanning items like a flat peace of metal.

The sample sits on a moveable mechanical assembly which is put in a position by hand under the ultrasonic dual beam lens. Because the placement under the lens is very critical to assure correct and accurate scanning results, a number of manual and electronically controlled movements are provided. Centering, closer placement to the transducer, and leveling of the sample are done with the manual controls. The final adjustments are done with electronic controls while viewing the returned ultrasound echoes on the supplied Tektronix 2465B oscilloscope. The transducer is placed at approximately 80 μm above the sample.

3.3.3 *Lens Housing and Matching Networks*

The transducer assembly is made up of three major parts:

1. Lens and Transducers
2. Housing
3. Matching network

1. The construction of the lens buffer rod and the transducers have previously been described in Section 3.1.2. The gold wire which is bonded to each of the transducers is connected to its corresponding coax connector mounted on the outside of the lens holder.

2. The housing is made from brass. This was chosen because it is easily worked and will allow solder connections to be made to it when needed. The height of the assembly closely matches that of the Leitz system lens in order to maintain the feature of optical focussing prior to acoustic sighting. The physical attachment of the holder to the BIR system is the same SMA connector as the Leitz system. The SMA connector is terminated with a 51Ω resistor so that when this transducer assembly is connected to the Leitz system it will provide a suitable termination, if required.

3. A matching network is generally needed to get the maximum signal into and out of the transducer. At the 1 GHz frequency every part of the ultrasound path attenuates the signal greatly. A mismatch also introduces excessive ringing of the signal. The 80 μm spacing between the transducer lens represents such a short time window that ring of the signal, however small has to be eliminated where possible. The matching network at least minimizes this ringing.

Figures 9 and 10 show the lens housing and the matching network respectively.

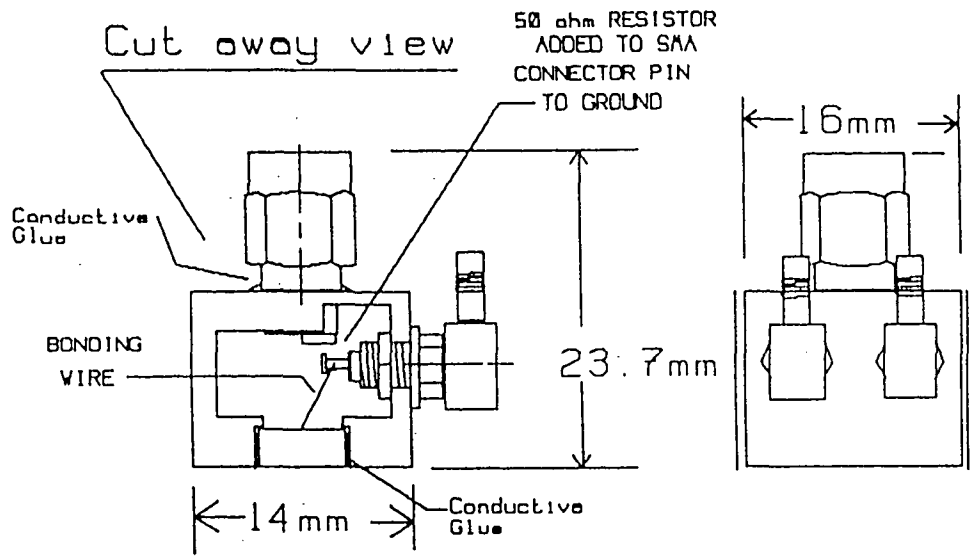

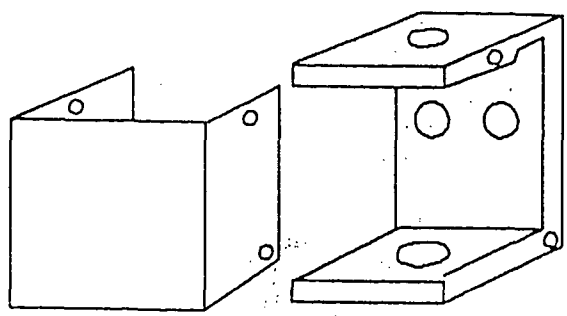

Figure 9. Lens housing.

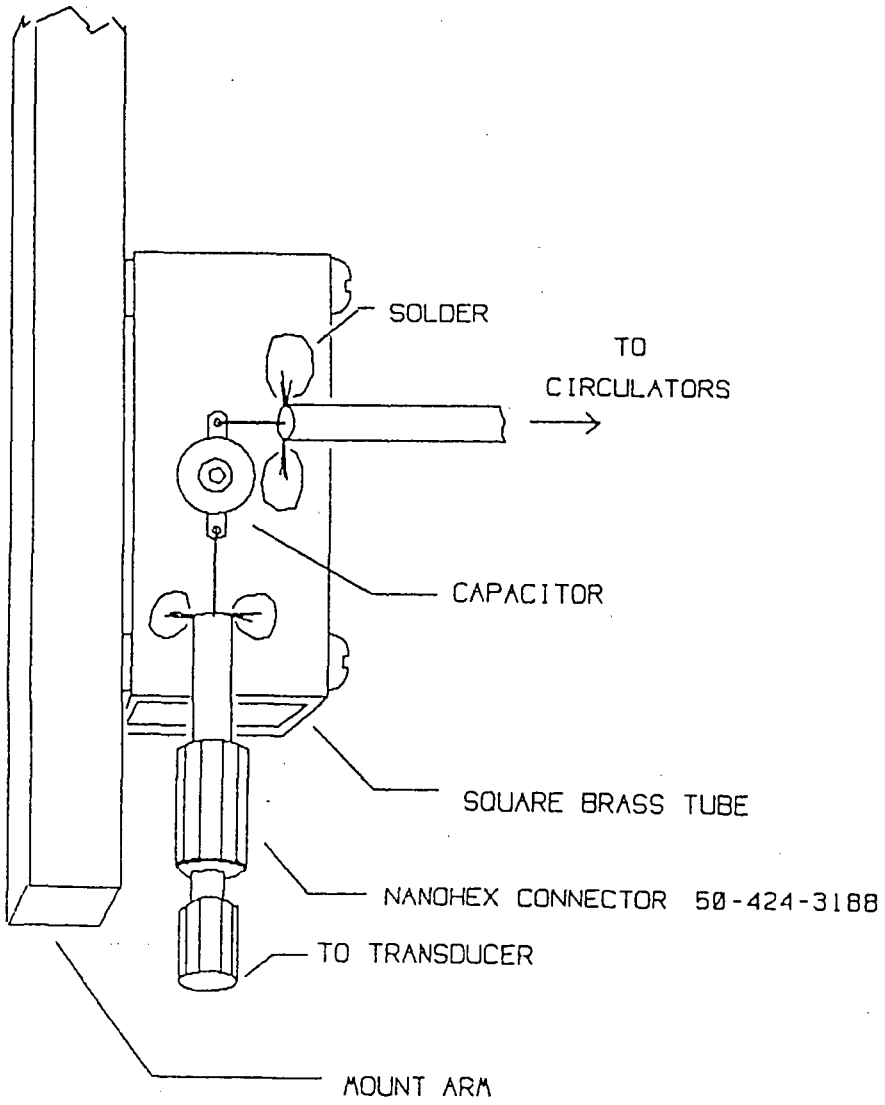

Figure 10. Matching networks.

3.4 Computer

The computer is an American Research Corporation (ARC) 386 Skyscraper type. A number of boards have been added to enhance the computers graphic capability, gather the picture data from the scanner's electronics, and allow the computer to control the scanner.

The special additions are as follows:

1. Keithley/Metrabyte DAS-50 board
2. Keithley/Metrabyte PIO-12 board
3. Pepper Pro 1280 Graphics Board & Mitsubishi Color Monitor (20")

The normal features included in the system are as follows:

4. 80 MB Hard Drive
5. 386/25MHz Co-processor
6. Irwin Tape Drive (40 MB)
7. 2 MB RAM
8. Panasonic Printer

1. The Keithley/Metrabyte DAS-50 A/D board receives and stores the image information as it comes from the scanner electronics. This is then transferred to the computers RAM and later to the hard disk. An image can be copied to the Irwin tape drive for storage. Images may also be stored on floppy disk.

2. A Keithley/Metrabyte PIO-12 board is used to interface the computer to the Klinger scanner.

3. The Pepper Pro 1280 Graphics Board is needed to drive the Mitsubishi Color Monitor which has a resolution of 1280 × 1024. The resolution of image scanned can be chosen by the operator (this is covered more in Section 3.5 Software), 512 × 512 is a common scan and two of these images can be put up on the screen side by side with this hardware.

The system will allow the operator to view a scan as it is being made thus providing the operator with a *quick look* before the scan has progressed to far and wasted time.

3.5 Software

This section summarizes the functions and usage of the software developed in support of this contract. The main functions of the software are to control and coordinate the XYZ 3-axis DC motor control precision moving stage (Klinger DCS750), the data acquisition system (Metrabyte DAS-50), the color display system (Pepper Pro 1280 color display control board and Mitsubishi Diamond Scan HL6905 color monitor), and the electronics for this microscope.

Two main programs can be invoked from DOS command level: NSCAN.EXE and NDISPLAY.EXE. Other assisting subprograms will be loaded automatically.

The first program NSCAN.EXE deals with the data acquisition and the synchronization between the data acquisition system and the motor control precision moving stage. This program is menu-driven. The second program NDISPLAY.EXE provides flexible image display features. The principles of operations will be described in the following sections. The detail usage of the software can be found in the user guide provided to NASA as part of this project.

3.5.1 *System Architecture*

The system architecture is shown in Figure 11. The 1 GHz differential phase acoustic lens is mounted on the DCS750 precision moving stage. The acoustic signal is transmitted and received through the electronics and then fed into the DAS-50 data acquisition system. The control of the Klinger DCS750 motor control moving stage is issued through an RS232 link. The data are acquired by and stored in DAS-50, and then transferred to hard disk at the end of the data acquisition. During the data acquisition, the image data are also displayed on the color display monitor through the Pepper Pro 1280 board.

The clock and trigger signal for data acquisition are provided by the DCS750 through a specially designed logic circuit under PC/AT's control. A number of motor control programs are automatically loaded into the precision motor control stage DCS750 at the NSCAN.EXE program initialization time. These motor control programs provides precise synchronization between the motor motion and the data acquisition system. The status of the electronics are also readable through the digital I/O of the PC/AT system.

The relationship between the software and various key elements of the system is shown in Figure 12. The data acquisition can be performed using NSCAN.EXE. This program commands the precision motor control stage DCS750 to follow a pre-determined scanning

path and the DAS-50 to take the data at proper time. The scanning data and parameters are stored onto the hard disk at the end of the data acquisition. The image data can be retrieved using NDISPLAY.EXE to display on the color monitor. The line scan or V(z) scan data can be retrieved using general graphic package, e.g. GRAPHER.

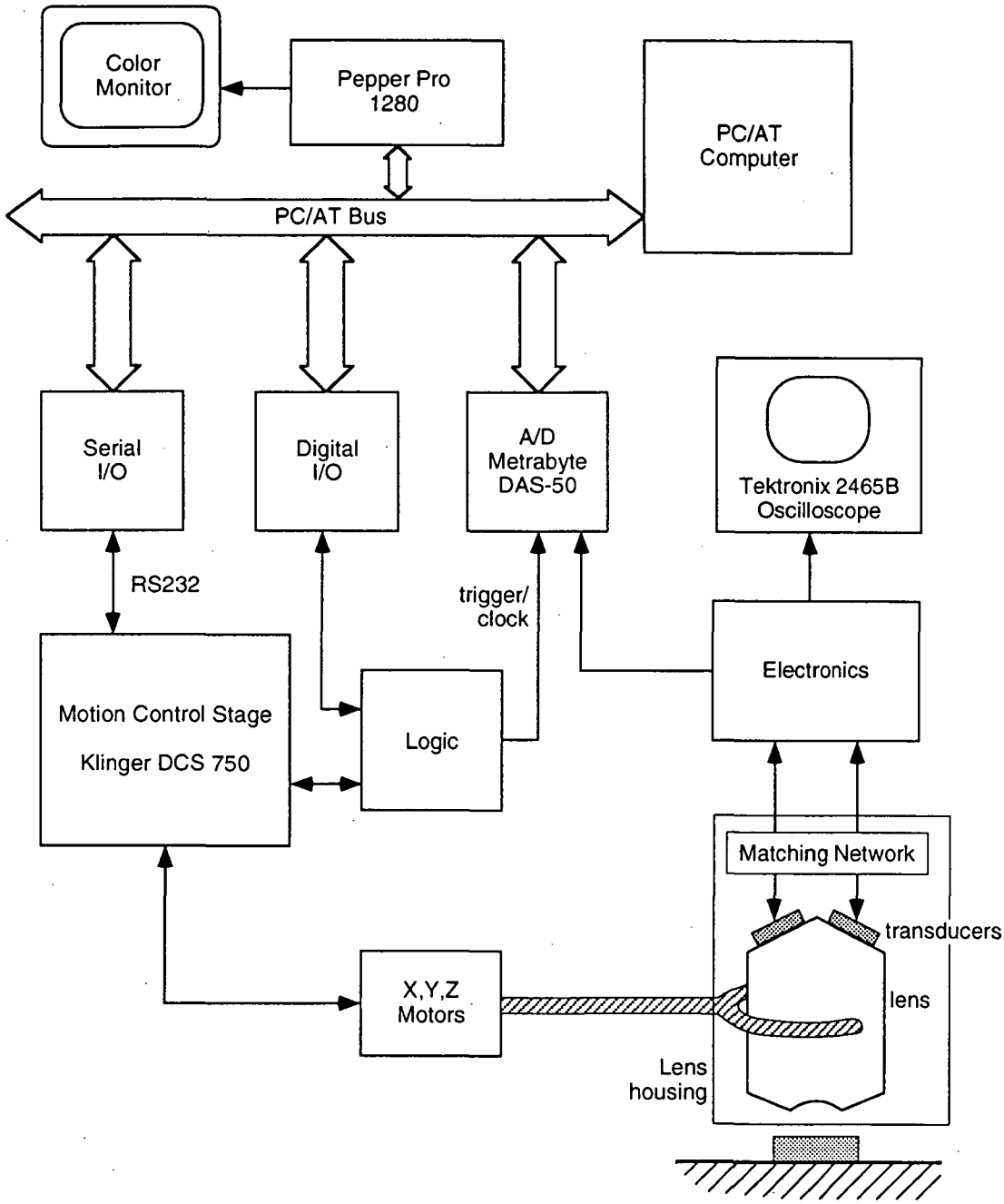

Figure 11. System Architecture.

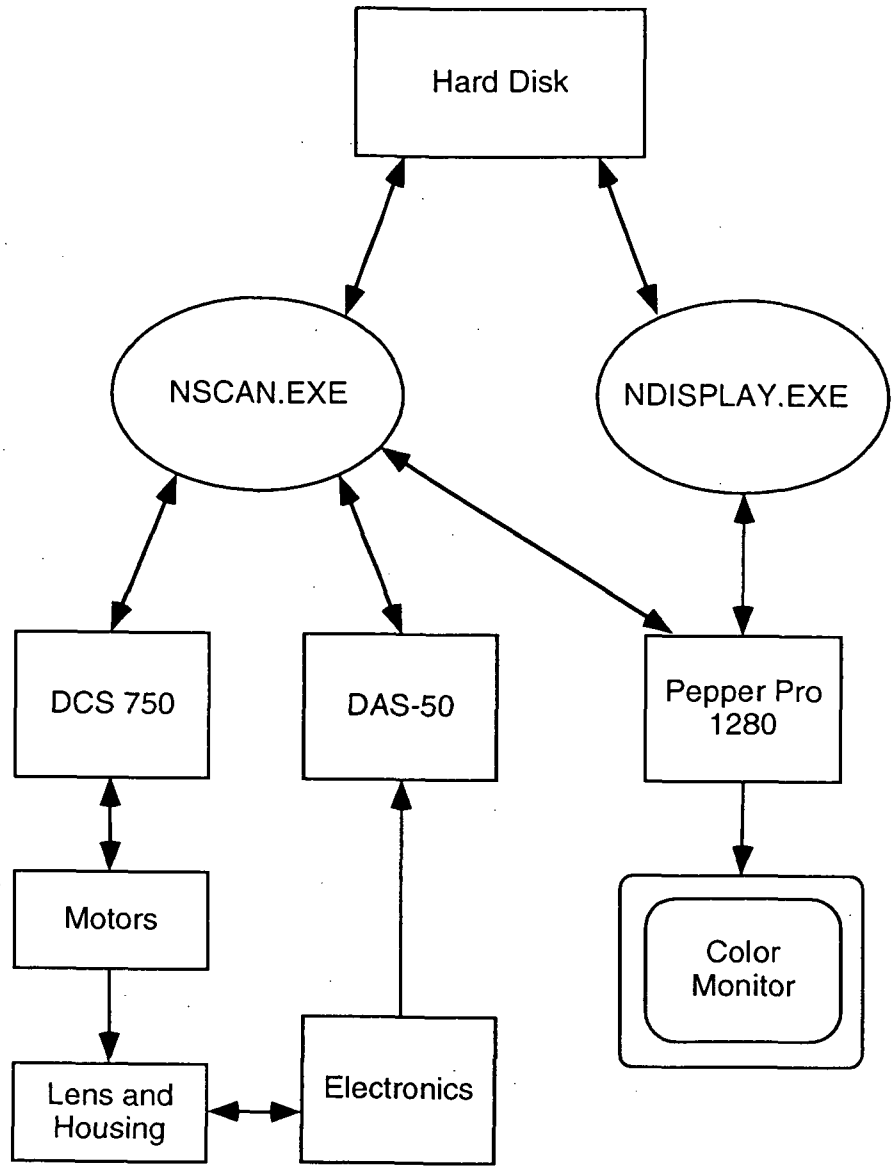

Figure 12. Relationship between software and hardware.

3.5.2 *Scanning parameters selection*

Two different scanning modes are supported in this differential phase scanning acoustic microscope, namely, line scan and raster scan. The line scan mode provides flexible scanning parameters along any of the following three axes: X, Y, or Z. The V(z) scan is one of the 4 options in line scan sub-menu. Raster scan is an image scan and can be treated as a collection of multiple X-axis line scan data. These two scanning modes can be selected from the main menu of the NSCAN.EXE program.

3.5.2.1 *Line scan and V(z) scan*

Scanning axis can be selected at the line scan sub-menu. Line scan direction is fixed and can not be changed. Step size (spatial sampling interval) of the line scan can be either 1, 2, or 4 μm. V(z) scan can be invoked by choosing the V(z) scan option at the line scan sub-menu. V(z) scan provides a better control of step size (0.5 μm).

In X, Y, or Z-axis line scan mode, the current transducer position is taken as the center position of the line scan. The transducer is moved toward the negative axis direction first and then moved toward the positive axis direction. The data are taken while the transducer moves toward the positive axis direction. At the end of the scan, the transducer is moved back to the original position.

In V(z) scan mode, however, the user can choose the current transducer position as either the center of the scan line or the starting position of the scan line. The first scanning mode corresponds to the "positive and negative Z scan" and the second mode corresponds the "negative Z scan only" in the V(z) scan sub-menu. In both scanning modes, the transducers will be brought back to the original position when the scanning is completed. Performing a regular line scan or V(z) typically takes about a few seconds.

The scanned data will be displayed on the PC/AT screen after the scan is completed. Two display modes are available: linear or logarithmic scale. The user can choose either to save the data or to re-adjust the sample position and re-scan it after scrutinizing the display of the line scan data.

3.5.2.2 *Raster scan*

Raster scan mode produces an image of the reflected acoustic signals. Four different possible sets of scanning parameters can be chosen:

(1) Standard scan: 256 x 256 pixels with 4 μm $\times$ 4 μm pixel size, the physical size of the scanning area is approximately 1 mm $\times$ 1 mm.

(2) Fine scan: 512 x 512 pixels with 2 μm $\times$ 2 μm pixel size, the physical size of the scanning area is approximately 1 mm $\times$ 1 mm.

(3) Quick scan: 128 x 128 pixels with 4 μm $\times$ 4 μm pixel size, the physical size of the scanning area is approximately 0.5 mm $\times$ 0.5 mm.

(4) Ultrafine scan: 512 x 512 pixels with 1 μm $\times$ 1 μm pixel size, the physical size of the scanning area is approximately 0.5 mm $\times$ 0.5 mm.

Scanning direction can be chosen either away from the user (+Y scan or bottom-up scan) or toward the user (-Y scan or Top-down scan). The names of top-down scan and bottom-up scan correspond to the display direction when looking at the color monitor.

Aside from these two classification of scanning modes, each scan mode can be either uni-directional or bi-directional. Uni-directional scan means the scan direction is always from -X toward +X axis direction and bi-directional scan means the scanning direction changes every line, in other words, at the first line the scanner scans from -X toward +X, at the second line it scans from +X toward -X, at the third line it scans from -X toward +X, etc. Uni-directional scan is a slower process but provides a better image quality. The scanning time for a bi-directional scan is much shorter than the uni-directional scan since no trace back is needed for each scanned line.

In summary, combining the 4 possible scanning sizes and resolution, 4 scanning directional control, the software provides 16 raster scanning modes in total. The user can apply different combination of the scanning modes to quickly set up a good scanning condition before taking the actual scan. A suggestion from BIR is to do bi-directional quick scans for both top-down and bottom-up modes, then finely adjust the sample position and level, and repeat this process till the best condition is achieved where a good (partial or total) image is observed on the color monitor. Then, depending upon the need of the applications, choose either the standard, quick, fine, or ultrafine scanning mode.

The scanning time for a raster scan varies from 11 minutes to 200 minutes. An estimate of the required scan time is shown on the screen when raster scan mode is chosen. For examples, a bi-directional quick scan takes about 11 minutes, an uni-directional quick scan takes about 25 minutes, a bi-directional standard scan takes about 35 minutes, an uni-directional standard scan takes about 81 minutes, a bi-directional fine scan takes

about 99 minutes, an uni-directional fine scan takes about 200 minutes, a bi-directional ultrafine scan takes about 76 minutes, and an uni-directional ultrafine scan takes about 125 minutes. Notes that the scan area for an ultrafine scan is only .5 mm × .5 mm while the scan area for a fine scan is 1 mm × 1 mm. This scanning time does not include the time spent for scanning parameters selection and the disk access time.

At the end of the raster scan, the transducer is always moved back to the original position before scanning. The raster scan can be aborted any time during the scan no matter what scanning mode the scanner is operating at. This can be done by pressing the Escape key on the PC/AT keyboard during scanning. The program will respond to this request at the end of the current scan line and then move the transducer back to the original position. This feature give the user a way to re-adjust the sample position, leveling, or any other electronic signal conditioning, and to re-start the scan. This may be necessary when a degradation of the image quality is observed on the color monitor during scanning which could be due to improper sample positioning and leveling, inappropriate electronic setting, or loss of coupling medium (i.e. water) .

The user is responsible for the reserving enough disk space to store the image and scan data. The program will report the required disk space at the time the use select the scanning mode so that the user has the opportunity to clean up the hard disk before scanning.

The image will be displayed on the color monitor and updated whenever an extra scan line data are acquired. The user can watch the partial image during scanning and determine whether the sample position and leveling is appropriate or not. The on-line display function only displays the image at fixed format. However, the user can retrieve the image after the scanning is completed using NDISPLAY.EXE program which provides much more image display features including pseudo color palette selection and zooming.

The user also has the option to save the scanning parameters into a file so that the user can retrieve the scanning information later.

3.5.3 *Image display*

The raster scan image can be retrieved and displayed using NDISPLAY.EXE program. The main function of this program is to control the Pepper Pro 1280 to display the image data. This program can be invoked from the DOS command level. The program will display the image on the color monitor and the user has to provide the image filename

and sizes information. The user can choose different zoom factors and pseudo color. Various color palettes are available. The image can be re-scaled if necessary. Proper re-scaling of the image data usually results a much better contrast to analyze the image.

3.5.4 *Data format*

The software produces two kinds of data files: line scan data and raster scan image.

The line scan (including V(z) scan) data are stored in ASCII text file format and can be read by many off-the-shelf graphic and data analysis software packages. The sampling index number is stored together with each datum in one single text line.

The raster scan image data are stored in binary format. Each datum is stored as a 16-bit integer. The sequence of the data storage is "X-axis"-major, i.e. the first line along X-axis is stored first, and then second line, and then third line, etc. The order of the data storage for each line has already been corrected. Either uni-directional or bi-directional or top-down or bottom-up scan produces the same order of image data. The image is always stored in top-down (+Y toward -Y) and left-to-right (-X toward +X) order. This allows an easy and unambiguous way to access the image file if the user wish to perform further image processing.

4. PERFORMANCE

Figures 13 - 17 show the outlook of the whole system. The mechanical support of the scanning stage is to the left of Figure 13 and the electronics cabinet is to the right of Figure 13. The computer system and the color monitor are shown in Figure 14. Figures 15 and 16 show the sample holder. The remote push button control panel of the scanning stage is shown on the right lower corner of Figure 15. All three adjustment knobs of the sample holder for adjusting the sample level can be seen from Figure 16.

Figure 17 shows the outlook of the electronics cabinet. They are (from top to bottom) the Tektronix oscilloscope 2465B, the Klinger DC motor controller DCS750, the Splitter/Mixer chassis, the Stanford delay generator DG535 and the detector chassis, the pulser chassis, and the power supplies. Figures 18 and 19 show typical high frequency circuits inside the electronics cabinet.

All of the electronic hardware and the scanning stages have been tested and the desired performance obtained. Control of the scanning stages with a predefined pattern and scan rate has been demonstrated. All of the drive circuitry, as described by the circuit given in Figure 7, has been tested with a 1 GHz dual beam lens as described in Table 1. Integrated test of the whole differential phase scanning acoustic microscope system including the lens, electronics, scanning stages, and control and display software have been tested and accepted

(1) at BIR on March 9, 1992 in presence of Dr. Patrick H Johnston of Composite NDE Research of NASA Langley Research Center and

(2) at NASA, Langley during the week of March 23 - 27, 1992.

This section describes the performance of the system.

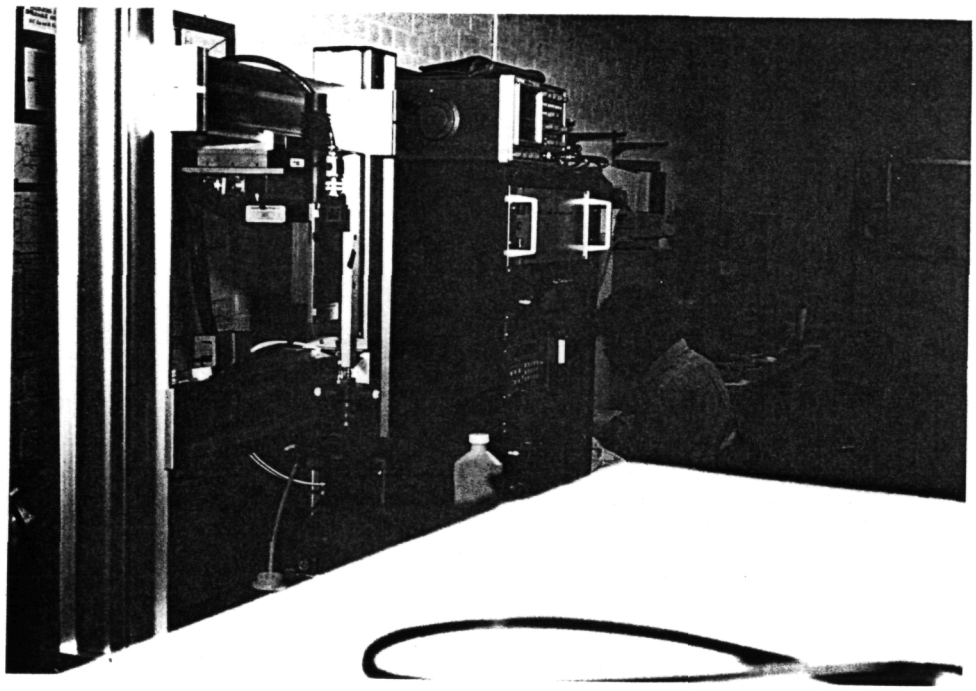

Figure 13. The scanning stage, the lens, the sample holder, and the electronics cabinet.

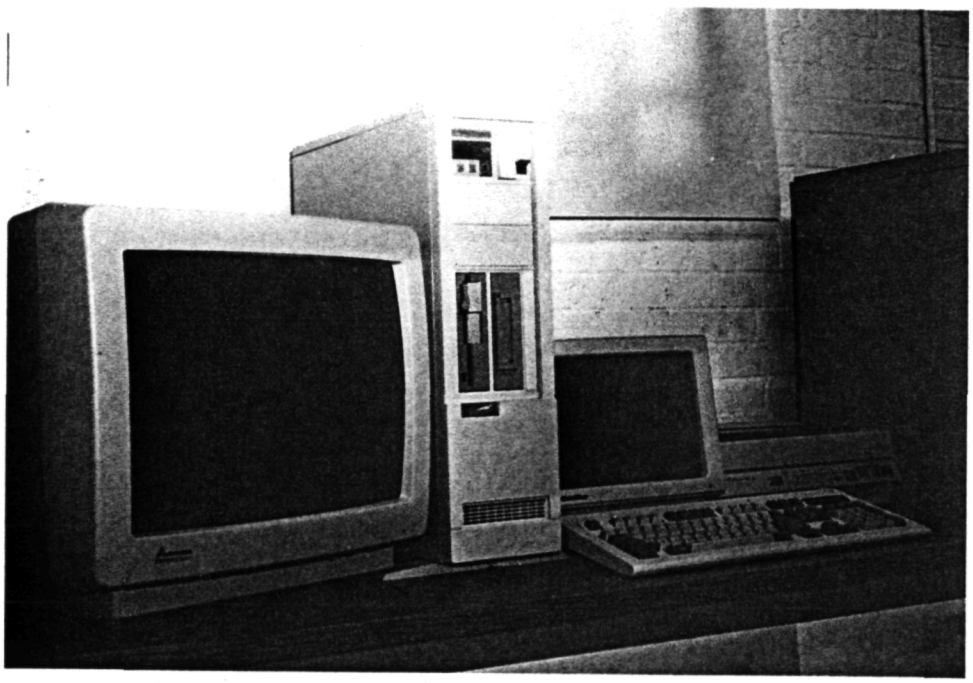

Figure 14. The computer system and the color monitor.

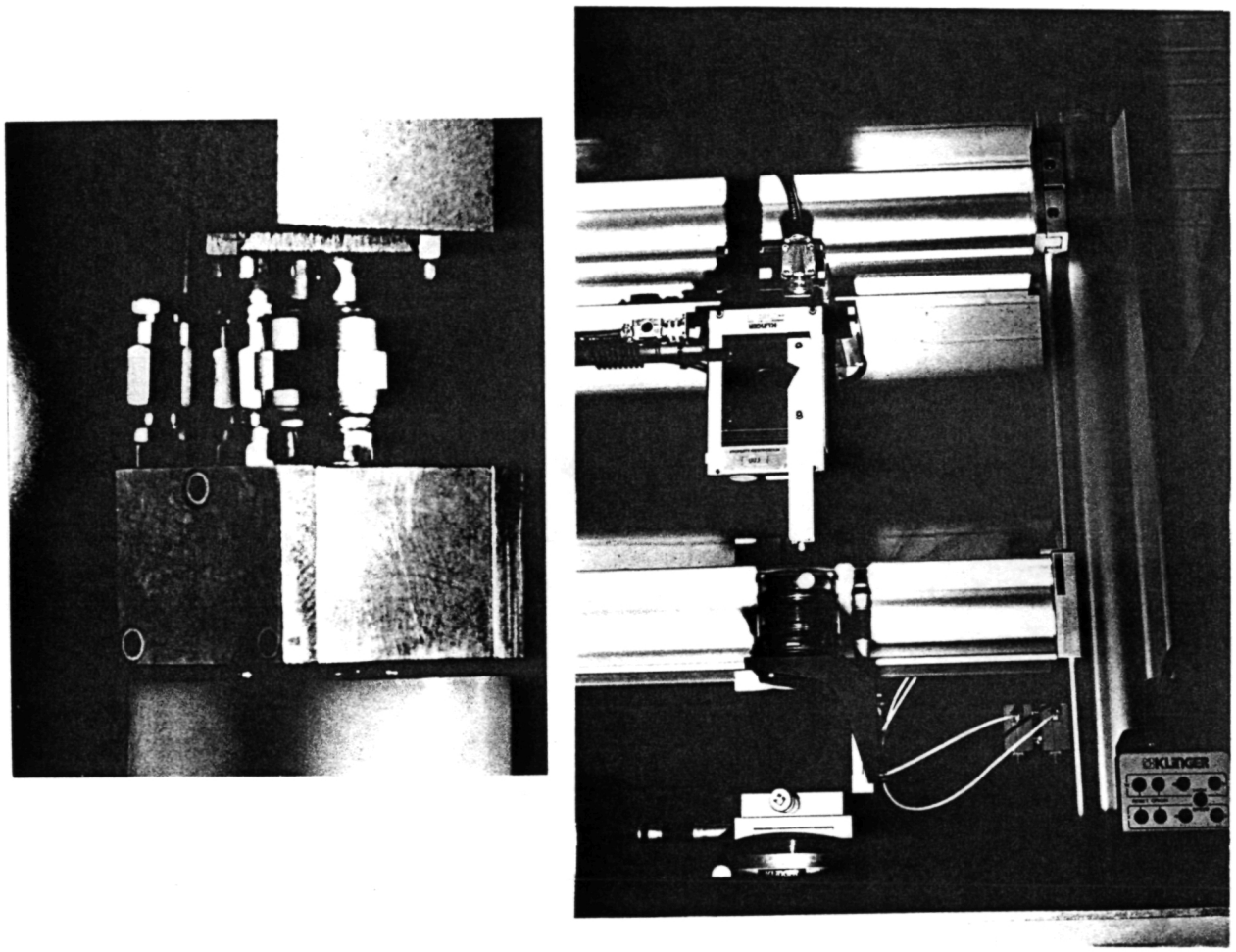

Figure 15. The scanning stage, the lens, and the sample holder.

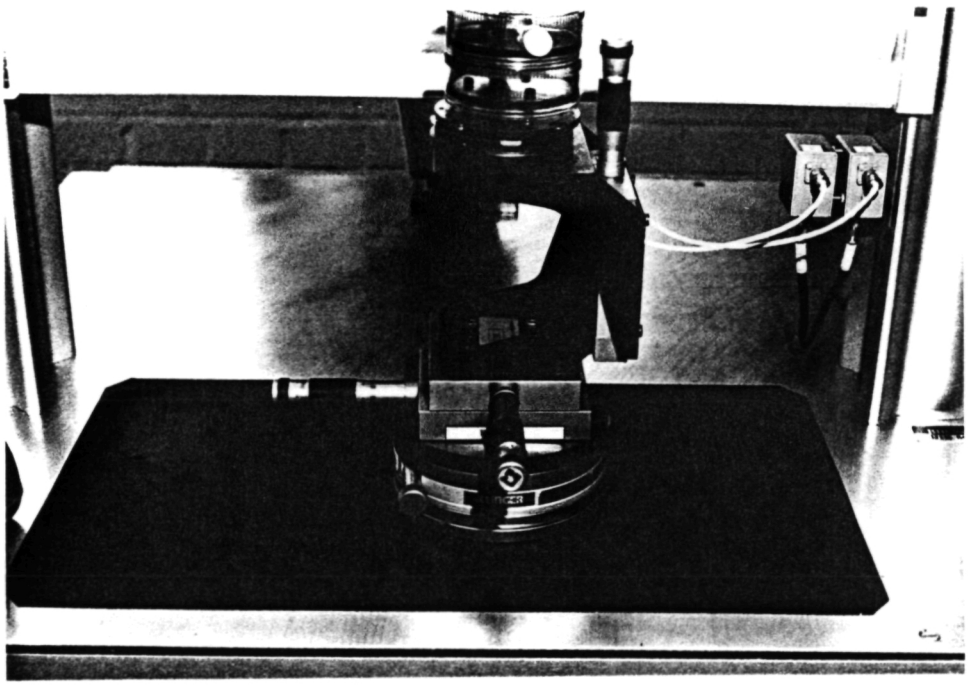

Figure 16. The sample holder.

Figure 17. Electronics cabinet.

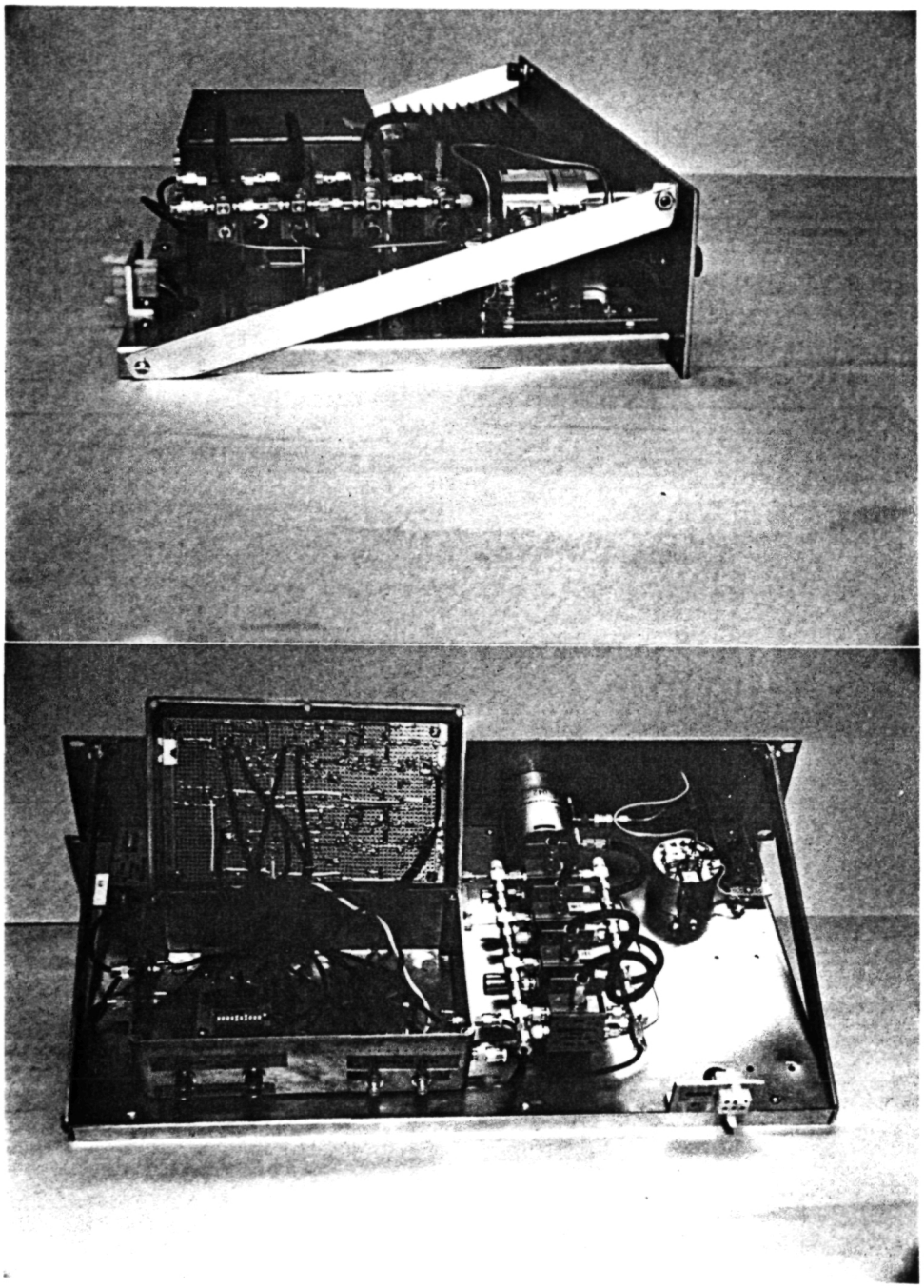

Figure 18. Pulser.

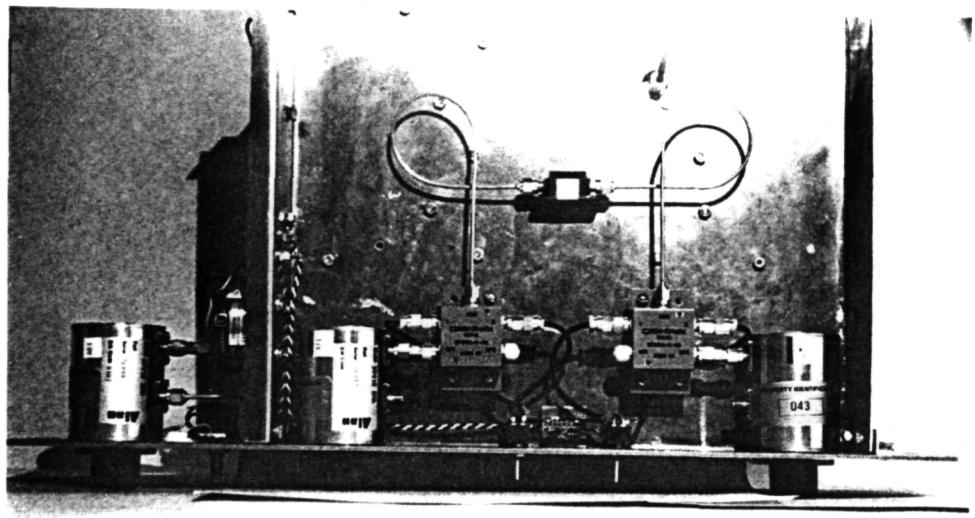

Figure 19. Splitter/Mixer.

4.1 Acoustics Performance

Although the Phase II work was a continuation of the work undertaken during the Phase I program the complexity of the lens and the fabrication process itself resulted in a number of problems in the early stage of the project. Almost all of the early stage problem focus on the lens itself, either in the way in which it is fabricated or the manner in which is mounted, i.e. the form of the housing and configuration.

4.1.1 *Lens and Transducers Performance*

Figures 20 and 21 show typical lens/water interface and sample echoes. Figures 22 and 23 show the optical microscopic images of the lens surface focusing at the outer rim of the aperture and on the spherical curvature.

The lens in structure has been previously defined, see Section 3.1.1. Each side of the lens, i.e. the individual transducers, can be exercised independently and the relative performance of each side was compared. For the working lens as shipped and installed with the system, the amplitude difference between the two transducers were approximately 0.8 dB. This difference of amplitude response was compensated using the two independent variable attenuators for each channel on the panel. After compensated at .83 GHz, the amplitude response of the two channels were nearly the same.

The frequency of the peak transducer response were closer to .83 GHz than the required 1 GHz despite the fact that the actual transducer dimensions corresponded closely to the theoretical values needed to achieve the required response. Although the peak frequency was not at 1 GHz, the overall system response, including the transducer response, was within only 5 dB range between the peak frequency (0.83 GHz) and 1 GHz as will be discussed in Section 4.2.1.

The lens was prone to *clouding over* resulting in a very low output. Figure 24 shows an example of the cloudy lens surface. This was originally attributed to the quality of water being used for the acoustic coupling but the use of demineralized water showed little signs of improvement in the decay in performance with time. Even with the lens thoroughly cleaned the performance still deteriorated with time. This can be remedied by regularly cleaning the lens.

The 3 dB pads in the original transducer design were removed and impedance matching networks were designed and fabricated to match the electronic response of the transducers at the peak frequency.

The theoretical focal length of the lens is given as approximately 80 μm. In practice the focal length was closer to 70 μm (see Figure 22) while all physical parameters of the lens were measured as being according to design.

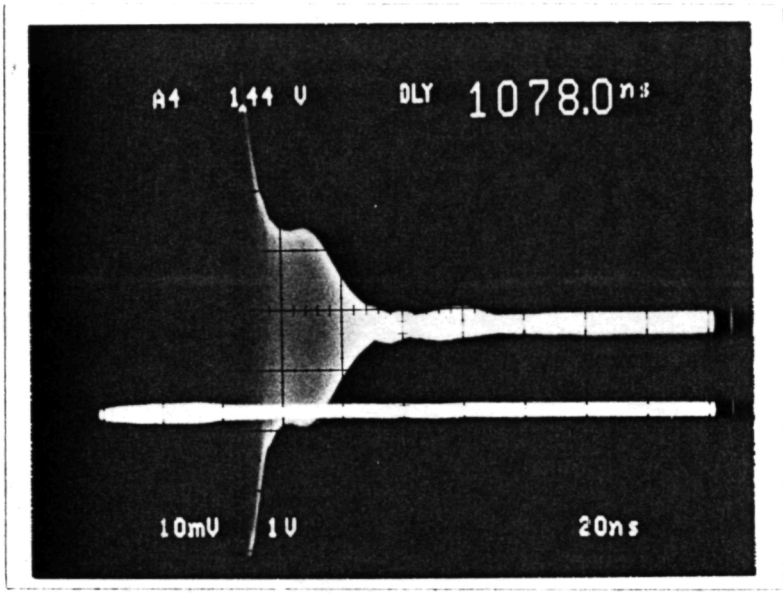

Figure 20. Typical lens/water interface echo.

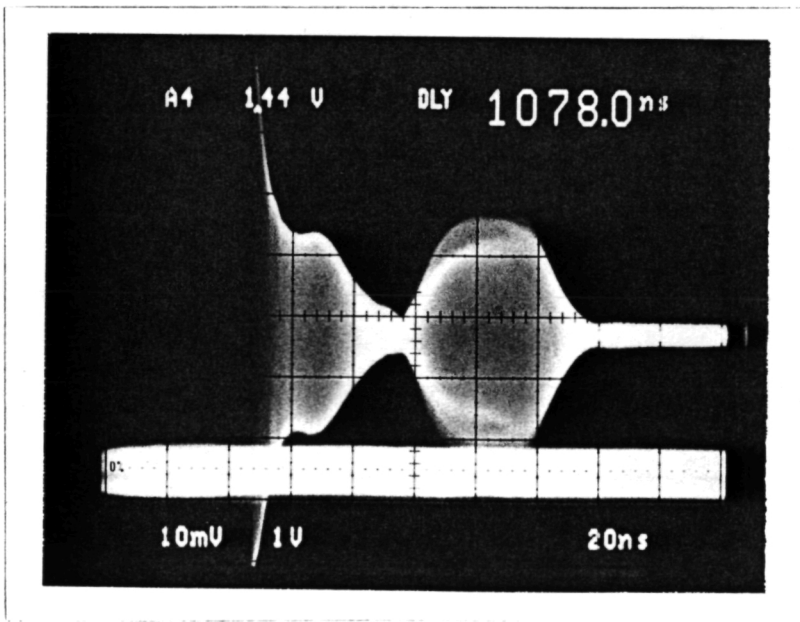

Figure 21. Typical sample echo.

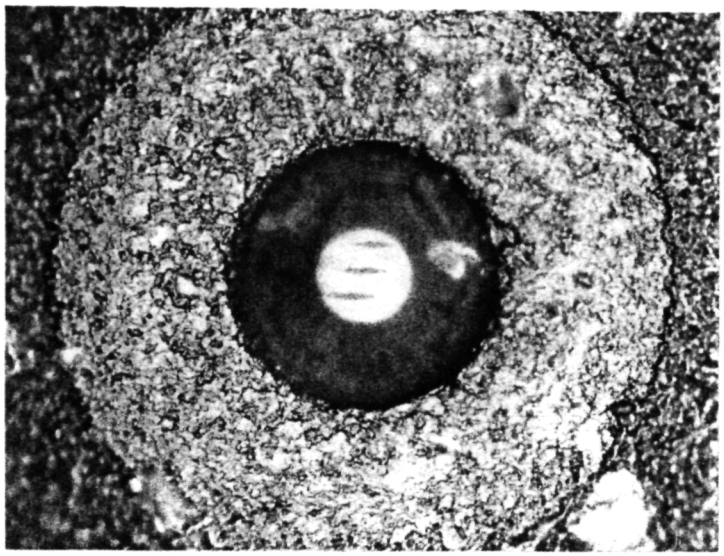

Figure 22. Optical microscopic image of the lens, focussing at the outer rim of the lens curvature.

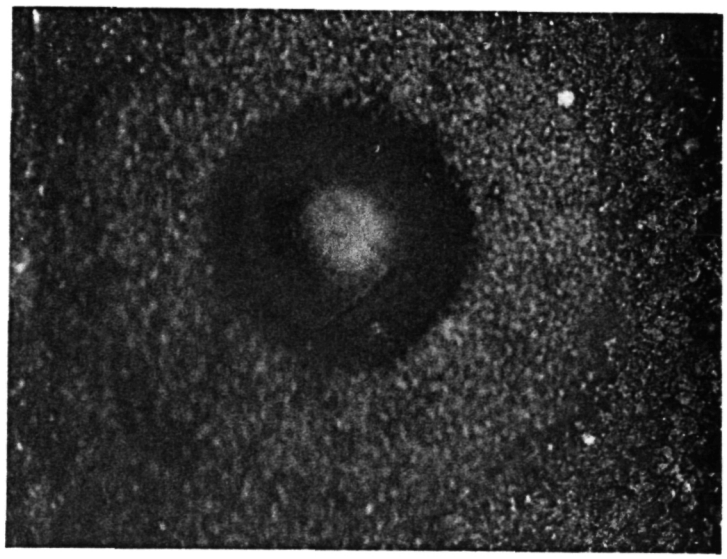

Figure 23. Optical microscopic image of the lens, focusing at the spherical curvature.

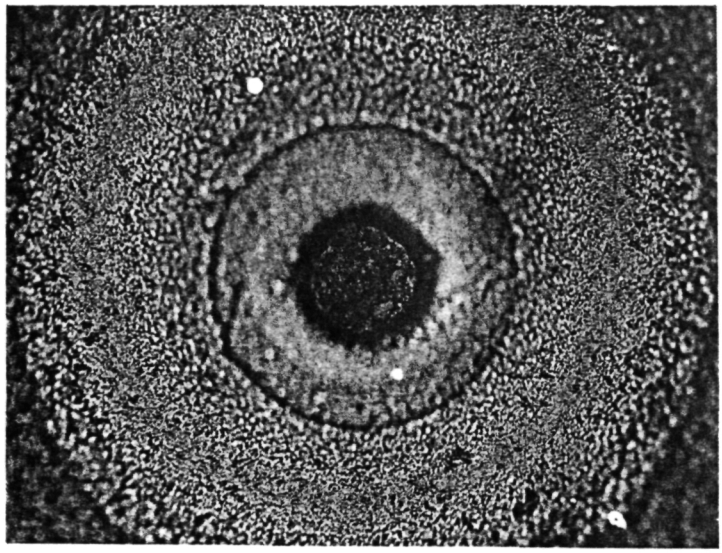

Figure 24. Optical microscopic image of the cloudy lens.

4.1.2 *Lens Mechanical Configuration*

The lens housing is designed in such a way as to enable the unit to interface with the Leitz microscope currently available at NASA Langley. However, no information on the Leitz system was obtained from Leitz, therefore, the lens housing was made to mechanically interface to the Leitz system but no scanning control or electronics interface to the Leitz system was performed.

The overall size of the unit had been fabricated to accommodate three connectors, namely one standard SMA (in order to mount to the existing Leitz fixture), and two subminiature connectors which interfaced directly to our electronics.

The matching network which interfaced the transducers to the electronics was placed on the supporting arm for the lens housing.

It was found to provide an improvement in performance if the acoustic coupling medium (water) was heated. On the Leitz this is achieved by means of a coil which surrounds the lens and, through conduction, heats the water at the lens aperture. However, the performance of this system is good without heating the water and therefore no water heating device was provided with this system.

The lens had a higher output when it was not normal to the surface being scanned. While this could be attributed to the lens being offset in the housing this could not be substantiated.

4.2 Electronics System Performance

All the electronics driving and receiving circuits, scanning stages, and scanning control and display software had been tested and satisfied all the specifications.

4.2.1 *System Frequency Response*

Figure 23 shows the overall system frequency response including the transducer response. It appears that a wide band performance has been achieved. The system response varies within 5 dB from .7 GHz to 1.3 GHz. It drops at lower and higher frequencies because of the limitation of some components (e.g. the circulators drops at below .7 GHz) and the low acoustic response of the transducers when not operating near the designed resonance frequency. The frequency of this plot was measured using the Startek 1500 high frequency counter. The peak response at .83 GHz was used as the reference (0 dB).

4.2.2 *Phase Detector Response*

Figure 24 shows the response of the phase detector. The phase detector response was obtained by injecting two sinusoids of same frequency (300 MHz) and known phase difference into the phase detector and observing the phase detector output on the oscilloscope. The 300 MHz signal was generated using a Hewlett-Packard 8656B Signal Generator. A Sage 6703-2/N variable delay which can varies from -22.5° to 22.5° was used to produce a phase shifted 300 MHz sinusoid. The phase difference between the two sinusoids were recorded from the oscilloscope readings. The systematic phase difference between the two oscilloscope channels and the cables were removed by a calibration step which fed the same 300 MHz sinusoid into both channels of the oscilloscope. These two phase shifted sinusoids were then fed into the two input limiters of the phase detector and the output of the phase detector was recorded. A linear curve fit was performed and the conversion factor between phase detector output and detected phase difference was 0.136°/mV (or 2.37×10^{-3} rad/mV) and the inverse conversion factor was 7.36 mV/deg.

4.2.3 *YIG Oscillator Frequency Drift*

The frequency of the YIG oscillators used to generate the pulse to drive the transducers and to mix the received echoes down to the 300 MHz I.F. was drifting over time. This

frequency drift was removed using a heater to keep the YIG oscillators working at constant frequency. Figure 25 shows the improvement of adding the heater. From this figure, the settling time for the YIG oscillators were estimated to be around 20-30 minutes. The users should allows this settling time for the system to stabilize the oscillation frequency in order to obtain the best scanned images.

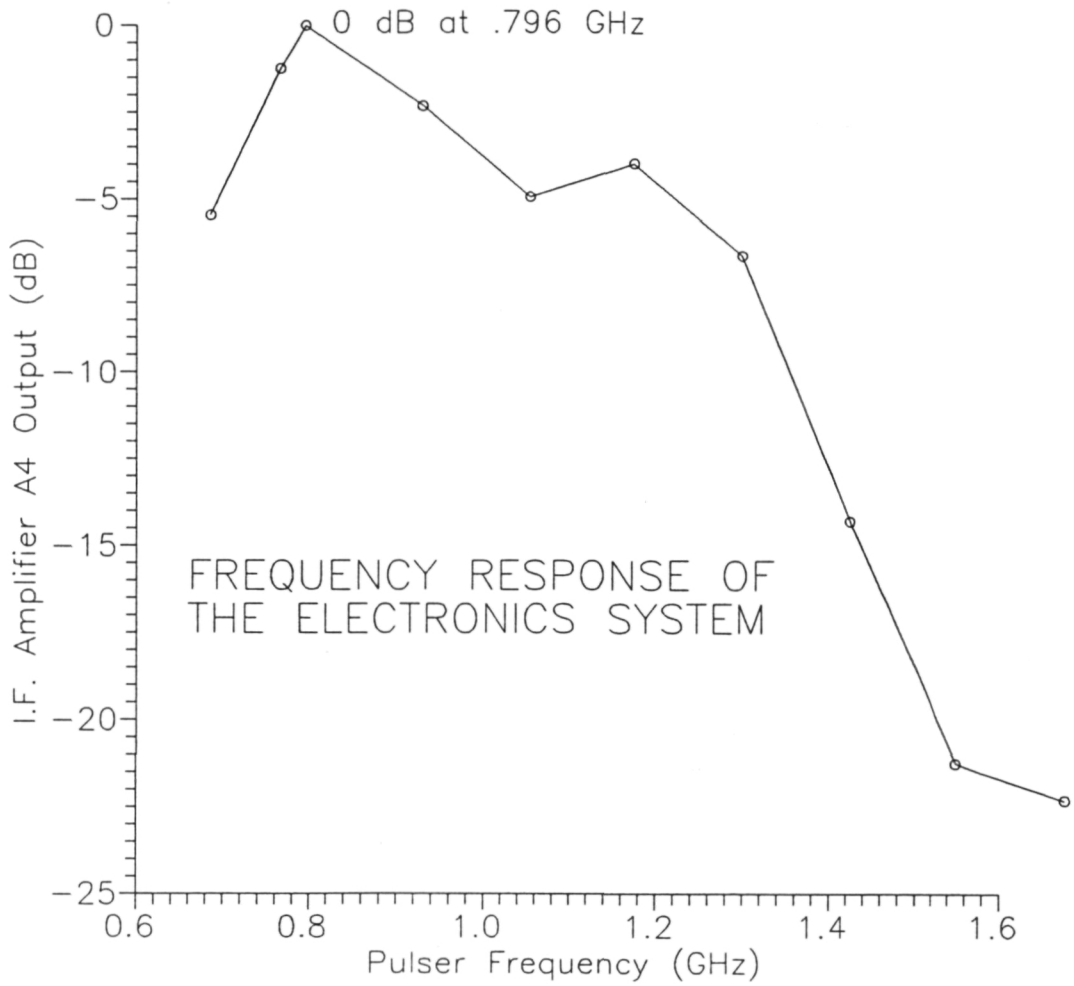

Figure 25. The overall system frequency response.

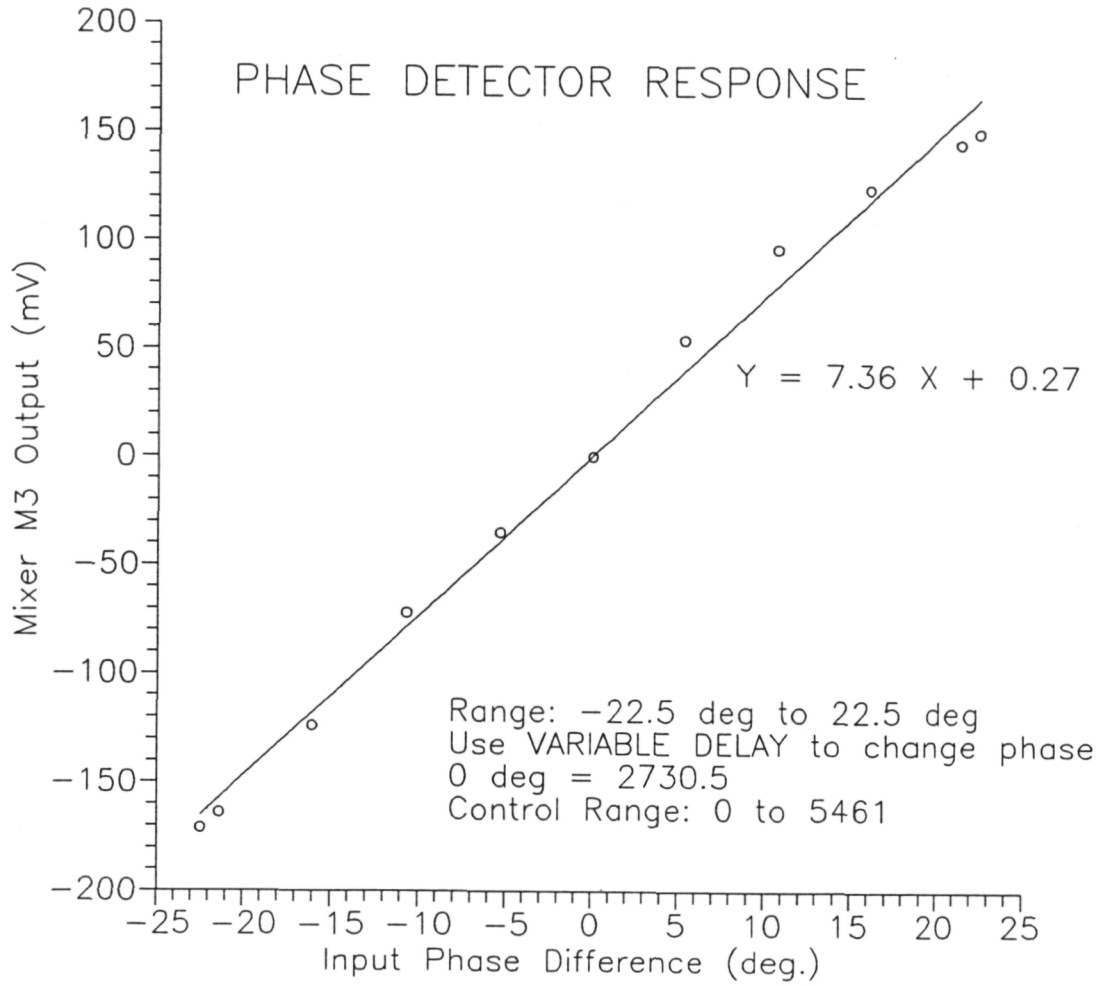

Figure 26. The phase detector response.

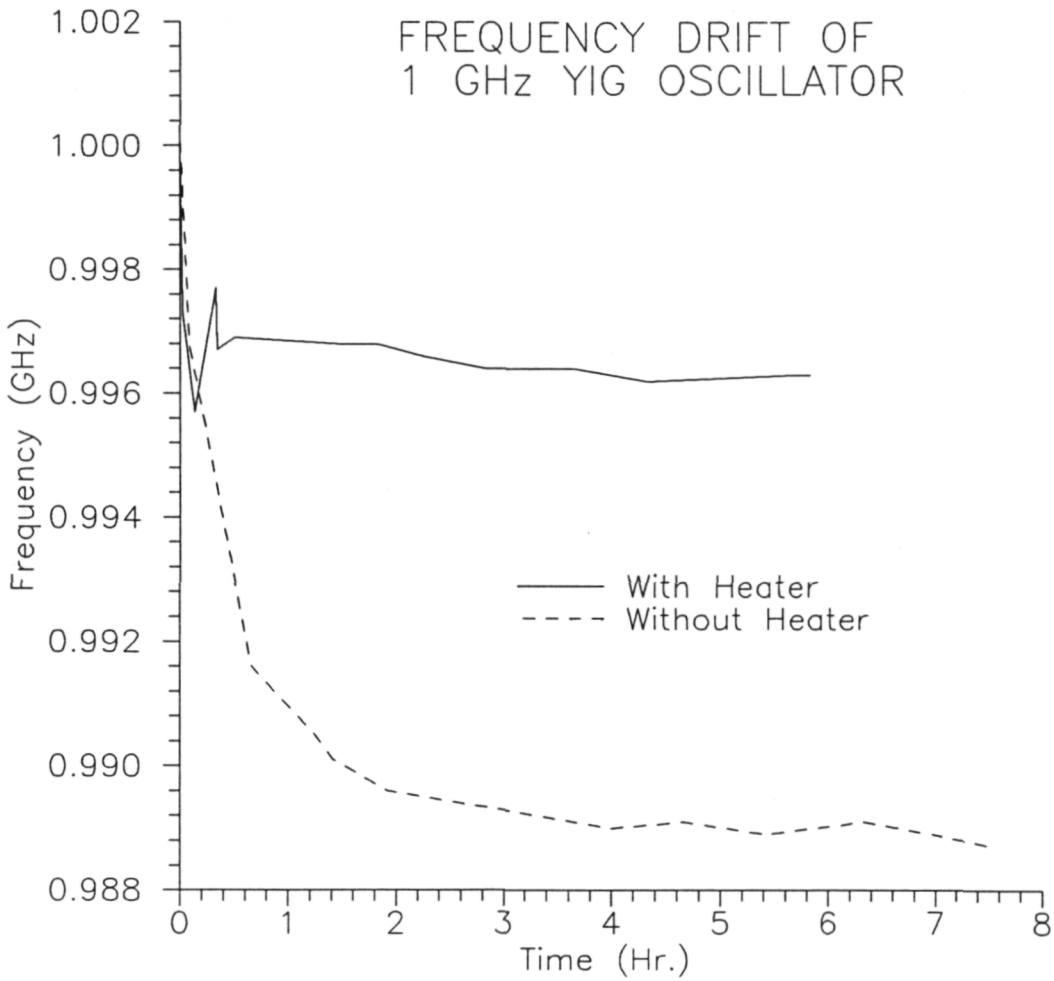

Figure 27. The frequency drift of the YIG oscillator.

4.3 Scanning Stages Performance

Sixteen scanning modes, including four scanning sizes/resolution and four directional control, are available for this system as described in Section 3.5.2.2. All scanning modes have been tested.

The Klinger scanning stages controller DCS750 provided a .1 μm resolution for the position control over the DC motors but it can be achieved only with a very long settling time (in the order of seconds). Therefore, a compromise was made to achieve a 1 μm scanning resolution with reasonable scanning speed. The scanning time for different scanning mode is listed in Table 2. It varies from 11 minutes to 200 minutes depending upon the scanning size and resolution.

Scan Mode	Image Size	Pixel Size (μm)	Scan Size (μm)	Scan† Time (min.)	Scan‡ Time (min.)
Standard	256×256	4×4	1×1	81	35
Fine	512×512	2×2	1×1	200	99
Quick	128×128	4×4	.5×.5	25	11
Ultrafine	512×512	1×1	.5×.5	76	125

†Uni-directional scan.
‡Bi-directional scan.

Table 2. Raster scan size and time.

To further increase the scanning speed, a bi-directional scanning mode as described in Section 3.5 was provided although slight motor back lash was observed for this bi-directional scanning mode. The scanning time for a bi-directional scan is normally around half that of uni-directional scan. The user can make his/her own trade-off between the image quality and scanning time.

The resolution of line scan and V(z) scan is .5 μm because that the scanning time is less stringent. It generally takes around 10 - 20 seconds to perform a line scan or a V(z) scan.

4.4 Software Performance

The software is divided into two main programs, a scanning control software and an image display software. The operation of the software is described in Section 3.5. Both software has been tested and satisfy the specifications.

The scanning time is currently limited by the scanning stages and the display time is limited by the disk access time and the available main memory. Images are stored in plain signed 16-bit binary integer format without coding. line scan and V(z) scan data are stored in text format. The data values are always in between -2048 to 2047 limited by the A/D conversion precision except the V(z) scan data are DC shifted to be in the range of 1 to 4096 so that one can take logarithmic operation without mathematical problems. This is summarized in the following table.

Scan Mode	Filename Extension	Data Range	Format
All	.SCN	Scan Parameters	ASCII text
Raster	.RAW	-2048 to 2047	Binary, 16-bit signed integer
V(z)	.DAT	1 to 4096	ASCII text
Line	.DAT	-2048 to 2047	ASCII text

Table 3. Data range and format.

For the display software, multiple image display, pseudo color palettes, image scaling, image zooming features are available and all had been tested. Twelve palettes are provided with this unit as listed in the following table.

	Name	Description
1.	GRAY	Standard linear gray scale
2.	BI-GRAY	Bi-directional linear gray scale
3.	RED	Linear red scale
4.	BLUE	Linear blue scale
5.	GREEN	Linear green scale
6.	GREEN2	Nonlinear green scale
7.	R-GREEN	Reverse linear green scale
8.	BLUE-RED	Linearly going from blue to dark to red
9.	CYAN-RED	Linearly going from cyan to dark to red
10.	GRN-RED	Linearly going from green to dark to red
11.	GRN2-RED	Nonlinearly going from green to dark to red
12.	GRN3-RED	Nonlinear red scale with green background

Table 4. System color/gray level palettes.

4.5 Theoretical Performance on Topographic Measurement

One of the applications of this differential phase acoustic microscope is to display the topographic changes of the sample surfaces. If all the phase changes are due to the topographic changes, then

$$\Delta\phi = \frac{4\pi f h}{c} \tag{8}$$

where $\Delta\phi$ is the phase difference in radian,
f = .83 GHz is the operating frequency,
c = 1.48 μm/ns is the speed of sound in the medium (water) at 20°C, and
h is a step topographic change of the surface.

Given the phase conversion factor of 0.136°/mV or 2.37×10^{-3} rad/mV as derived in Section 4.2.2, and the measured electronics noise floor of 1 mV_{pp} random noise (using oscilloscope filter, see Figure 28), and assume that a signal-to-noise ratio of 2 is required to observe a recognizable feature in the scanned image, the theoretical performance is 6.7 Å. Since the system has a filter of 46 dB at 600 MHz (where the 1 mV_{pp} noise was observed using the oscilloscope filter) which is slightly worse than the oscilloscope filter, the expected performance is about 10 - 20 Å. However, due to the difficulty in preparing and scanning a sample with a precise 20 Å step, this theoretical performance has not yet been experimentally verified at the time of shipping and installation.

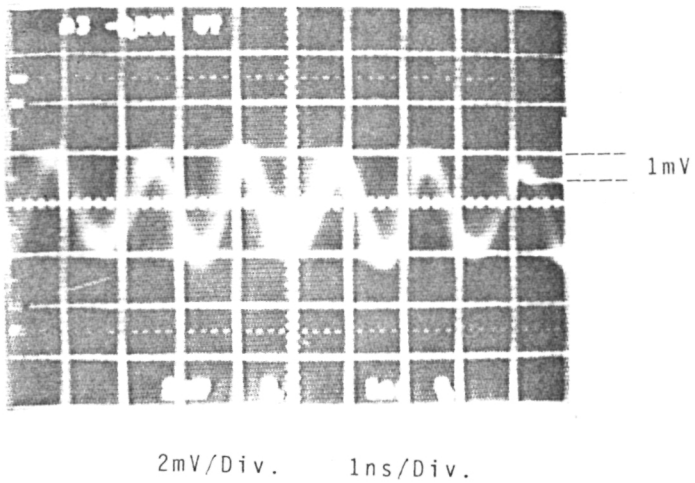

Figure 28. Noise floor of the phase detector.

4.6 Imaging Experiments

Several imaging experiments were performed a system integration test. Figures 29-39 show the scanning results on various test samples and operating at different scanning modes. A vertical gray scale and a vertical pixel index coordinate are shown to the left of each scanned image. A horizontal bar showing the physical size is also show at the lower left corner of each scanned image.

Figure 29 demonstrates a differential phase scan on a piece of milled aluminum. The milled pattern shows up clearly in the image. As a direct comparison, Figure 30 is a optical microscopic image the same milled aluminum in approximately same magnification and same area.

Figures 31 and 32 are the scans performed on an integrated circuit. Figure 31 is a differential phase scan and Figure 32 is a optical microscopic image.

Figure 33 is a differential phase scan of a metal sample. The structure of the fiber in the sample is clearly displayed in the image. Figure 34 shows an optical microscopic image of this sample.

Figures 35 and 36 are the scanned amplitude and differential phase acoustic microscopic images for the composite sample #1 provided by NASA, Langley respectively. Comparing these two figures, the image quality improvement of the differential phase scan over the conventional amplitude scan is obvious. Figure 37 shows an optical microscopic image of the sample.

Figures 38 is a scanned image on the composite sample #2 provided by NASA, Langley. This is a combined scan. The top portion (area-1) is a differential phase scan result, with -10 dB gain adjustment for the band showing at the lower end of area-1. The center portion (area-2) is a amplitude scan, with refocussing performed at the lower end of area-2. The lower portion (area-3) is a differential amplitude scan. The structure is most clearly displayed using differential phase/amplitude scanning. Also notice that the gain and the focussing are different for the differential phase and differential amplitude scans in this image. Figure 39 shows an optical microscopic image of the sample.

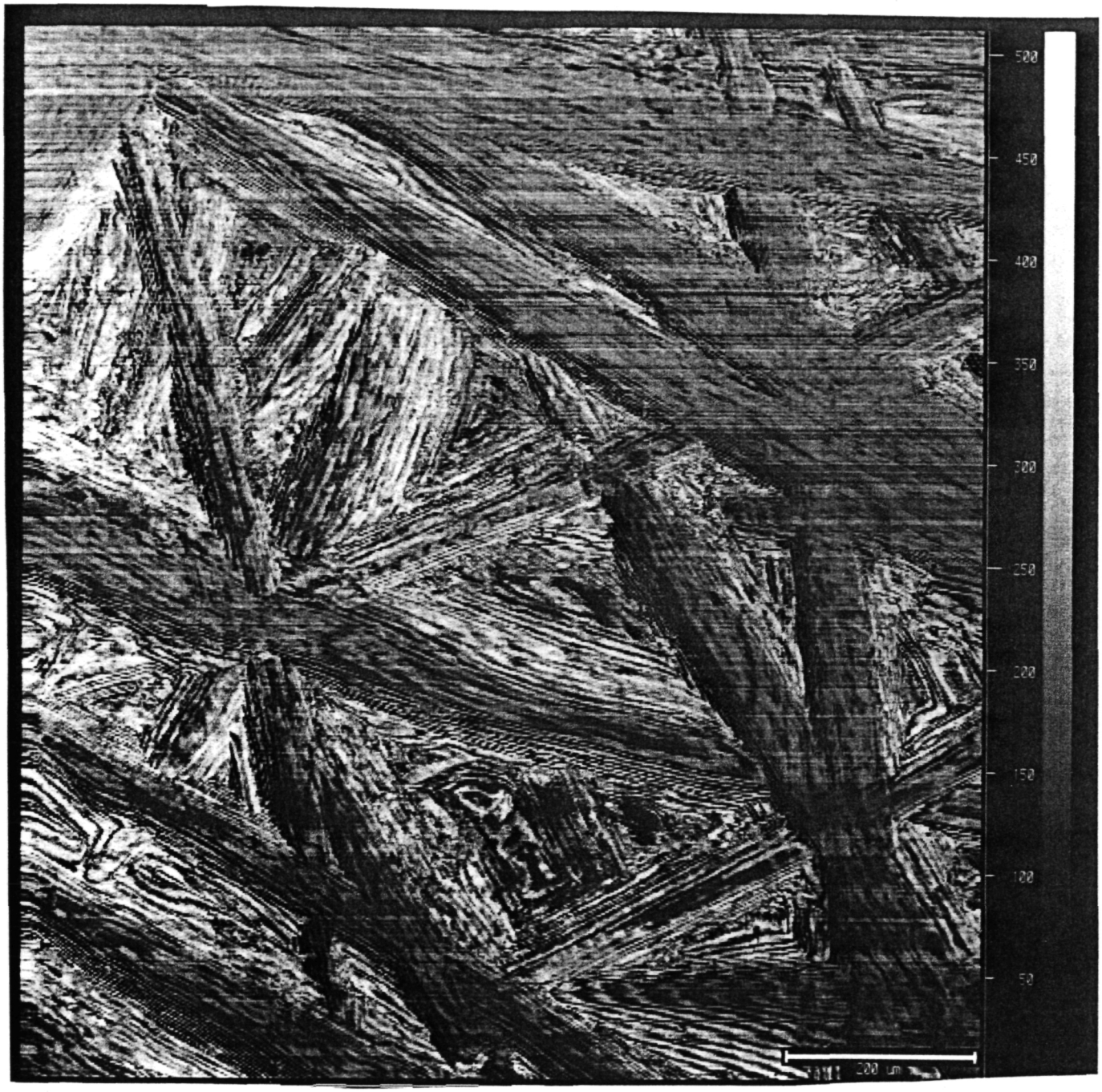

Figure 29. Differential phase acoustic microscopic image of the milled aluminum.

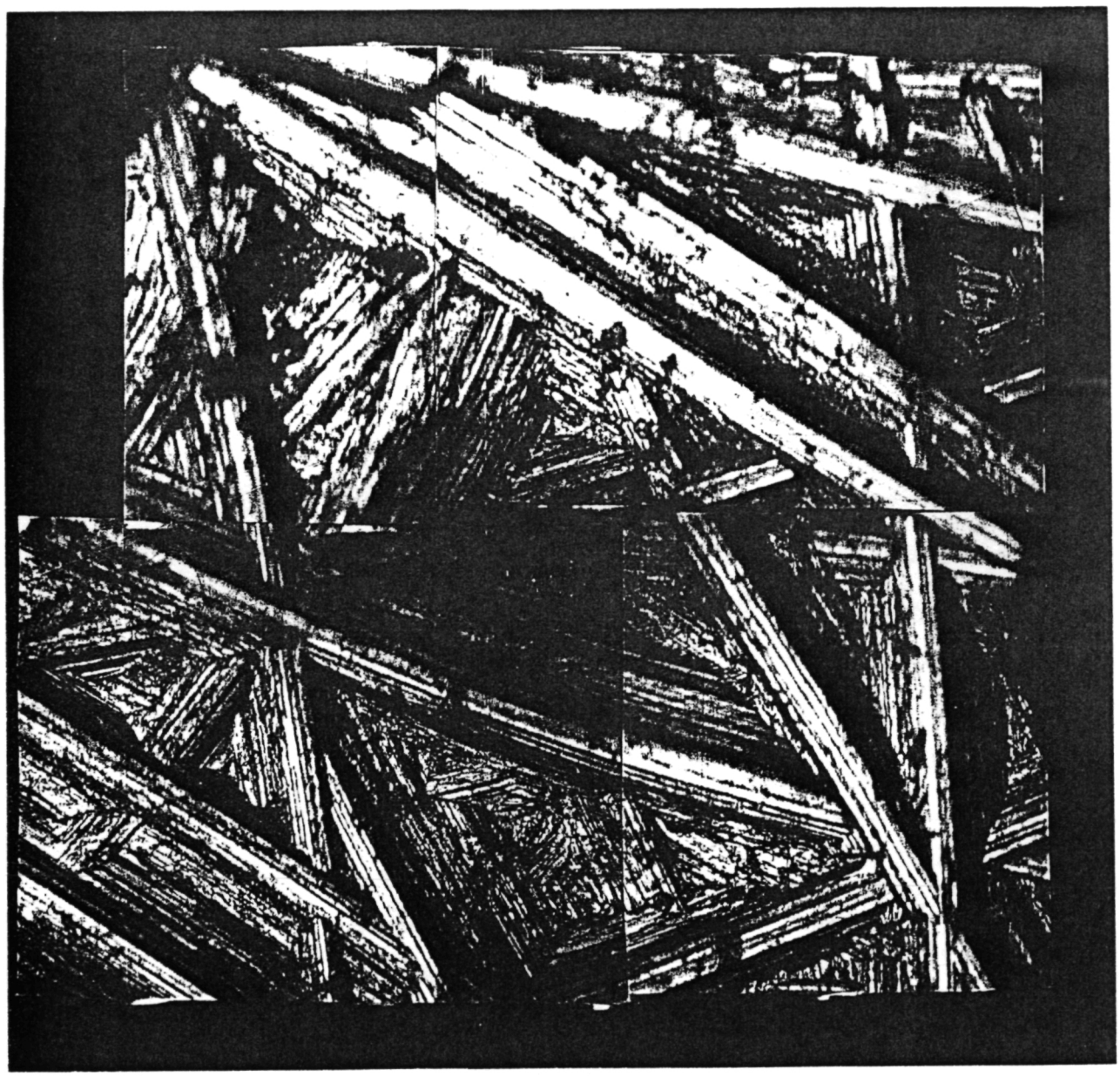

Figure 30. Optical microscopic image of the milled aluminum.

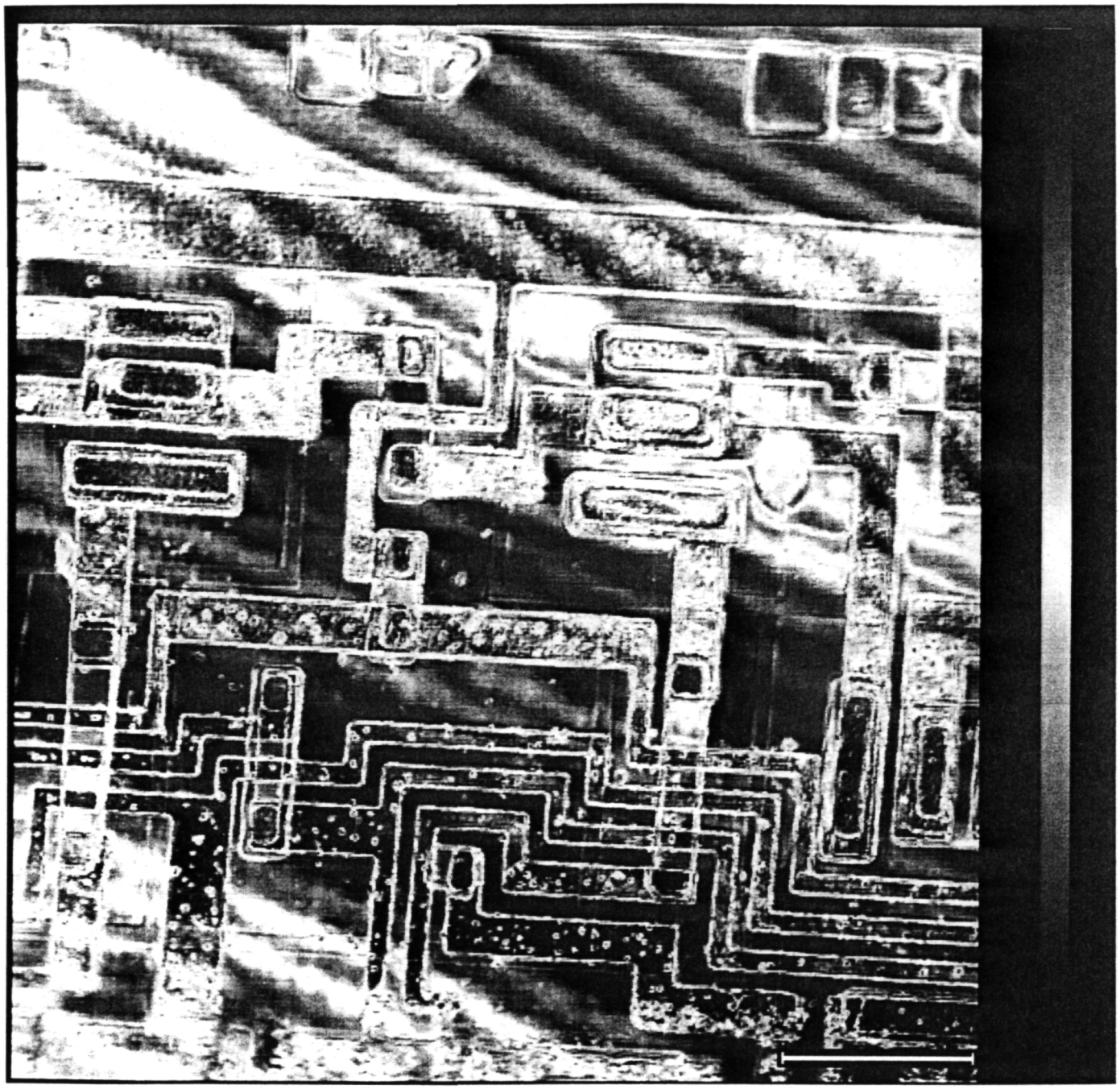

Figure 31. Differential phase acoustic microscopic image of an integrated circuit.

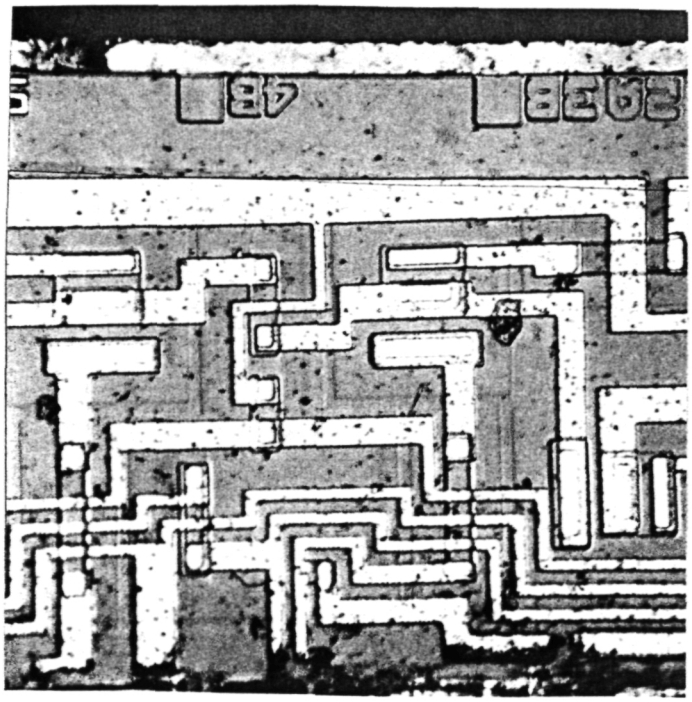

Figure 32. Optical microscopic image of an integrated circuit.

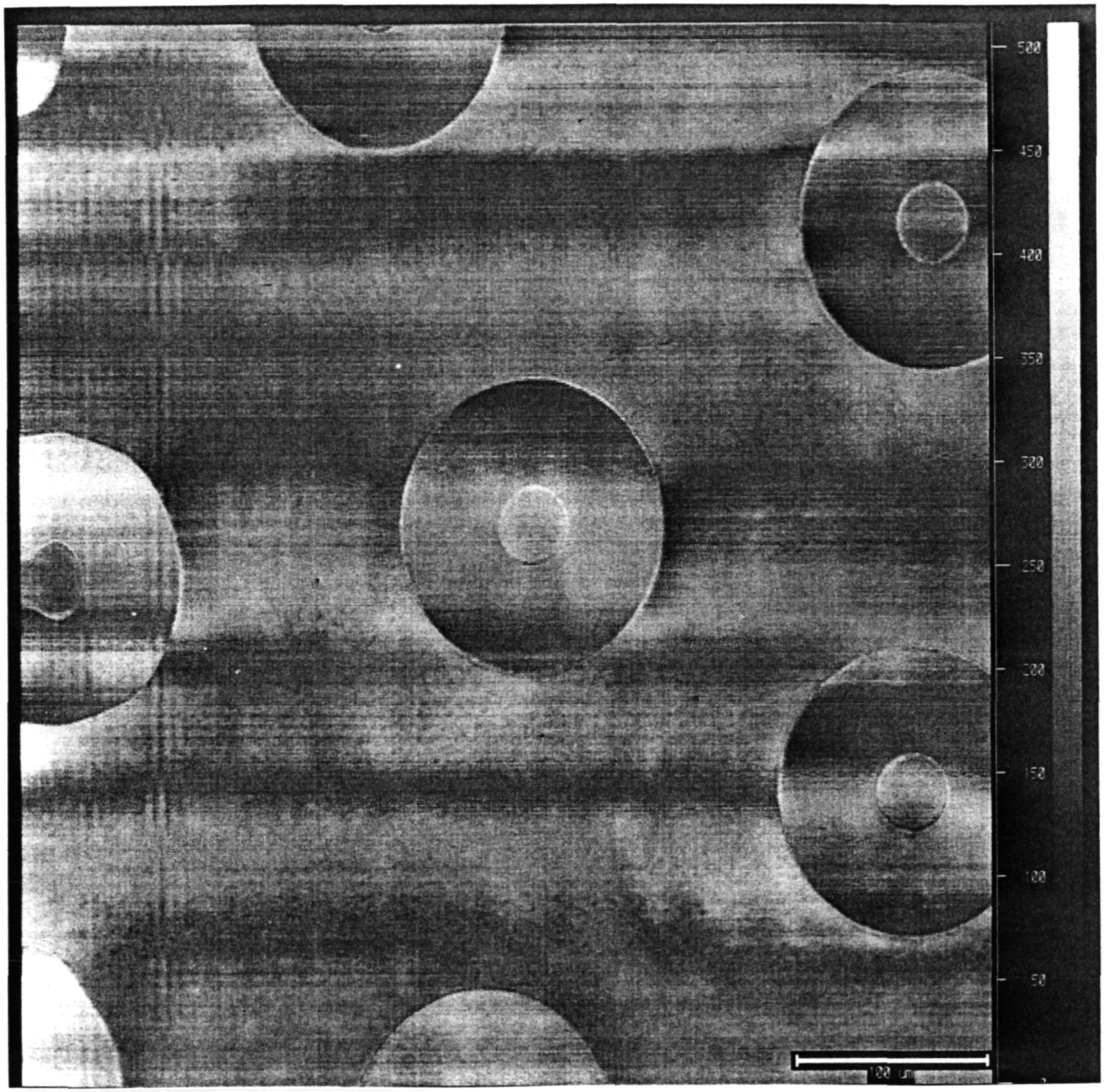

Sample courtesy NASA
Lewis Research Center

Figure 33. Differential phase acoustic microscopic image of the metal sample.

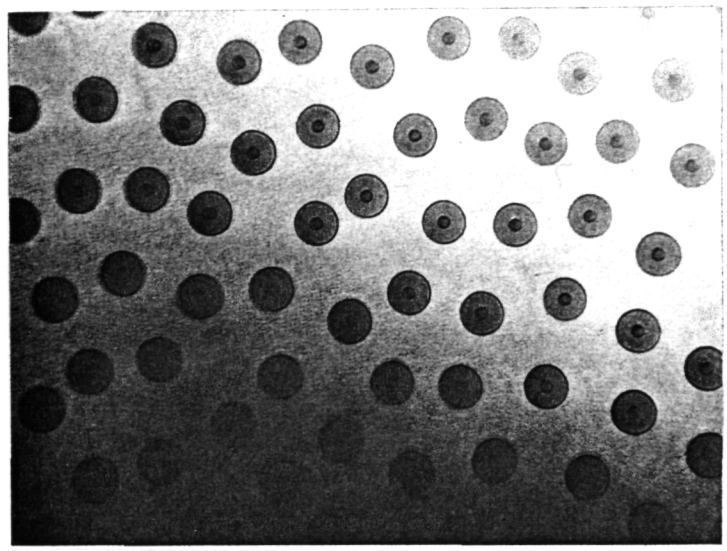

Sample courtesy NASA
Lewis Research Center

Figure 34. Optical microscopic image of the metal sample.

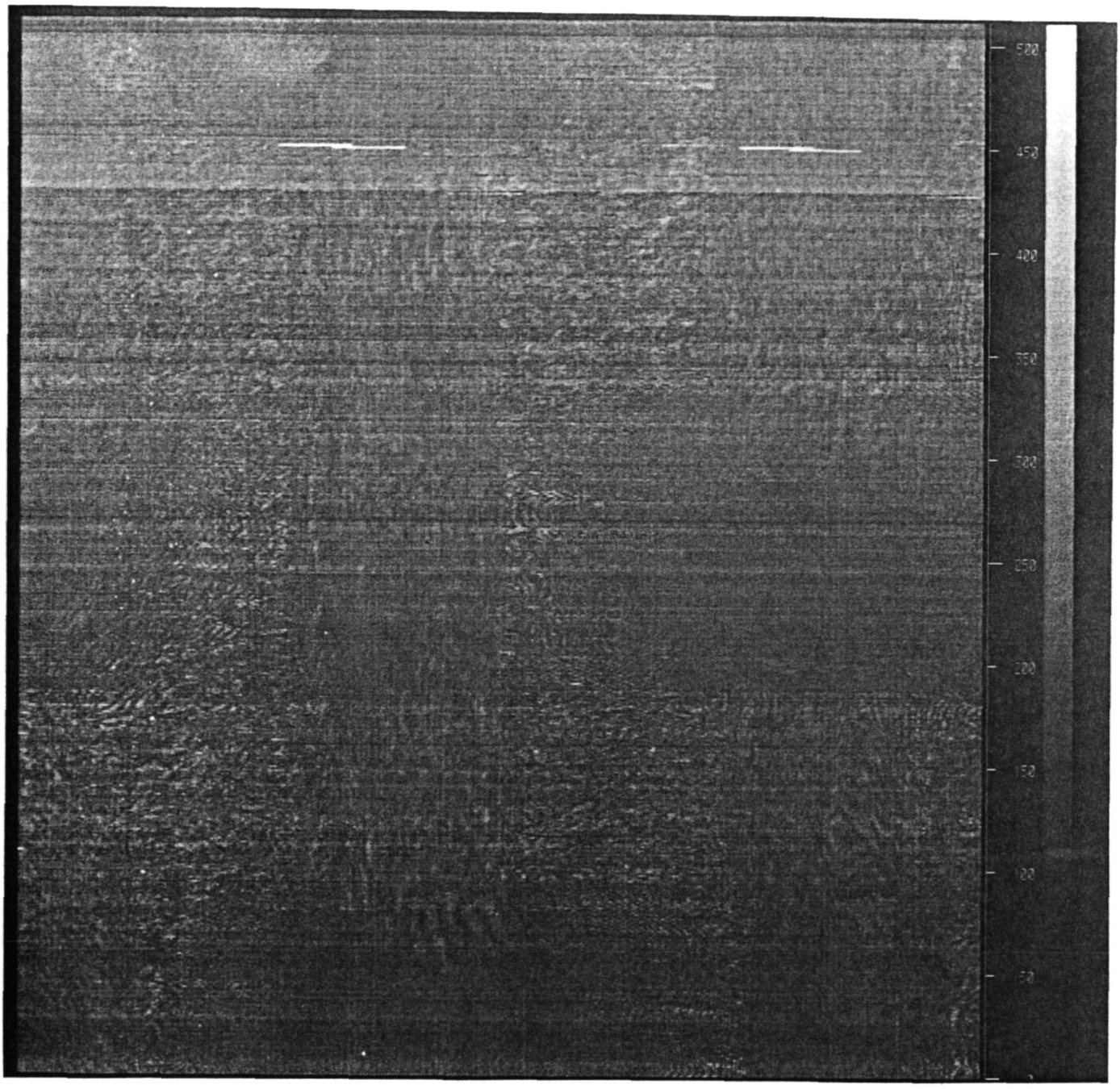

Figure 35. Amplitude acoustic microscopic image of composite #1.

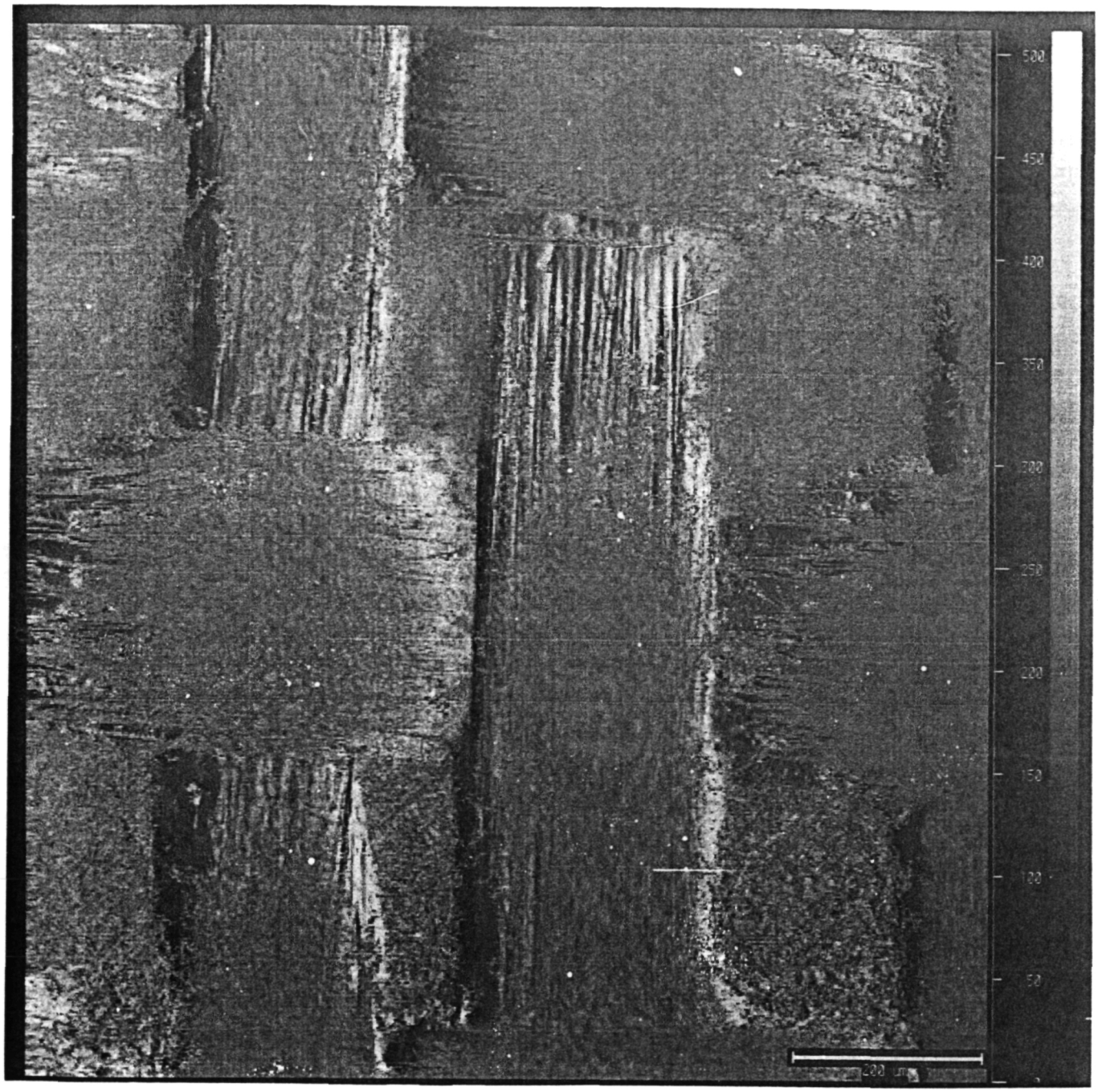

Figure 36. Differential phase acoustic microscopic image of composite #1.

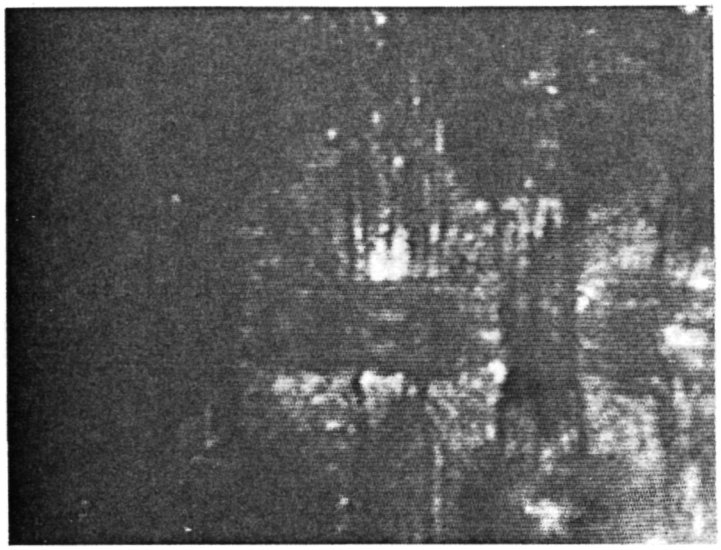

Figure 37. Optical microscopic image of composite #1.

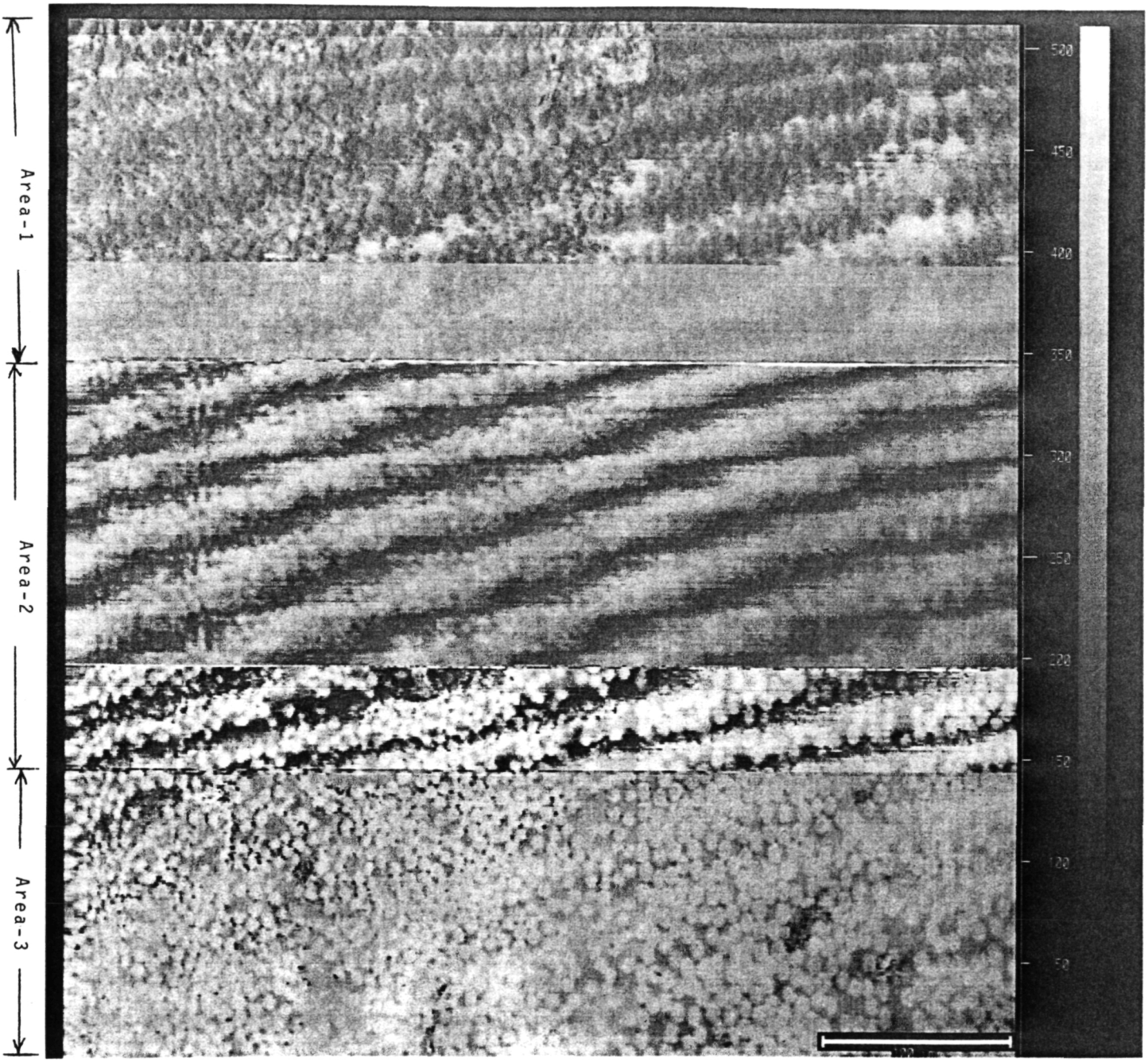

Figure 38. Combined scanning modes of acoustic microscopic image of composite #2.

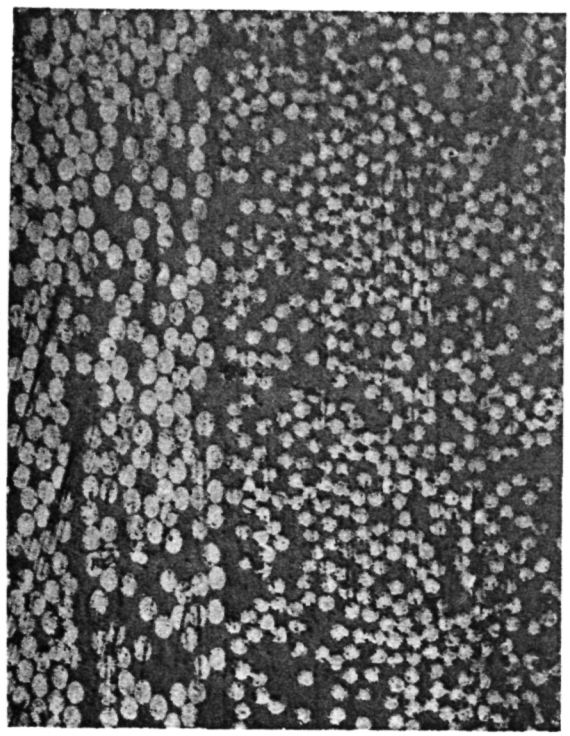

Figure 39. Optical microscopic image of composite #2.

4.7 V(z) and line scan

Tests of the line and V(z) scans had been performed on various samples. Figures 40 and 41 are example line scan and V(z) scan on the NASA composite samples #1 and #2. Figure 42 shows a conventional V(z) plots on the glass slide. As a direct comparison, the V(z) scan of the same material obtained using the 50 MHz system is shown in Figure 43. The spacing of peaks of the V(z) curves of the two plots indicates that the measurements of the acoustic signature of the same material at 1 GHz and at 50 MHz report the same results. Operating at high frequency of 1 GHz, this system provides a better spatial resolution than the 50 MHz system. With the two pulsers and four receiving modes, this system even provides more novel ways to obtain novel acoustic signature. For example, Figure 44 shows a pitch-catch V(z) plot where only one pulser and only the amplitude channel of the opposite receiver were turned on. Figure 45 shows other two novel V(z) plots displaying the differential phase and differential amplitude signal while the transducer was moving toward the sample. The differential phase V(z) plot shows twice frequency in voltage changes than that of a conventional V(z) scan. This will at least increase the accuracy of the measurement of the Rayleigh wave propagation speed using V(z) scan.

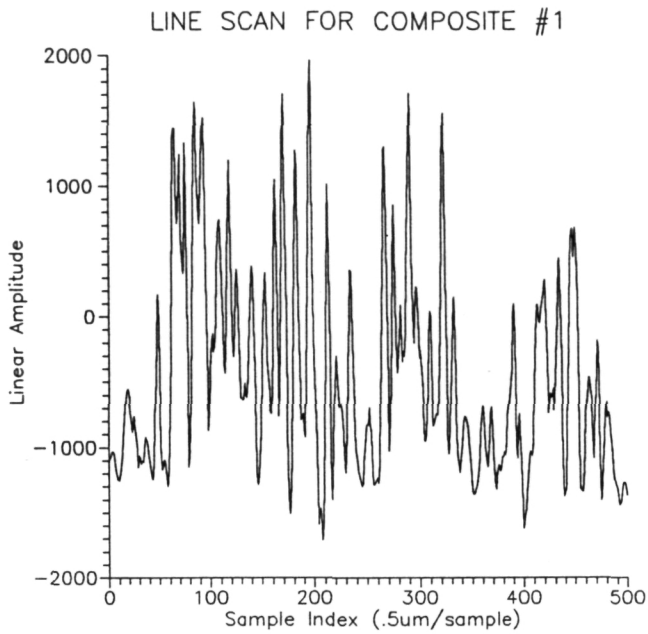

Figure 40. Conventional amplitude line scan plot of the composite #1.

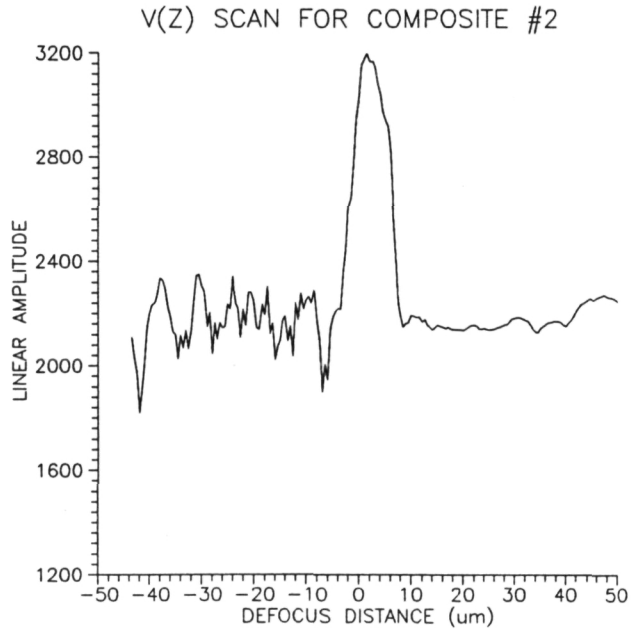

Figure 41. Conventional amplitude V(z) plot of the composite #2.

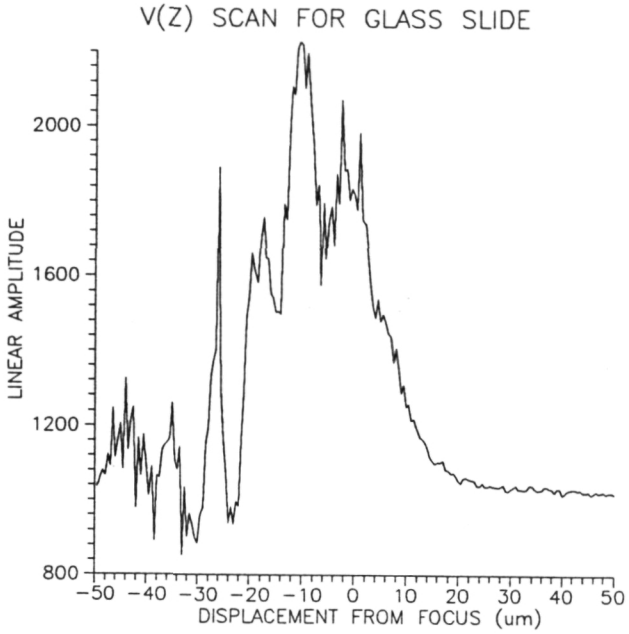

Figure 42. 1 GHz conventional V(z) plot of glass slide.

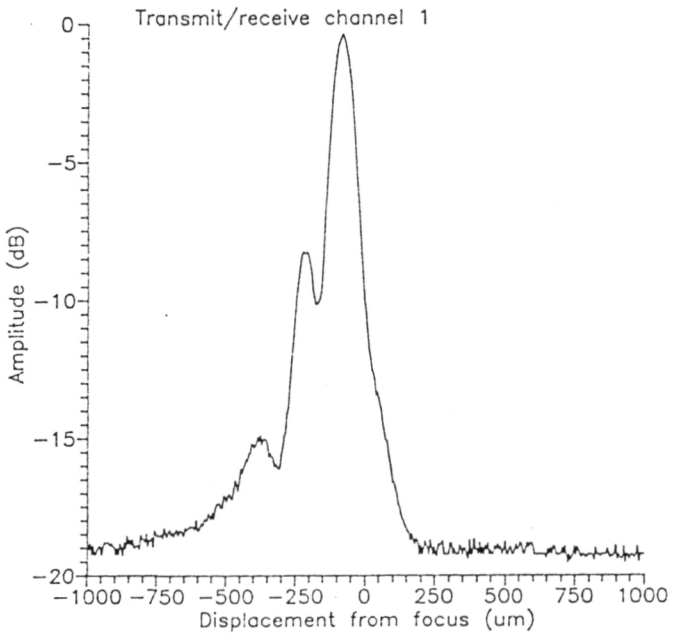

Figure 43. 50 MHz conventional V(z) plot of glass slide.

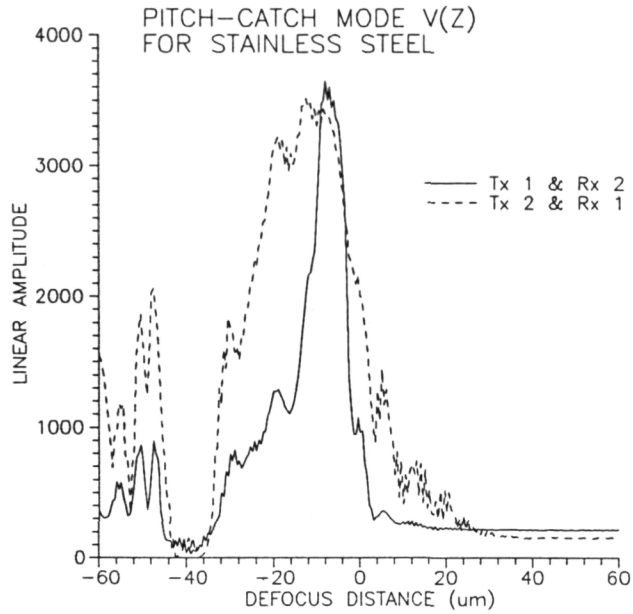

Figure 44. Novel V(z) plot of glass slide — pitch-catch mode.

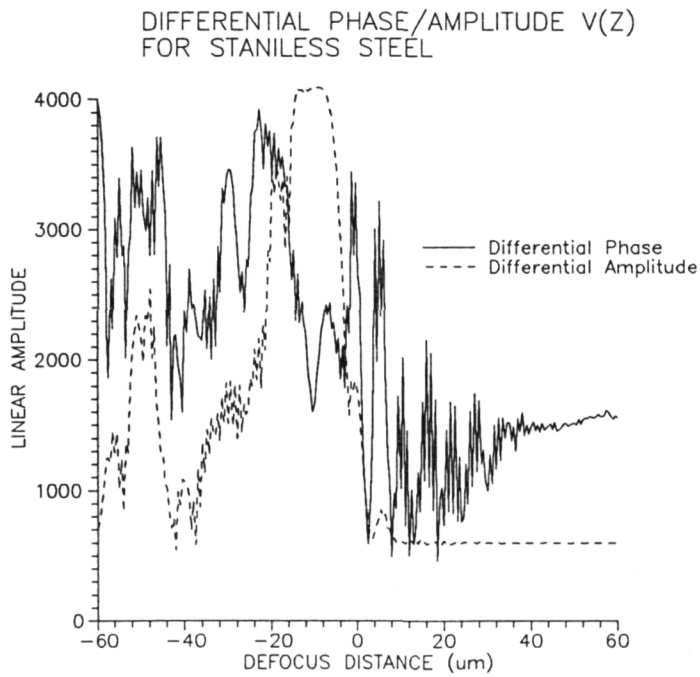

Figure 45. Novel V(z) plot of glass slide — differential phase/amplitude.

5. PRODUCT DEVELOPMENT

5.1 Objectives

Having delivered the microscope to NASA and effectively finished the Phase II contract it is believed that we have a product that can be further developed and subsequently market we have no intention of entering the competitive field of the acoustic microscope. We could not compete with other companies already established in the field.

It is, and always has been, our considered opinion that the device will be marketed as an *add-on* device which will be marketed as a feature capable of being added to an existing microscope. Our initial review indicated that this is practically possible and, if low cost, should be attractive to the current microscope manufacturers.

5.2 Third party interest

We had previously stated that we had had discussions with companies currently producing acoustic microscopes, namely:

1. Leitz (Wetzlar, Germany);
2. Sonoscan (Bensonville, Illinois);
3. Olympus of Japan (New Hyde Park, New York).

In all cases we are still progressing a relationship. Interest in the device as an *add-on* has been expresses by at least one of the parties. This is being pursued further, in parallel with the assessment and applications of the microscope by NASA.

REFERENCES

[1] Lemons, R.A. and C.F. Quate, *Applied Physics Letters*, 24, p.163, 1974.

[2] Quate, C.F., A. Atalar, and H.K. Wickramasinghe, "Acoustic Microscopy with Mechanical Scanning - A Review", *Proceedings of the IEEE*, 67, p. 1092, 1979.

[3] Nikoonahad, M:, "Recent Advanced in High Resolution Acoustic Microscopy", *Contemporary Physics*, 25, No. 2, p. 129, 1984.

[4] Nikoonahad, M., "Reflection Acoustic Microscopy for Industrial NDE", *Research Techniques for Nondestructive Testing* (R.S. Sharpe, ed.), Chapter 7, Vol 7, p. 217, 1984.

[5] Nikoonahad, M., "Differential Phase Contrast Acoustic Microscopy Using Tilted Transducers", *Electronics Letters*, 23, No. 10, p. 489, 1987.

[6] Nikoonahad, M., "New Techniques in Differential Phase Contrast Acoustic Microscopy Using Tilted Transducers", *Acoustical Imaging*, Vol 16, 1987.

[7] Nikoonahad, M., "Differential amplitude contrast in acoustic microscope", *Applied Physics Letters*, 51, No. 21, p. 1687, 1987.

[8] Nikoonahad, M. and E.A. Sivers, "Dual-beam differential amplitude contrast scanning acoustic microscopy", *Acoustical Imaging*, Vol 17, 1989.

[9] Wickramasinghe, H.K. and M. Hall, *Electronics Letters*, 12, p. 637, 1976.

[10] Souquet, J. and G.S. Kino, *Journal of Applied Physics*, 47, p. 5482, 1976.

[11] Kessler, L.W., P.R. Palermo, and A. Korpel, "Practical High Resolution Acoustic Microscopy", *Acoustic Holography*, Vol 5, p. 15, 1974.

[12] Ilic, D.B., G.S. Kino, and A.R. Selfridge, *Rev. Sci. Instrum.*, 50, p. 1527 , 1979.

[13] Ilic, D.B., G.S. Kino, A.R. Selfridge, and F.E. Stanke, in *Proceedings of the IEEE Ultrasonics Symposium,* 79CH1482-9SV, 1979.

[14] Nikoonahad, M., G.Q. Yue, and E.A. Ash, "Subsurface Broadband Acoustic Microscopy of Solids Using Reduced Aperture Lenses", in *Review of Progress in Quantitative NDE* (B.O. Thompson and D.E. Chimenti, eds.), Vol 2B, p. 1611 1982.

[15] Yue, G.Q., M. Nikoonahad, and E.A. Ash, *Proceedings of the IEEE Ultrasonics Symposium*, p. 93, 1982.

[16] Tjotta, J.N. and Tjotta, S., "An analytical model for the near field of a baffled piston transducer", *J. Acoust. Soc. Am.*, 68, 334-339, 1980.

APPENDICES — Schematics and Drawings

1.	2380-B001-EBD-1	Electronics Cabinet Detailed Block Diagram
2.	2380-A002-PIC	Klinger Mechanical Stages with Modular Support
3.	2380-A003-PIC	Klinger Mechanical Scanning Stages
4.	2380-A004-PPD	1 GHz Dual Beam Quartz Lens #1
5.	2380-A005-ASD	1 GHz Lens Holder
6.	2380-B008-ESD	Switch Drive Board
7.	2380-A009-FPD	Mount Arm
8.	2380-A010-EBD	General Block Diagram
9.	2380-A011-ESD	Pulser Chassis Wiring
10.	2380-A012-ESD	Splitter/Mixer Chassis
11.	2380-A013-TSP	General Timing Diagram
12.	2380-A014-ESD	X-scan Detector and Clock Trigger Switch
13.	2380-A015-ESD	Scanner Trigger and Clock Cabling
14.	2380-A016-ESD	Detector Chassis
15.	2380-A017-ESD	Rx gate Delay
16.	2380-A018-ESD	Sample/Hold & Video Amp A8
17.	2380-A019-ESD	Video Amp A5 & Filter F5
18.	2380-A020-SCF	Main Cabinet (Front Panel Layout)
19.	2380-A021-ESD	300 MHz Amps A6 & A7
20.	2380-A022-ESD	Power Supply Chassis
21.	2380-A023-ESD	Video Amp A9, & Filters F6 & F8
22.	2380-A024-ESD	Video Amp A10
23.	2380-A025-ESD	Transducer Matching Network

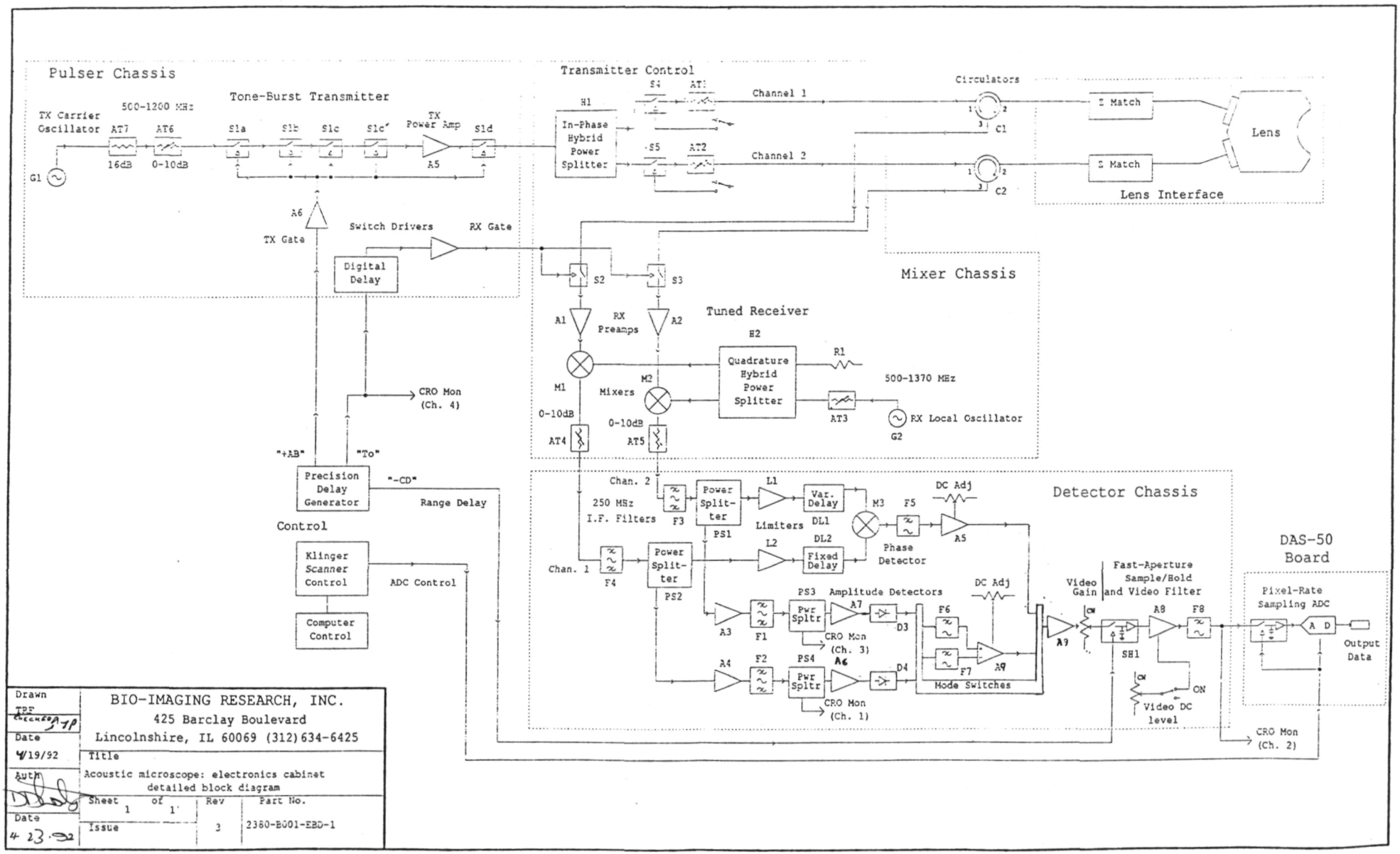

Drawn TRF	BIO-IMAGING RESEARCH, INC.		
Checked SAP	425 Barclay Boulevard		
Date 4/19/92	Lincolnshire, IL 60069 (312) 634-6425		
Auth	Title: Acoustic microscope: electronics cabinet detailed block diagram		
Date 4 23 92	Sheet 1 of 1	Rev 3	Part No. 2380-B001-EBD-1
	Issue		

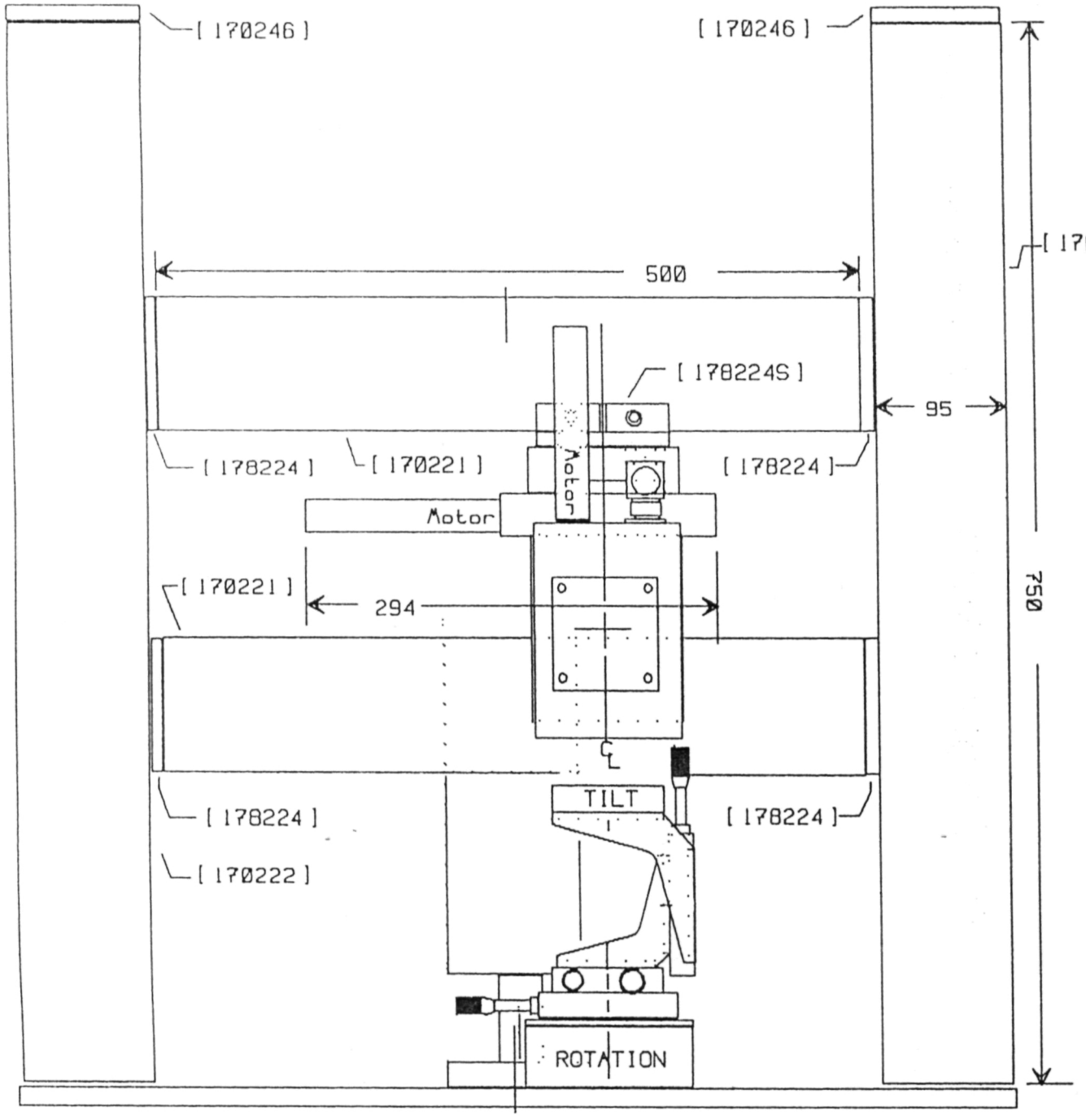

BIO-IMAGING RESEARCH, INC
425 BARCLAY BLVD.
LINCOLNSHIRE, IL
60069
PHONE 708/634-8425

NAME: KLINGER MECHANICAL SCANNING STAGES WITH MODULAR SUPPORTS.

DRAWING NUMBER 2380-A002-PIC	PAGE 1 OF 2
DATE: 23JULY90	BY: T Pusateri

Generic cadd file: IG-KMFV3

Dimensions in Millimters

CHECKED AUTH.

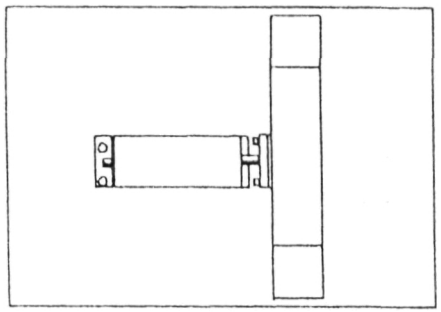

TOP VIEW
OF SUPPORTS

BIO-IMAGING RESEARCH, INC. 425 BARCLAY BLVD. LINCOLNSHIRE, IL 60069 PHONE 708/634-6425

NAME: KLINGER MECHANICAL SCANNING STAGES WITH MODULAR SUPPORTS.

DRAWING NUMBER: 2380-A002-PIC | PAGE 2 OF 2

DATE: 24JUL90 BY: T Puoteri

Generic cadd file: IG-KMSV3

Dimensions in Millimters

CHECKED AUTH

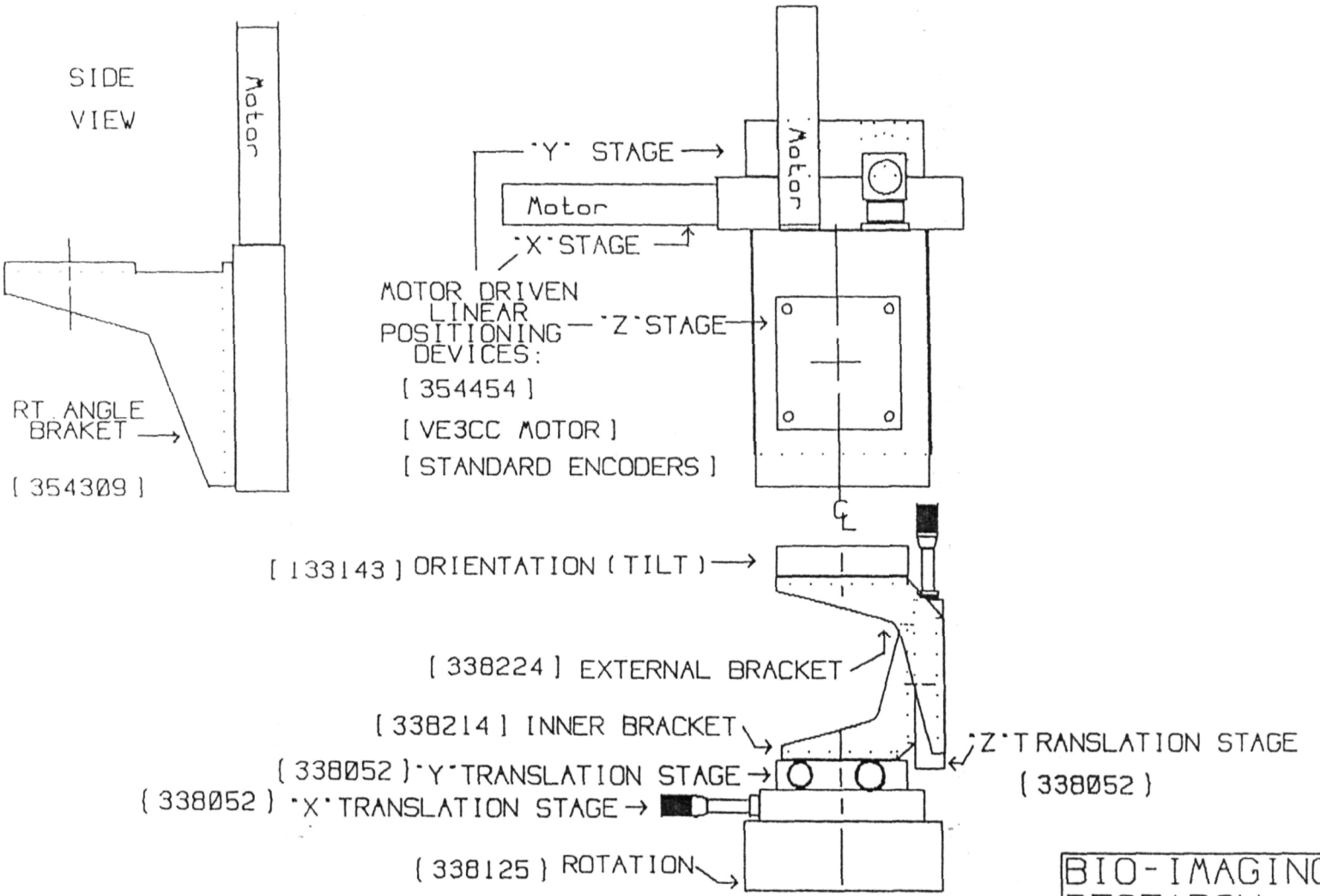

BIO-IMAGING RESEARCH, INC. 426 BARCLAY BLVD. LINCOLNSHIRE, IL 60069 PHONE 708/634-8425

NAME: KLINGER MECHANICAL SCANNING STAGES

DRAWING NUMBER: 2380-A003-PIC

DATE: 24JULY90 BY: T. PUSATERI

Generic cadd file: IG-MEC-4

CHECKED AUTH.

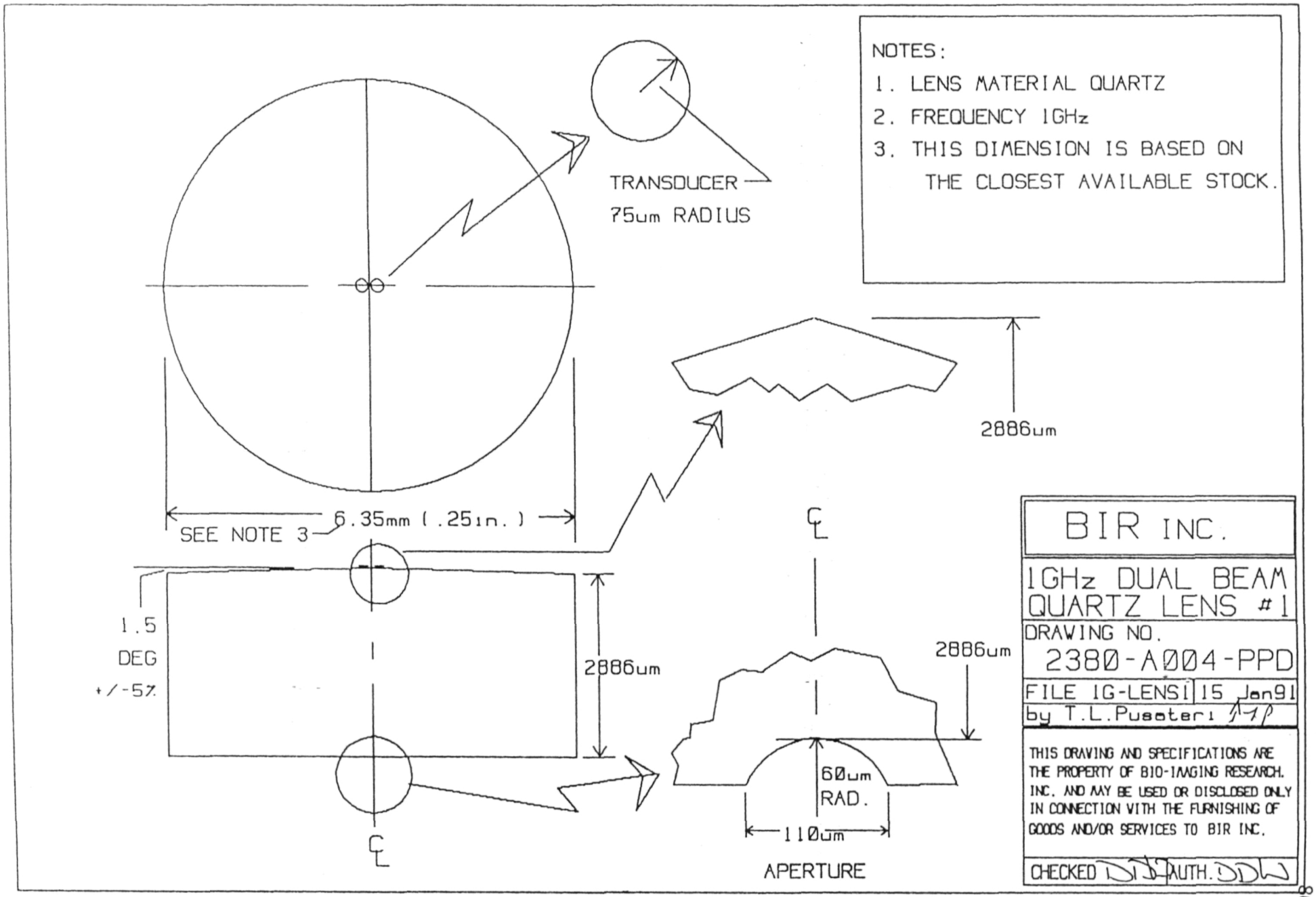
NOTES:
1. LENS MATERIAL QUARTZ
2. FREQUENCY 1GHz
3. THIS DIMENSION IS BASED ON THE CLOSEST AVAILABLE STOCK.
TRANSDUCER
75um RADIUS
2886um
6.35mm (.25in.)
SEE NOTE 3
1.5
DEG
+/-5%
2886um
2886um
60um
RAD.
110um
APERTURE
BIR INC.
1GHz DUAL BEAM
QUARTZ LENS #1
DRAWING NO.
2380-A004-PPD
FILE 1G-LENS1 15 Jan91
by T.L.Pusateri
THIS DRAWING AND SPECIFICATIONS ARE THE PROPERTY OF BIO-IMAGING RESEARCH, INC. AND MAY BE USED OR DISCLOSED ONLY IN CONNECTION WITH THE FURNISHING OF GOODS AND/OR SERVICES TO BIR INC.
CHECKED
AUTH.

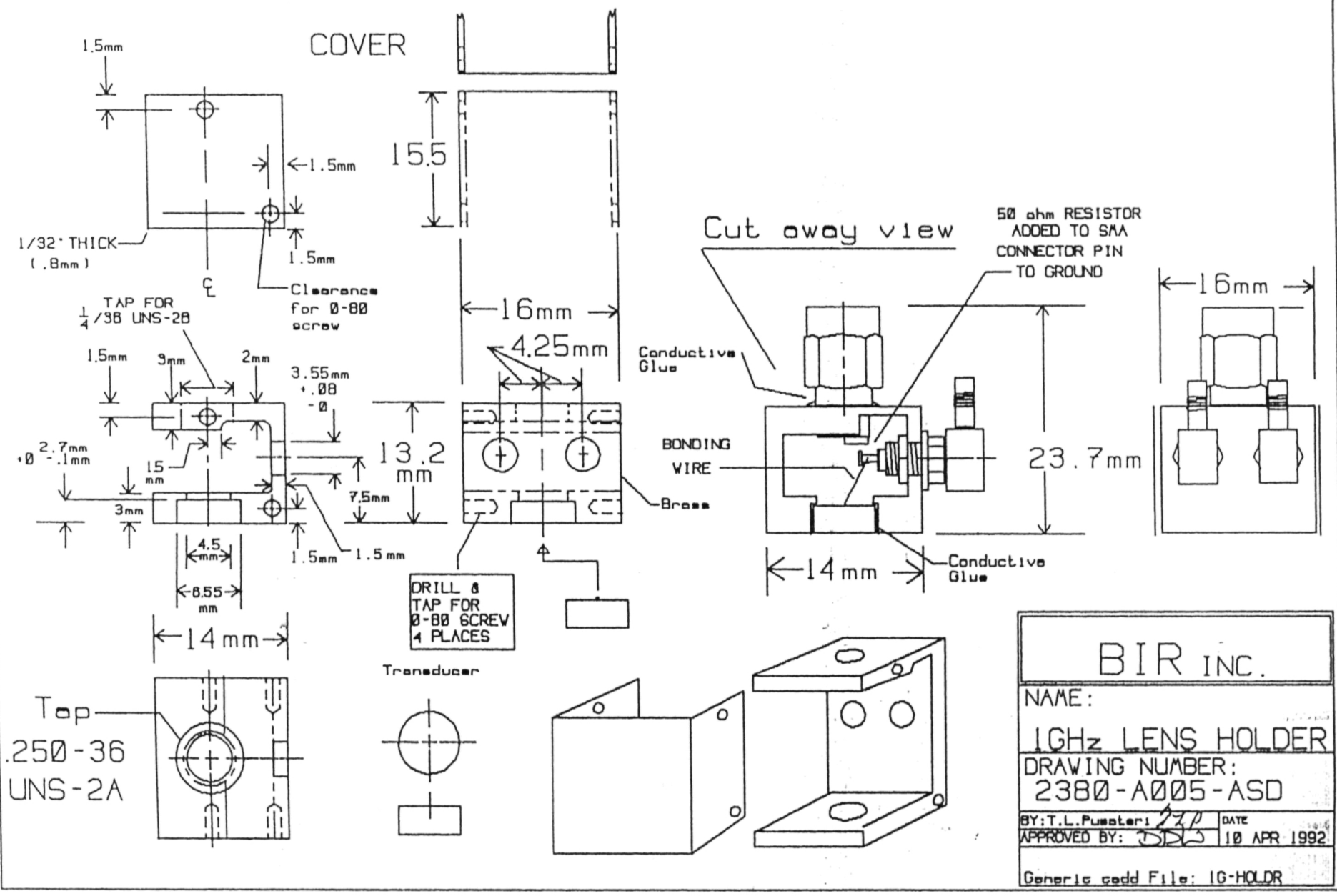
COVER
1.5mm
1.5mm
1.5mm
1/32" THICK
(.8mm)
Clearance
for 0-80
screw
15.5
16mm
4.25mm
TAP FOR
1/4/38 UNS-2B
1.5mm
3mm
2mm
3.55mm
+.08
-0
2.7mm
+0 -.1mm
1.5
mm
13.2
mm
7.5mm
3mm
4.5
mm
8.55
mm
1.5mm
1.5mm
14mm
DRILL &
TAP FOR
0-80 SCREW
4 PLACES
Transducer
Tap
.250-36
UNS-2A
Cut away view
50 ohm RESISTOR
ADDED TO SMA
CONNECTOR PIN
TO GROUND
Conductive
Glue
BONDING
WIRE
Brass
23.7mm
14mm
Conductive
Glue
16mm
BIR INC.
NAME:
1GHz LENS HOLDER
DRAWING NUMBER:
2380-A005-ASD
BY:T.L.Pusateri
APPROVED BY:
DATE
10 APR 1992
Generic cadd File: 1G-HOLDR

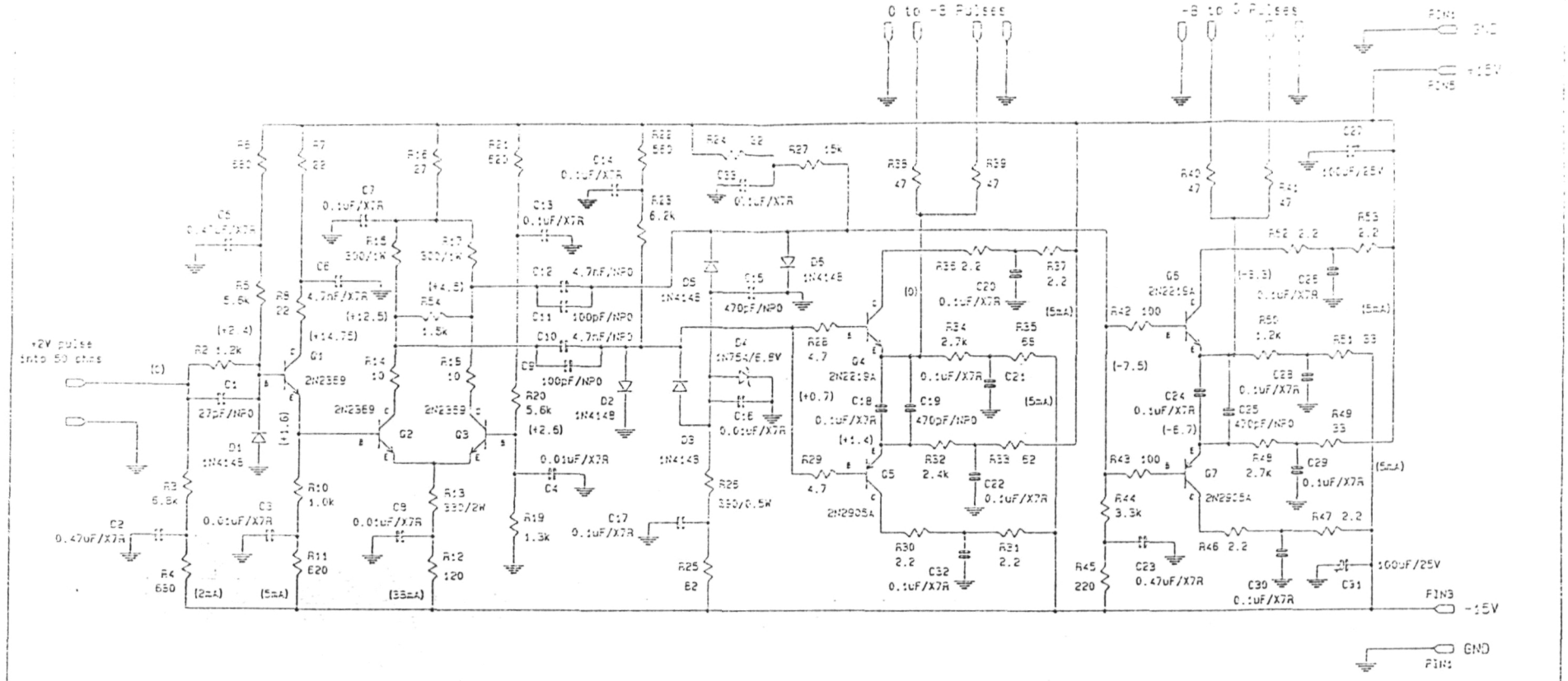

Drawn IRF	BIO-IMAGING RESEARCH, INC. 425 Barclay Boulevard Lincolnshire, IL 60069 (708)634-6425	
Date 5/23/91	Title Switch driver board	
Appr	Sheet 1 of 1	Rev
Date 4-23	Issue	Part No. 2390-8686-ESC

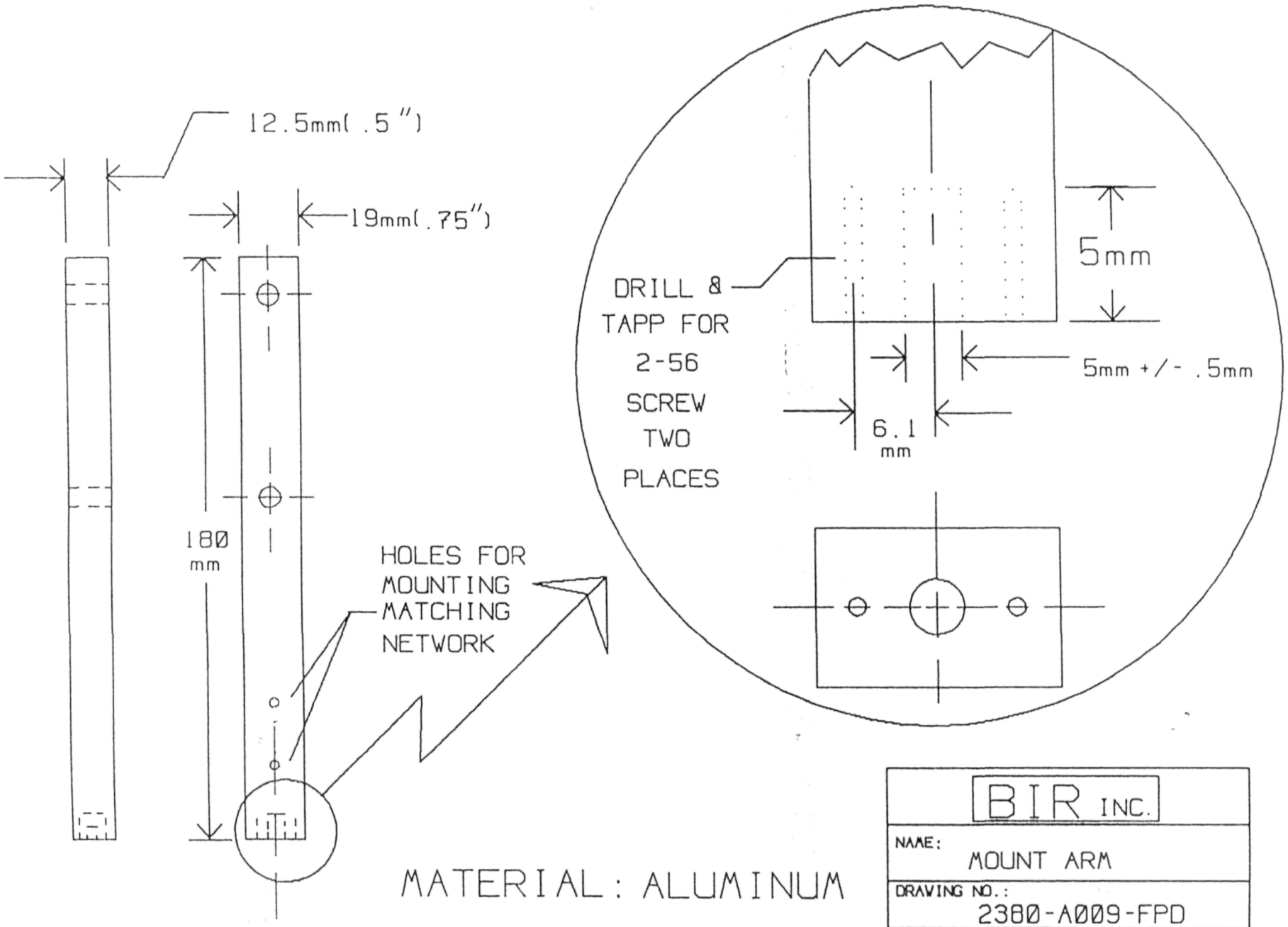

MATERIAL: ALUMINUM

BIR INC.	
NAME: MOUNT ARM	
DRAWING NO.: 2380-A009-FPD	
GENERIC CADD FILE: 1G-MOUNT	
BY : T.L.PUSATERI	DATE:
APPROVED:	8 APR 92

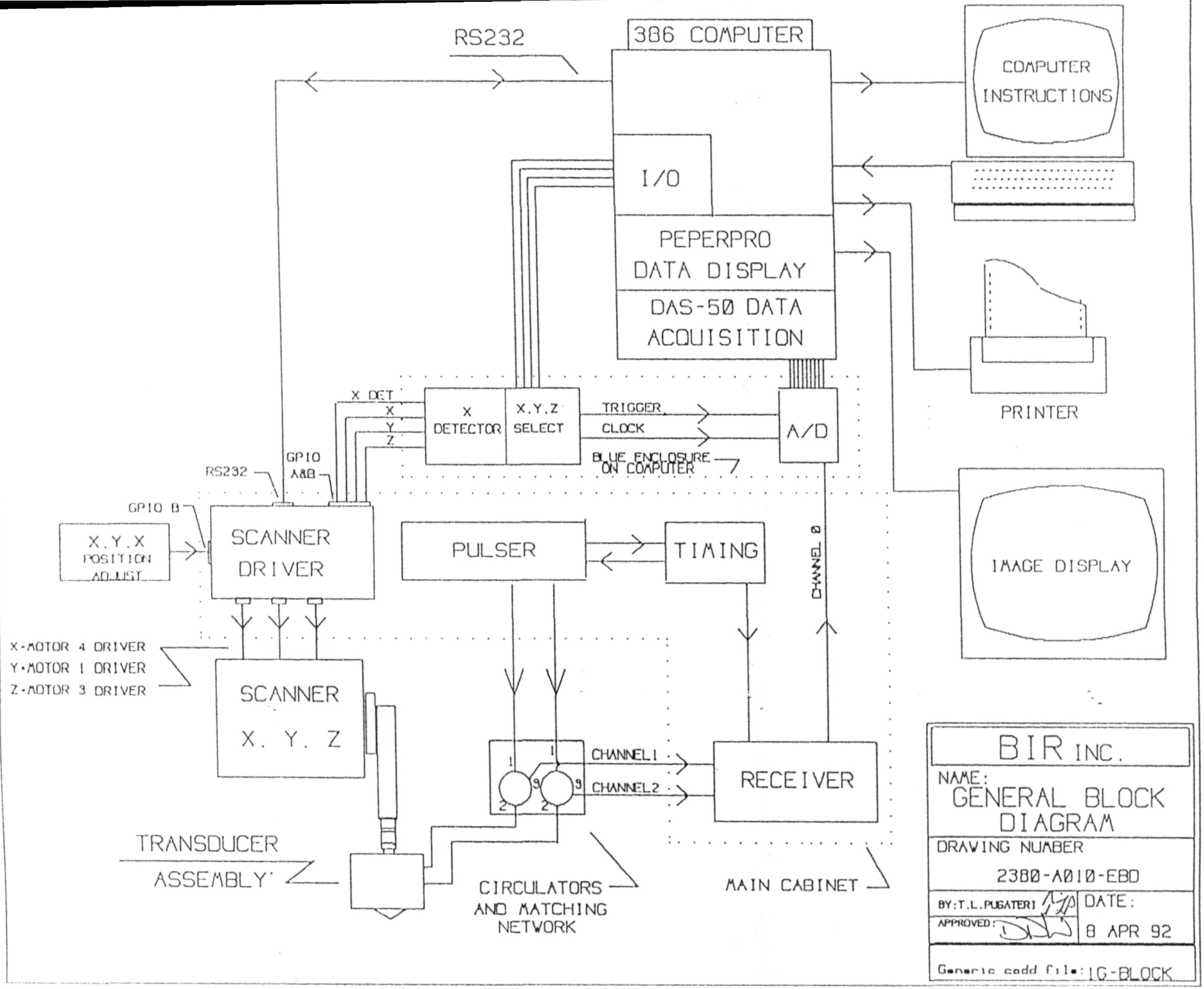
RS232
386 COMPUTER
COMPUTER INSTRUCTIONS
I/O
PEPERPRO DATA DISPLAY
DAS-50 DATA ACQUISITION
PRINTER
X DET
X
Y
Z
X DETECTOR
X.Y.Z SELECT
TRIGGER
CLOCK
A/D
BLUE ENCLOSURE ON COMPUTER
RS232
GPIO A&B
GPIO B
X.Y.X POSITION ADJUST
SCANNER DRIVER
PULSER
TIMING
CHANNEL 0
IMAGE DISPLAY
X-MOTOR 4 DRIVER
Y-MOTOR 1 DRIVER
Z-MOTOR 3 DRIVER
SCANNER X. Y. Z
CHANNEL1
CHANNEL2
RECEIVER
TRANSDUCER ASSEMBLY
CIRCULATORS AND MATCHING NETWORK
MAIN CABINET
BIR INC.
NAME:
GENERAL BLOCK DIAGRAM
DRAWING NUMBER
2380-A010-EB0
BY:T.L.PUGATER1
DATE:
APPROVED:
8 APR 92
Generic cadd file: IG-BLOCK

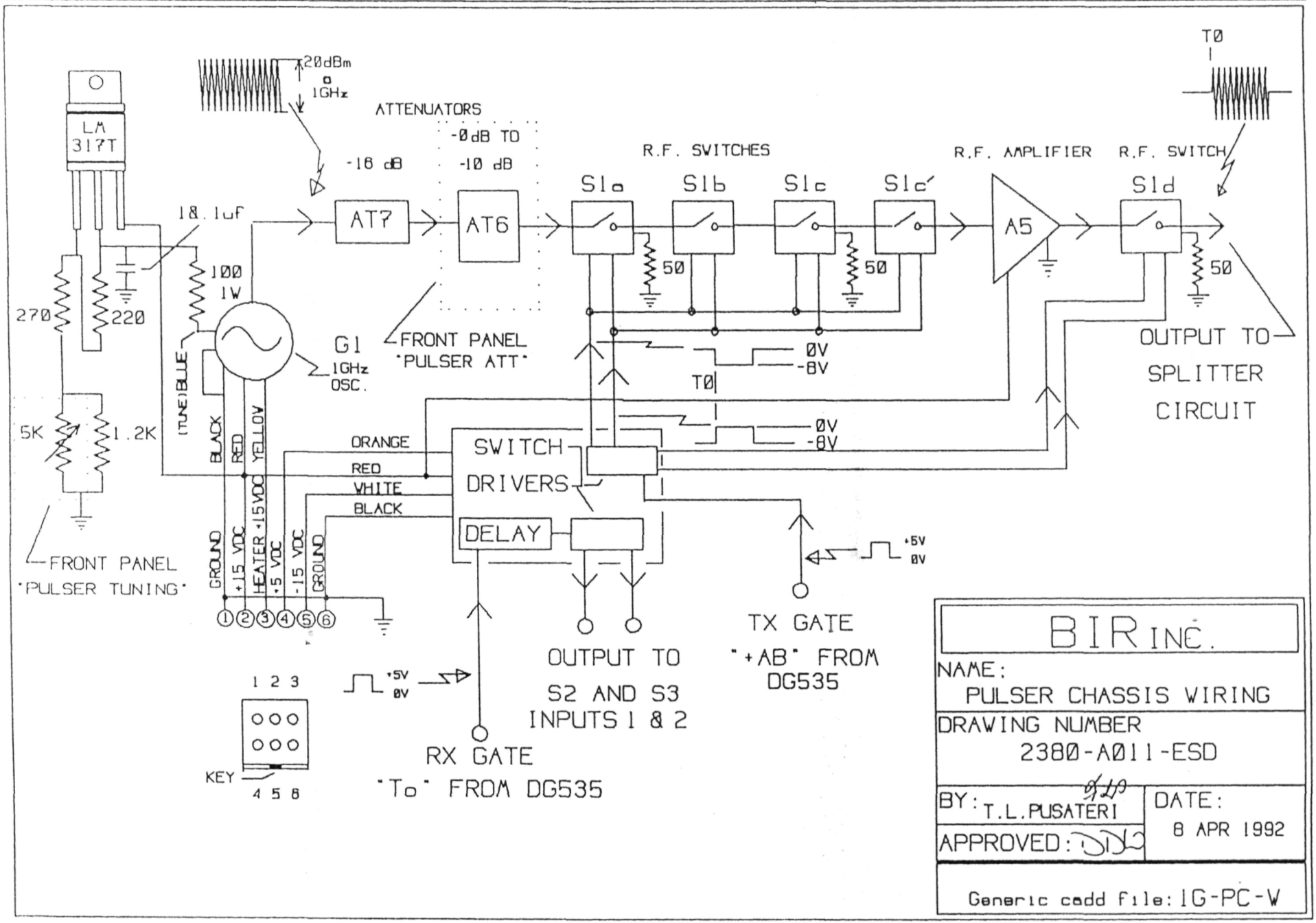
LM 317T
20dBm @ 1GHz
ATTENUATORS
-0dB TO -10 dB
-16 dB
AT7
AT6
R.F. SWITCHES
S1a
S1b
S1c
S1c'
R.F. AMPLIFIER
A5
R.F. SWITCH
S1d
T0
18.1uF
100 1W
270
220
5K
1.2K
G1
1GHz OSC.
FRONT PANEL "PULSER ATT"
FRONT PANEL "PULSER TUNING"
50
0V
-8V
OUTPUT TO SPLITTER CIRCUIT
SWITCH DRIVERS
DELAY
ORANGE
RED
WHITE
BLACK
BLUE (TUNE)
BLACK
RED
YELLOW
GROUND
+15 VDC
HEATER +15VDC
+5 VDC
-15 VDC
GROUND
1 2 3 4 5 6
KEY
4 5 6
+5V
0V
RX GATE "To" FROM DG535
OUTPUT TO S2 AND S3 INPUTS 1 & 2
TX GATE "+AB" FROM DG535
BIR INC.
NAME: PULSER CHASSIS WIRING
DRAWING NUMBER 2380-A011-ESD
BY: T.L.PUSATERI
DATE: 8 APR 1992
APPROVED:
Generic cadd file: 1G-PC-W

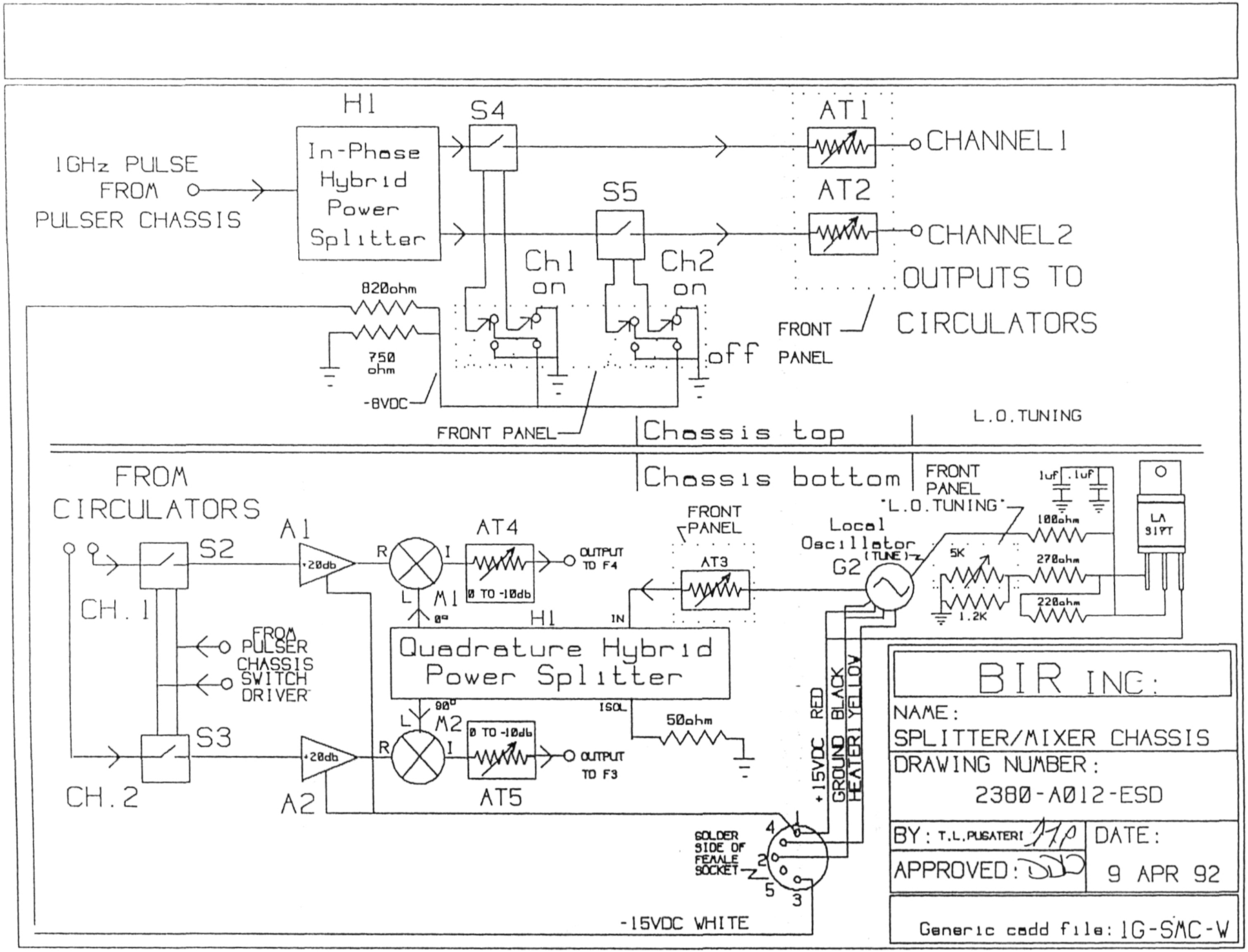
H1
S4
AT1
1GHz PULSE FROM PULSER CHASSIS
In-Phase Hybrid Power Splitter
CHANNEL 1
S5
AT2
CHANNEL 2
Ch1 on
Ch2 on
OUTPUTS TO CIRCULATORS
820ohm
750 ohm
-8VDC
off
FRONT PANEL
FRONT PANEL
Chassis top
L.O.TUNING
Chassis bottom
FROM CIRCULATORS
A1
S2
AT4
FRONT PANEL
AT3
Local Oscillator
G2
(TUNE)
FRONT PANEL
"L.O.TUNING"
1uf
.1uF
100ohm
5K
270ohm
220ohm
1.2K
LA 3197
+20db
R
I
L
M1
0°
0 TO -10db
OUTPUT TO F4
H1
IN
CH.1
FROM PULSER CHASSIS SWITCH DRIVER
Quadrature Hybrid Power Splitter
90°
M2
ISOL
50ohm
S3
CH.2
A2
AT5
OUTPUT TO F3
+15VDC RED
GROUND BLACK
HEATER YELLOW
SOLDER SIDE OF FEMALE SOCKET
-15VDC WHITE
BIR INC.
NAME:
SPLITTER/MIXER CHASSIS
DRAWING NUMBER:
2380-A012-ESD
BY: T.L.PUSATERI
DATE:
APPROVED:
9 APR 92
Generic cadd file: 1G-SMC-W

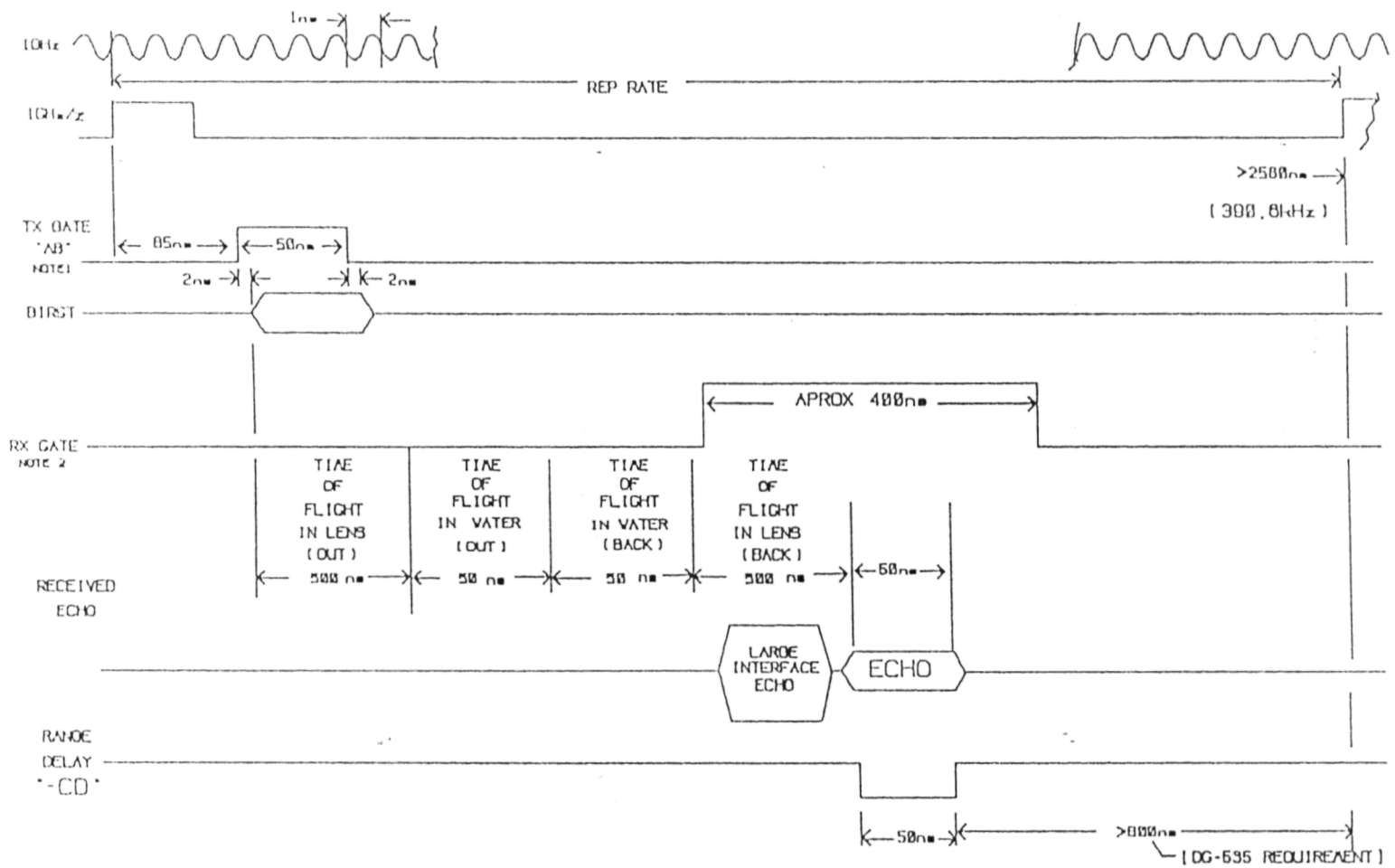

NOTE 1: RF SWITCHS S1A, S1B, S1C, S1C', AND S1D ARE SWITCHED ON.

NOTE 2: RF SWITCHS S2 AND S3 ARE SWITCHED ON.

BIR INC.	
NAME: 1GHz ULTRASOUND MICROSCOPE TIMING	
DRAWING NUMBER 2300-A013-TSP	
BY: T.L. PUSATERI	DATE:
APPROVED:	9 APR 92
Generic cadd file: 1G-TIME	

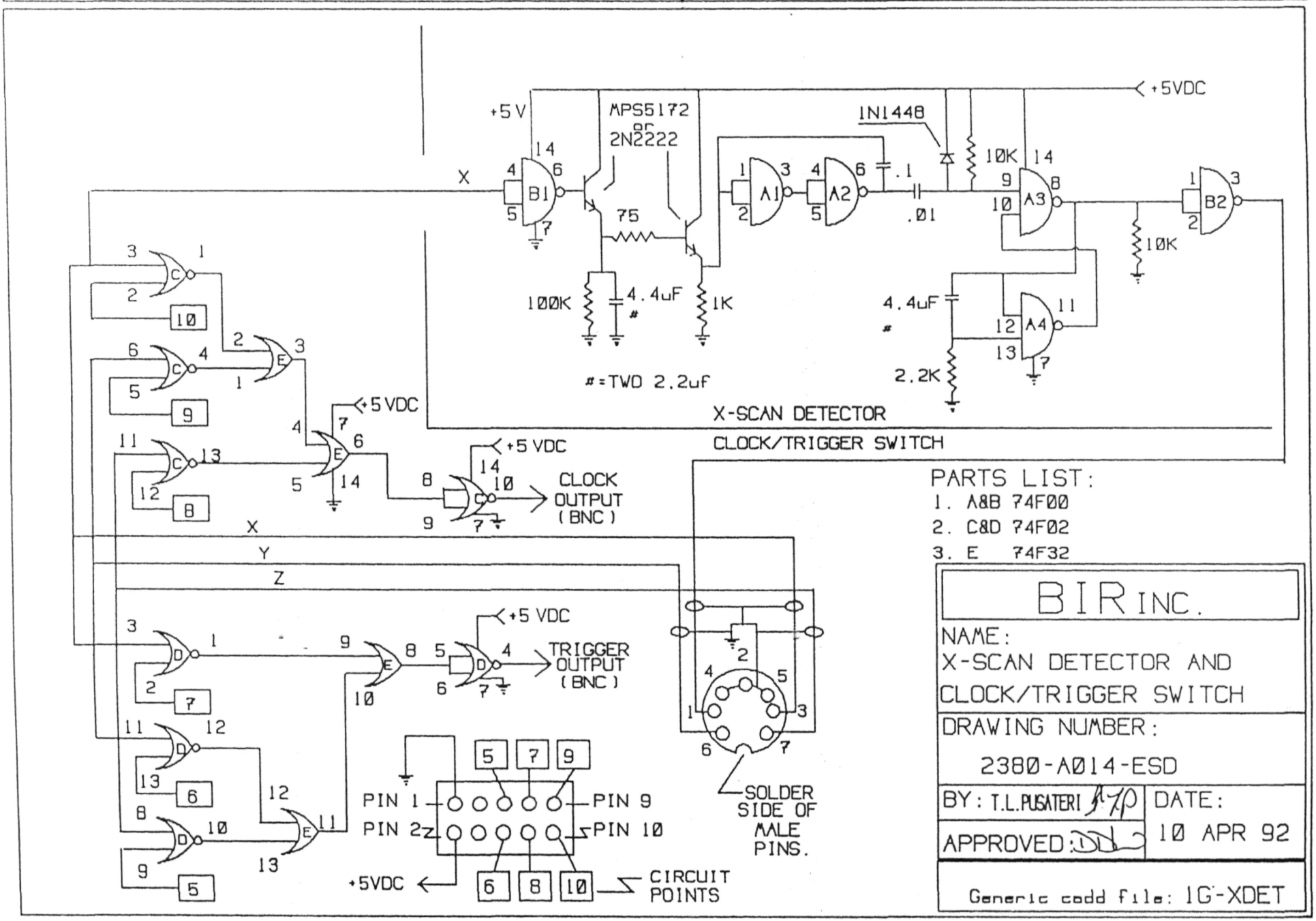
+5V
MPS5172
or
2N2222
+5VDC
1N1448
X
B1
A1
A2
.1
.01
10K
A3
B2
75
100K
4.4uF
#
1K
4.4uF
#
2.2K
A4
#=TWO 2.2uF
X-SCAN DETECTOR
CLOCK/TRIGGER SWITCH
+5 VDC
CLOCK
OUTPUT
(BNC)
X
Y
Z
TRIGGER
OUTPUT
(BNC)
PIN 1
PIN 2
PIN 9
PIN 10
+5VDC
CIRCUIT
POINTS
SOLDER
SIDE OF
MALE
PINS.
PARTS LIST:
1. A&B 74F00
2. C&D 74F02
3. E 74F32
BIR INC.
NAME:
X-SCAN DETECTOR AND
CLOCK/TRIGGER SWITCH
DRAWING NUMBER:
2380-A014-ESD
BY: T.L.PUSATERI
DATE:
APPROVED:
10 APR 92
Generic cadd file: 1G-XDET

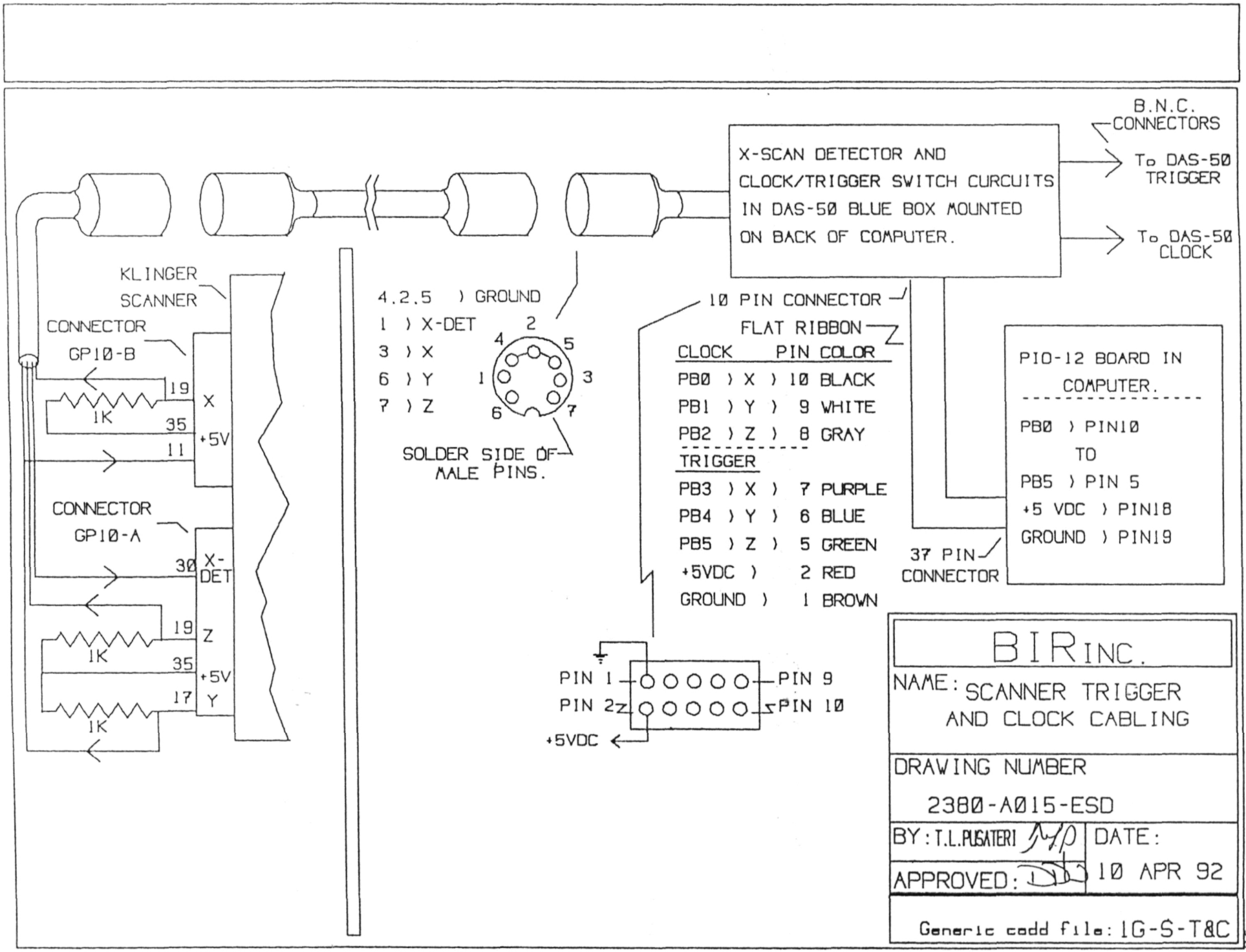
B.N.C.
CONNECTORS
X-SCAN DETECTOR AND
CLOCK/TRIGGER SWITCH CURCUITS
IN DAS-50 BLUE BOX MOUNTED
ON BACK OF COMPUTER.
To DAS-50
TRIGGER
To DAS-50
CLOCK
KLINGER
SCANNER
CONNECTOR
GP10-B
19
1K
35
11
X
+5V
CONNECTOR
GP10-A
30
X-
DET
19
1K
35
17
1K
Z
+5V
Y
4,2,5) GROUND
1) X-DET
3) X
6) Y
7) Z
SOLDER SIDE OF
MALE PINS.
10 PIN CONNECTOR
FLAT RIBBON
CLOCK PIN COLOR
PB0) X) 10 BLACK
PB1) Y) 9 WHITE
PB2) Z) 8 GRAY
TRIGGER
PB3) X) 7 PURPLE
PB4) Y) 6 BLUE
PB5) Z) 5 GREEN
+5VDC) 2 RED
GROUND) 1 BROWN
37 PIN
CONNECTOR
PIO-12 BOARD IN
COMPUTER.
PB0) PIN10
TO
PB5) PIN 5
+5 VDC) PIN18
GROUND) PIN19
PIN 1
PIN 2
PIN 9
PIN 10
+5VDC
BIR INC.
NAME: SCANNER TRIGGER
AND CLOCK CABLING
DRAWING NUMBER
2380-A015-ESD
BY: T.L.PUGATERI
DATE:
APPROVED:
10 APR 92
Generic cadd file: 1G-S-T&C

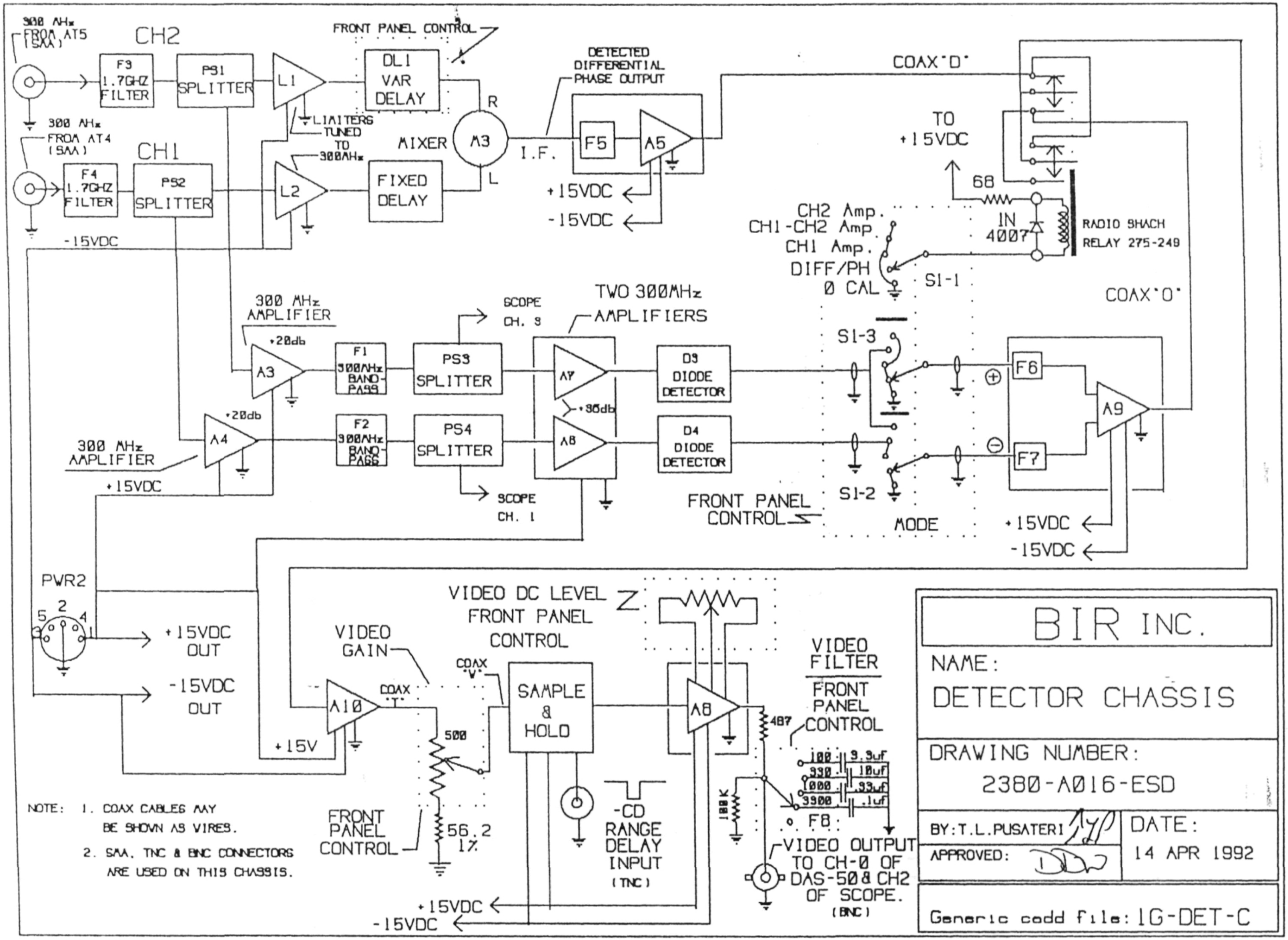
300 MHz FROM AT5 (SMA)
CH2
F3 1.7GHZ FILTER
PS1 SPLITTER
L1
FRONT PANEL CONTROL
DL1 VAR DELAY
DETECTED DIFFERENTIAL PHASE OUTPUT
COAX "D"
300 MHz FROM AT4 (SMA)
CH1
F4 1.7GHZ FILTER
PS2 SPLITTER
L2
LIMITERS TUNED TO 300MHz
MIXER
A3
R
L
FIXED DELAY
I.F.
F5
A5
+15VDC
-15VDC
TO +15VDC
68
IN 4007
RADIO SHACH RELAY 275-249
CH2 Amp.
CH1-CH2 Amp.
CH1 Amp.
DIFF/PH
Ø CAL
S1-1
COAX "O"
-15VDC
300 MHz AMPLIFIER
+20db
A3
F1 300MHz BAND-PASS
PS3 SPLITTER
SCOPE CH. 2
TWO 300MHz AMPLIFIERS
A7
+30db
D3 DIODE DETECTOR
S1-3
F6
A9
F7
A4
F2 300MHz BAND-PASS
PS4 SPLITTER
A8
D4 DIODE DETECTOR
S1-2
300 MHz AMPLIFIER
+15VDC
SCOPE CH. 1
FRONT PANEL CONTROL
MODE
+15VDC
-15VDC
PWR2
5 2 4 3 1
+15VDC OUT
-15VDC OUT
VIDEO DC LEVEL FRONT PANEL CONTROL
VIDEO GAIN
COAX "V"
COAX "T"
A10
+15V
500
SAMPLE & HOLD
A8
VIDEO FILTER
FRONT PANEL CONTROL
487
100 3.3uf
330 .1uf
1000 .33uf
3300 .1uf
F8:
VIDEO OUTPUT TO CH-0 OF DAS-50 & CH2 OF SCOPE. (BNC)
FRONT PANEL CONTROL
56.2 1%
-CD RANGE DELAY INPUT (TNC)
+15VDC
-15VDC
NOTE: 1. COAX CABLES MAY BE SHOWN AS WIRES.
2. SMA, TNC & BNC CONNECTORS ARE USED ON THIS CHASSIS.
BIR INC.
NAME:
DETECTOR CHASSIS
DRAWING NUMBER:
2380-A016-ESD
BY: T.L.PUSATERI
APPROVED:
DATE:
14 APR 1992
Generic cadd file: IG-DET-C

C-2.

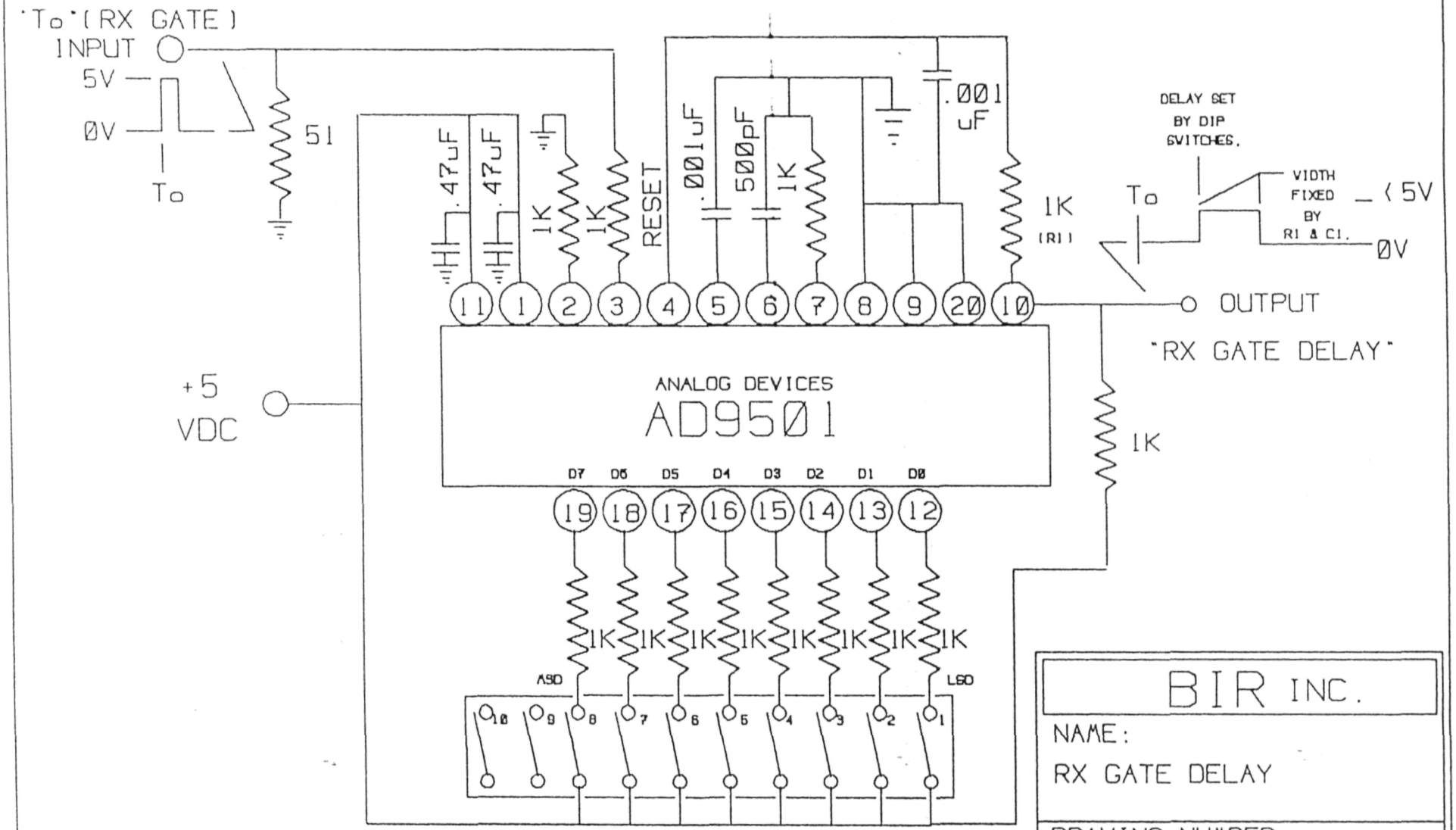

NOTES: 1. GATE DELAY CONTROLS SET AT BIR TO 1-2-3-4-7 ON.

2. THIS CIRCUIT IS LOCATED ON THE PULSER CHASSIS INSIDE THE CAST ALUMINUM BOX.

BIR INC.	
NAME: RX GATE DELAY	
DRAWING NUMBER 2380-A017-ESD	
BY: T.L.PUSATERI	DATE: 14 APR 92
APPROVED:	
Generic cadd file: 1G-DELAY	

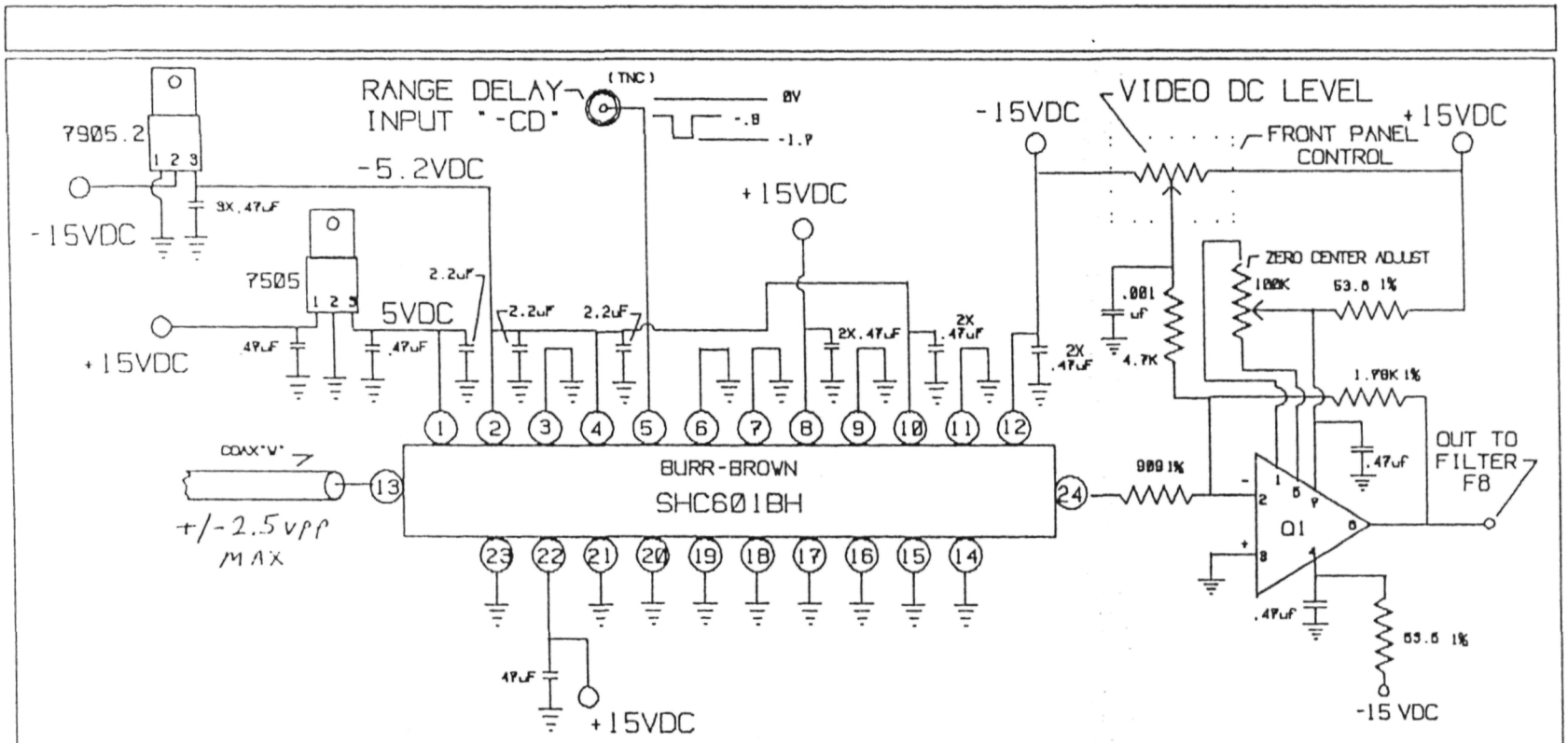

1. 1% RESISTERS ARE USED TO REDUCE NOISE.

2. Q1 PRECICION MONOLITHICS INC OP-15, PRECICION JFET-INPUT OPERATIONAL AMPLIFIER.

B.I.R. INC.	
NAME: SAMPLE/HOLD AND VIDEO AMP A8	
DRAWING NUMBER 2380-A18-ESD	
BY: T.L.PUSATERI	DATE:
APPROVED:	14 APR 92
Generic cadd file: 1G-S&H	

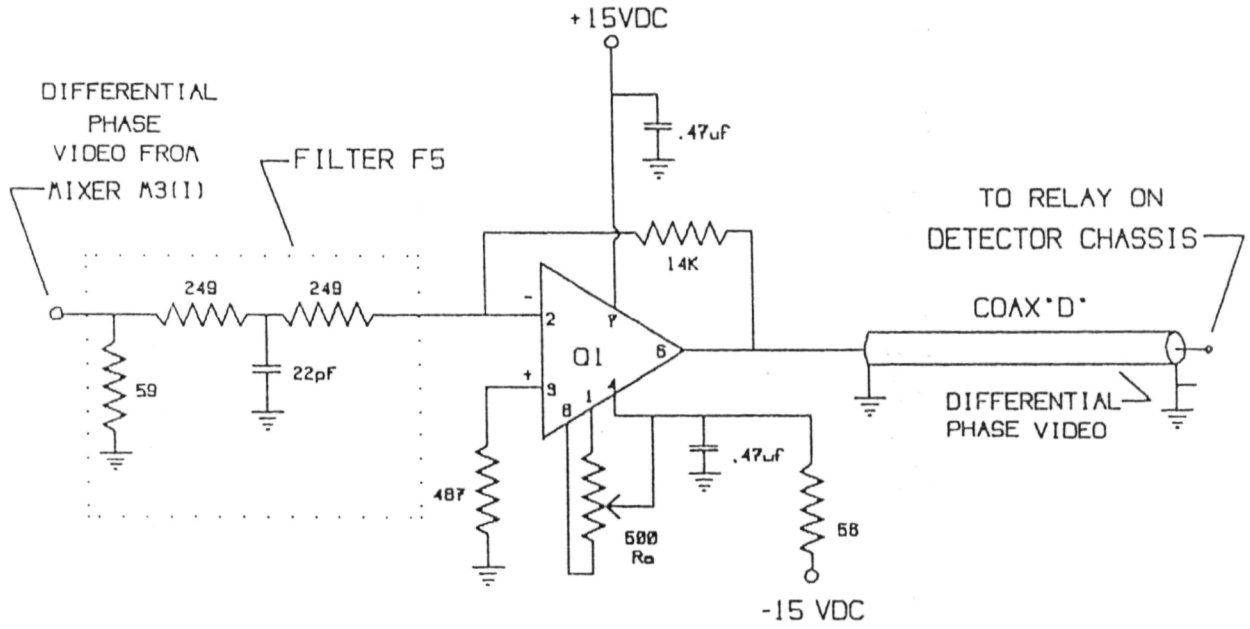

NOTES:

1. ALL RESISTORS EXECPT FOR Ra & Rb ARE 1% TO REDUCE NOISE.
2. Q1 IS ANALOG DEVICES AD849JN.

B.I.R. INC.	
NAME: VIDEO AMP A5 AND FILTER F5	
DRAWING NUMBER 2380-A019-ESD	
BY: T.L.PUSATERI	DATE: 14 APR 92
APPROVED:	
Generic cadd file: 1G-VAMP1	

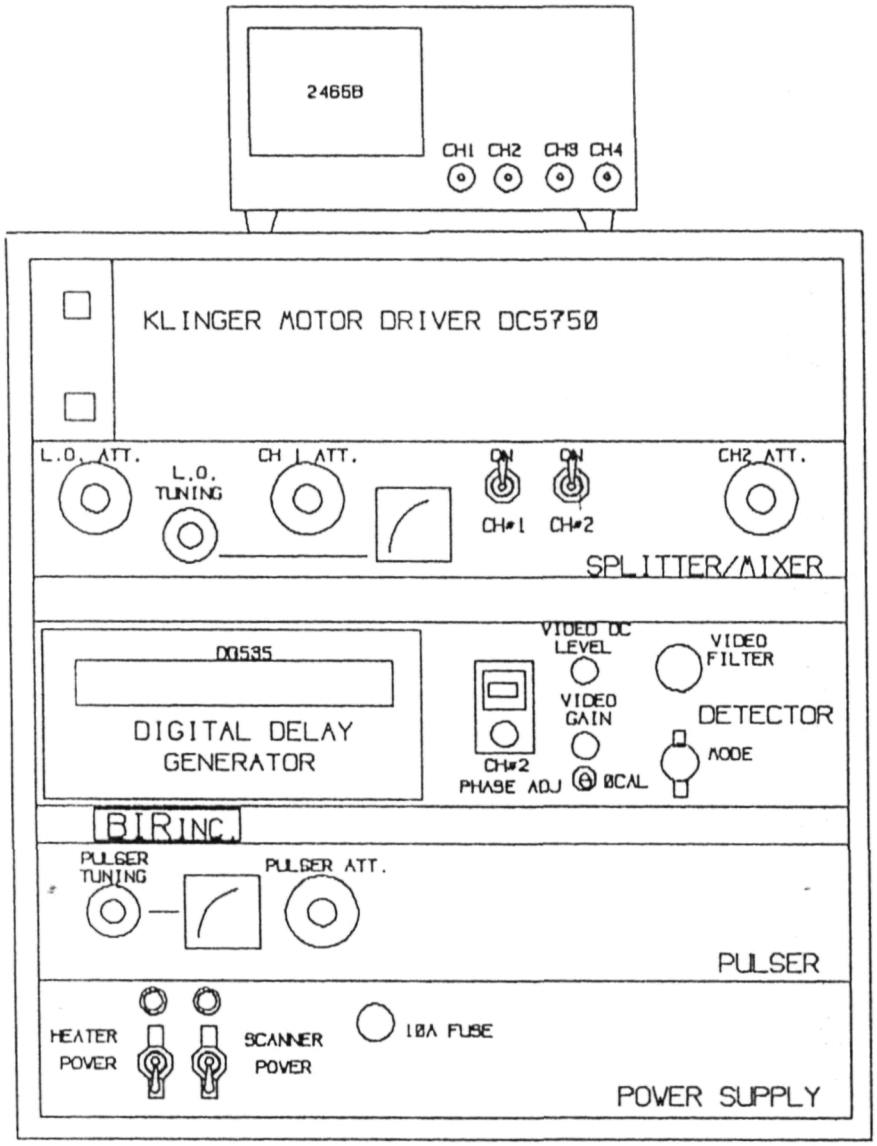

OSCILLOSCOPE INPUTS
(CRO-Mon)

CH1) Channel 1 of Transducer
ONE CABLE LABELED 'CH1'.

CH2) Video output to Computer
TWO CABLES LABELED 'OUT' & 'OUT'.

CH3) Channel 2 of Transducer
ONE CABLE LABELED 'CH2'. WITH A 50 OHM TERMINATION.

CH4) 'To' timing signal
TWO CABLES LABELED 'To' & 'To'.

Use RECALL 1 to use settings stored in the oscilloscope's memory.

BIR INC.

NAME:

MAIN CABINET

DRAWING NUMBER

2380-A020-SCF

BY: T.L.PUSATERI

DATE: 8 APR 92

CHECKED:

APPROVED:

Generic cadd file: 1G-MAINC

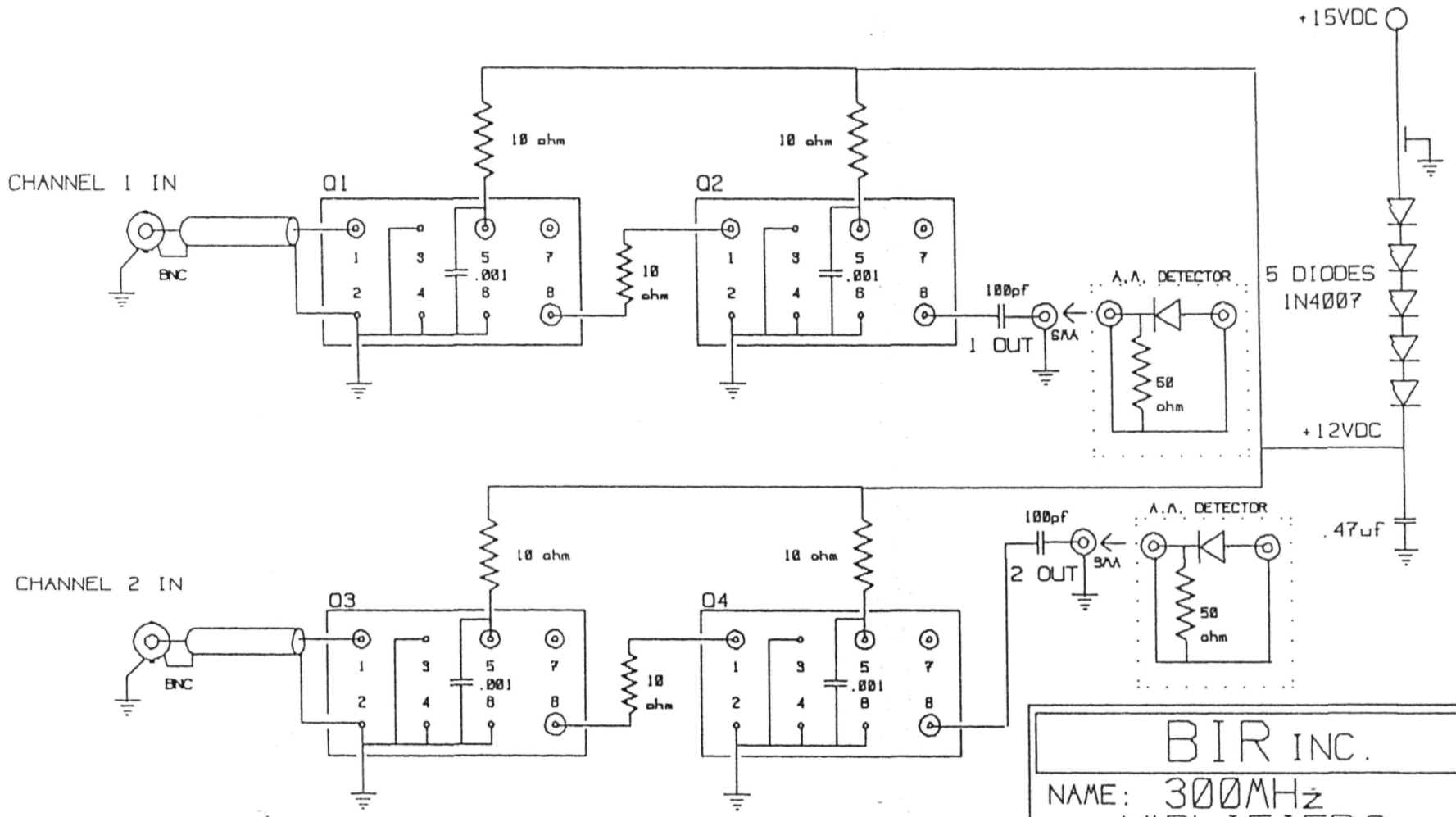

NOTES: Q1. Q2. Q3. & Q4 ARE MINI-CIRCUITS PART NO. MAN-2.
EACH AMPLIFIER HAS 18db GAIN. 1db COMPRESSION AT +9dbm.

AM DETECTORS:

D3 & D4 ARE MIDISCO COAXIAL DETECTORS MDC1087-N. SMA TYPE.

BIR INC.

NAME: 300MHz AMPLIFIERS A6 & A7

DRAWING NUMBER 2380-A021-ESD

BY: T.L.PUSATERI

APPROVED:

DATE: 14 APR 1992

Generic cadd file: IG-300MC

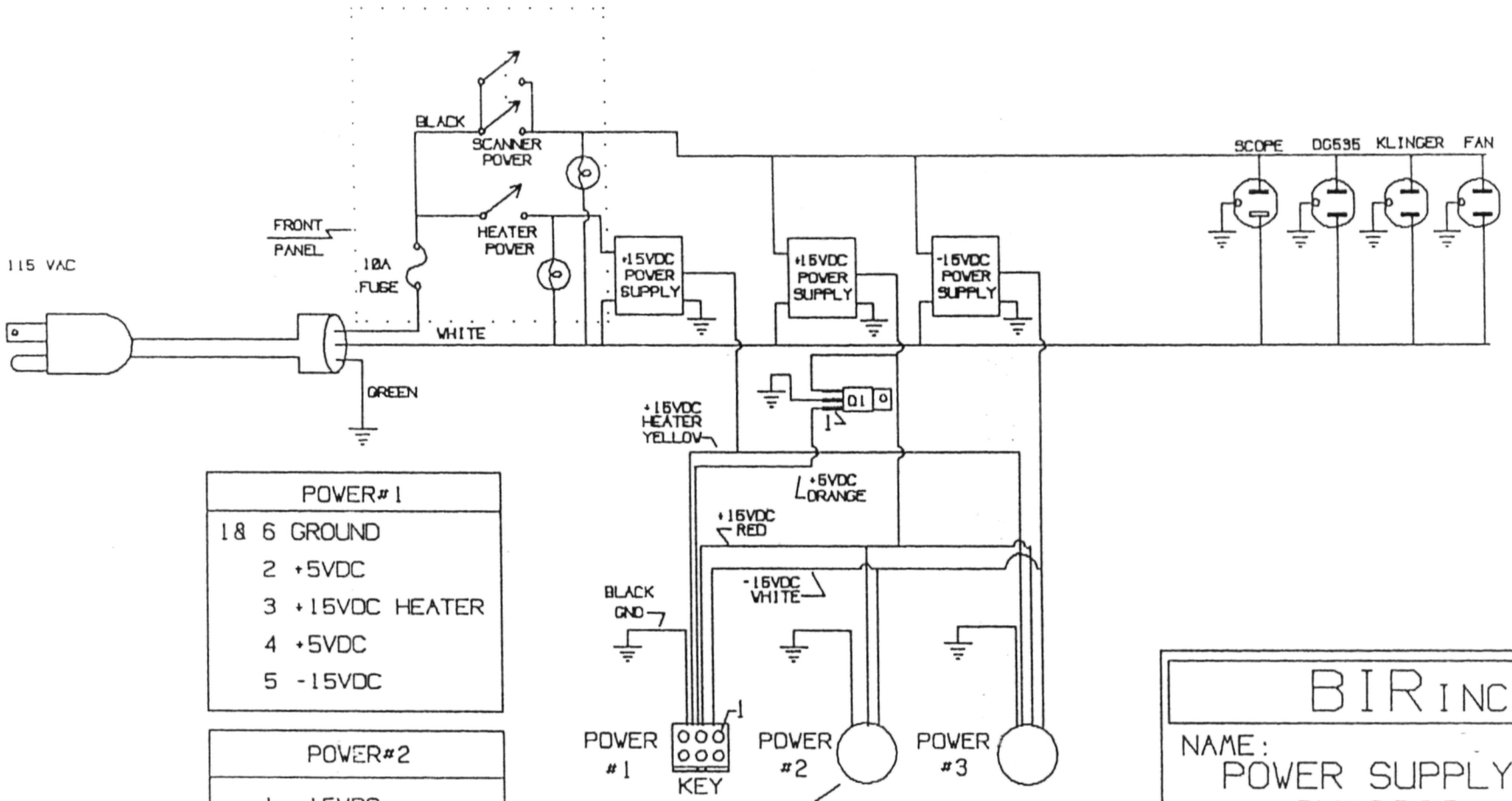

POWER#1	
1 & 6	GROUND
2	+5VDC
3	+15VDC HEATER
4	+5VDC
5	-15VDC

POWER#2	
1	+15VDC
2	GROUND
3	-15VDC
4	——
5	——

NOTE: Q1=7805

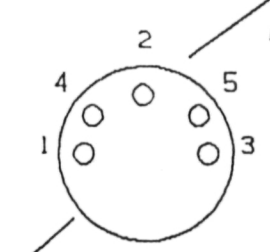

SOLDER SIDE OF MALE PLUG

POWER#3	
1	+15VDC
2	GROUND
3	-15VDC
4	+15VDC HEATER
5	——

BIR INC.

NAME: POWER SUPPLY CHASSIS

DRAWING NUMBER 2380-A022-ESD

BY: T.L.PUSATERI TLP DATE: 7 APR 1992

APPROVED: DDW

Generic cadd file: 1G-PWRSP

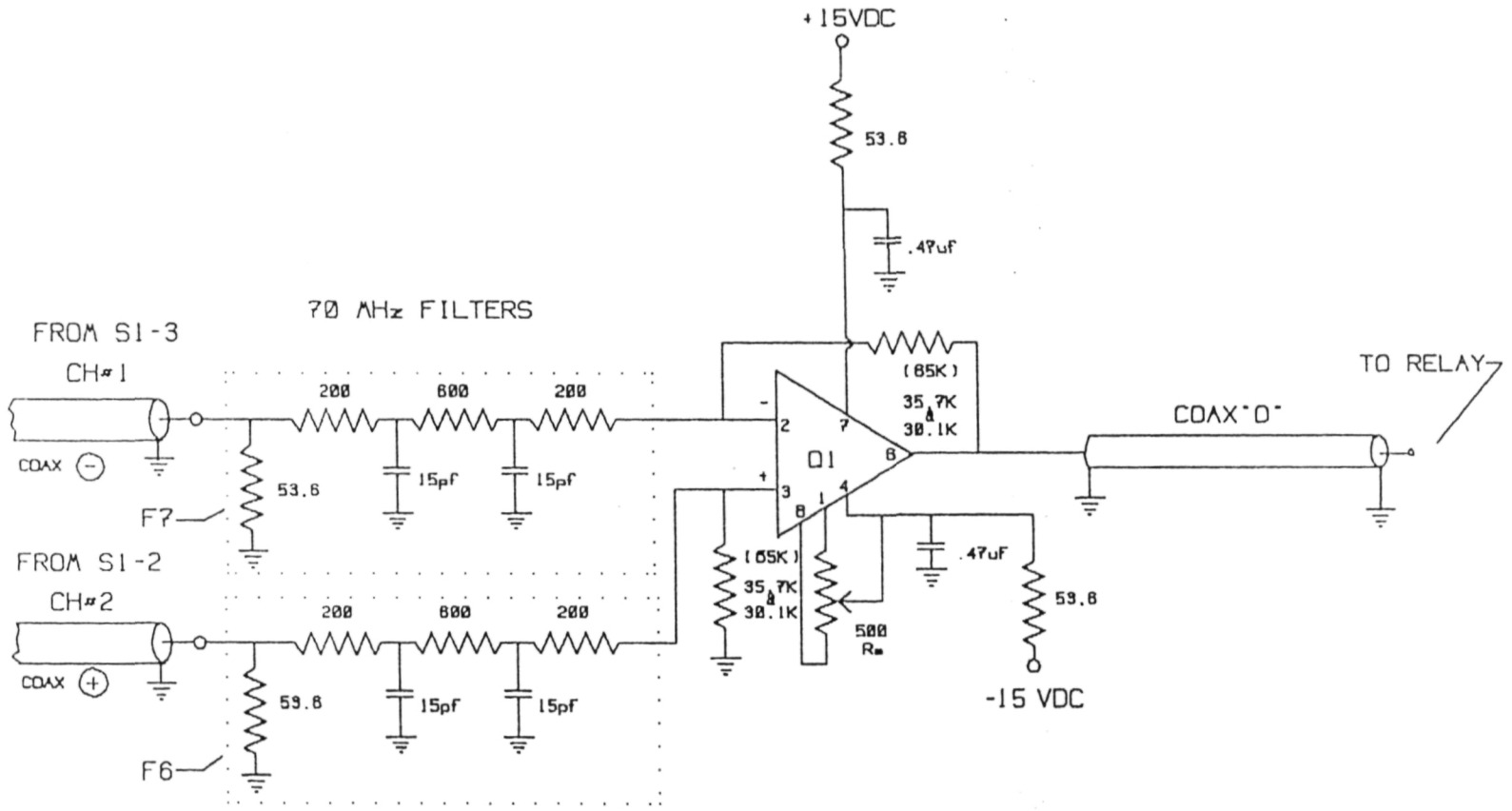

NOTES:

1. 1% RESISTERS ARE USED TO REDUCE NOISE.
2. Q1 IS ANALOG DEVICES AD849JN.
3. GAIN APROX 65.

BIR INC.	
NAME: VIDEO AMP A9 AND FILTERS F6 & F7	
DRAWING NUMBER: 3280-A023-ESD	
BY: T.L.RUSATERI	DATE:
APPROVED:	15 APR 92
Generic cadd file: IG-AMPA9	

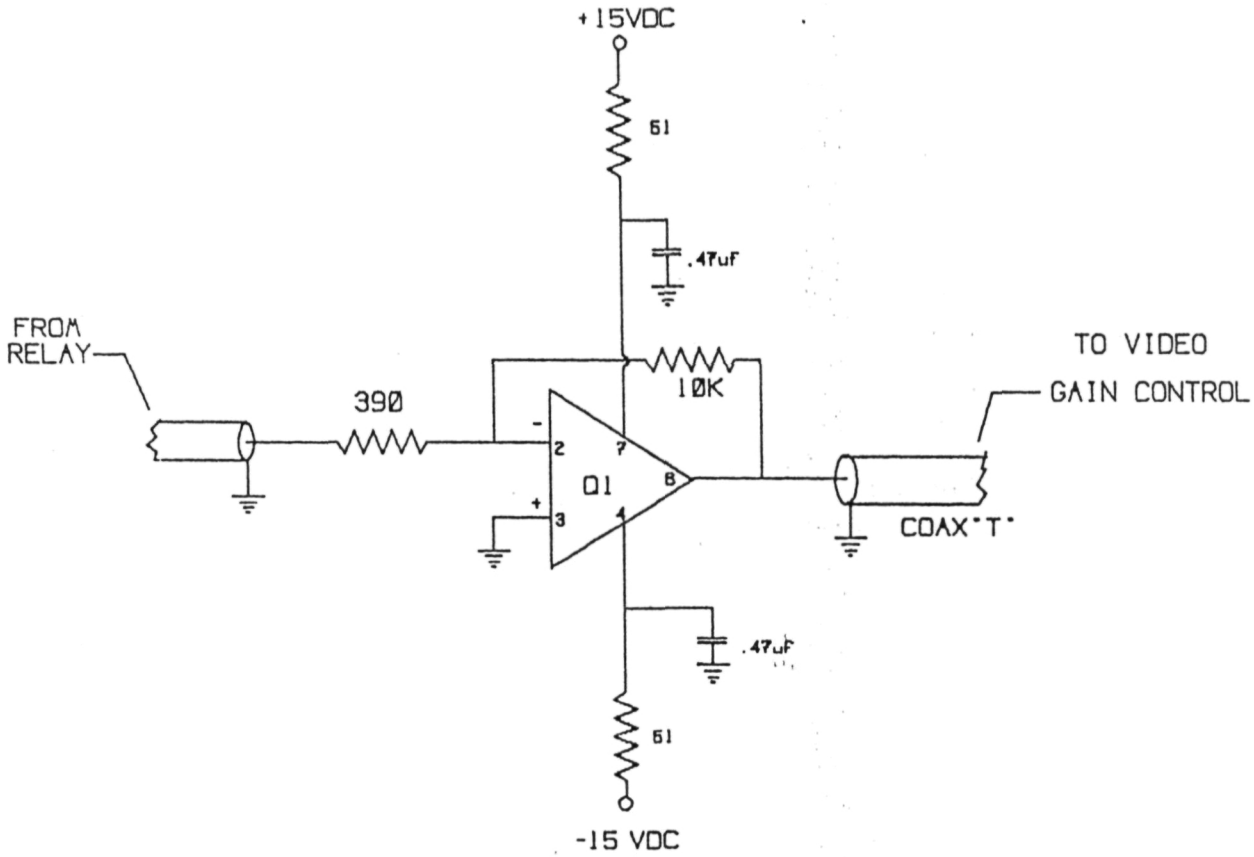

NOTES:

1. GAIN APROX 2

BIR INC.	
NAME: VIDEO AMP A10	
DRAWING NUMBER: 3280-A024-ESD	
BY: T.L. PUSATERI	DATE:
APPROVED:	15 APR 92
Generic cadd file: 1G-AMPAX	

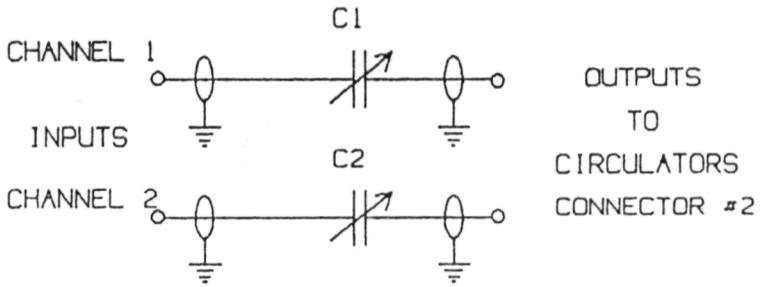

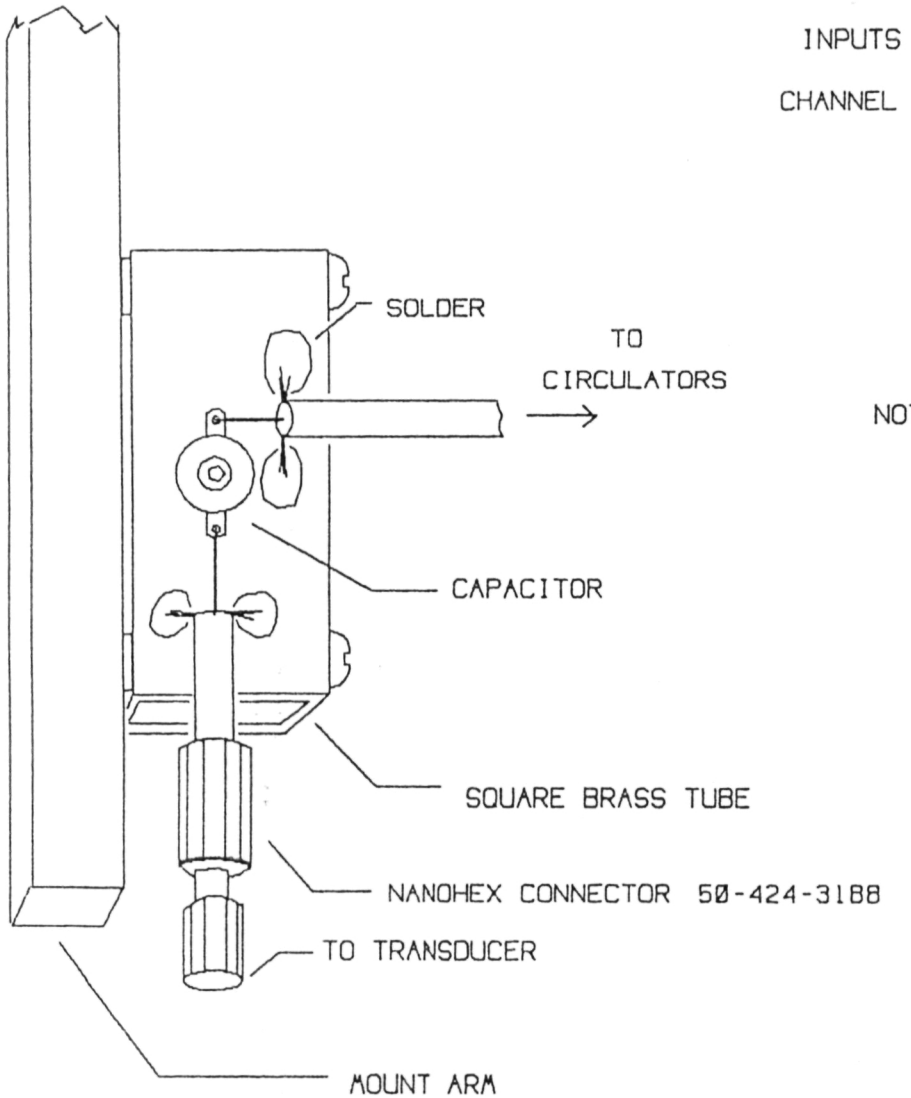

NOTE: 1. CAPACITORS C1 & C1 ARE
JOHANSON (JMC) CV98K200 5 TO 20 pF

BIR INC.	
NAME: TRANSDUCER MATCHING NETWORK	
DRAWING NUMBER: 2380-A025-ESD	
BY: T.L.PUSATERI	DATE:
APPROVED:	20 APR. 92
Generic cadd file: IG-NET	

REPORT DOCUMENTATION PAGE

1. AGENCY USE ONLY (Leave blank)	2. REPORT DATE	3. REPORT TYPE AND DATES COVERED
	May 1992	Contractor Report

4. TITLE AND SUBTITLE

Differential Phase Acoustic Microscopy for Micro-NDE

5. FUNDING NUMBERS

C NAS1-19099

WU 324-02-00

6. AUTHOR(S)

D.D. Waters, T.L. Pusateri, and S.R. Huang.

7. PERFORMING ORGANIZATION NAME(S) AND ADDRESS(ES)

BIO-IMAGING RESEARCH, INC.
425 Barclay Boulevard
Lincolnshire, IL 60069

8. PERFORMING ORGANIZATION REPORT NUMBER

BIR-2380

9. SPONSORING/MONITORING AGENCY NAME(S) AND ADDRESS(ES)

National Aeronautics and Space Administration
Langley Research Center
Hampton, VA 23665-5225

10. SPONSORING/MONITORING AGENCY REPORT NUMBER

NASA CR-189617

11. SUPPLEMENTARY NOTES

Langley Technical Monitor: Patrick H. Johnston
Final Report

12a. DISTRIBUTION/AVAILABILITY STATEMENT

FOR U.S. GOVERNMENT AGENCIES ONLY

Subject Category 71

12b. DISTRIBUTION CODE

13. ABSTRACT *(Maximum 200 words)*

A differential phase scanning acoustic microscope (DP-SAM) was developed, fabricated, and tested in this project. This includes the acoustic lens and transducers, driving and receiving electronics, scanning stage, scanning software, and display software. This DP-SAM can produce mechanically raster-scanned acoustic microscopic images of differential phase, differential amplitude, or amplitude of the time gated returned echoes of the samples. The differential phase and differential amplitude images provide better image contrast over the conventional amplitude images. A specially designed miniature dual beam lens was used to form two foci to obtain the differential phase and amplitude information of the echoes. High image resolution (1 μm) was achieved by applying high frequency (around 1 GHz) acoustic signals to the samples and placing two foci close to each other (1 μm). Tone burst was used in this system to obtain a good estimation of the phase differences between echoes from the two adjacent foci. The system can also be used to extract the V(z) acoustic signature. Since two acoustic beams and four receiving modes are available, there are 12 possible combinations to produce an image or a V(z) scan. This provides an unique feature of this system that none of the existing acoustic microscopic systems can provide for the micro NDE applications. The entire system, including the lens, electronics, and scanning control software, has made a competitive industrial product for nondestructive material inspection and evaluation and has attracted interest from existing acoustic microscope manufactures.

14. SUBJECT TERMS	15. NUMBER OF PAGES
Differential phase scanning acoustic microscopy, phase contrast ultrasonic microscopy, SAM, nondestructive evaluation, NDE, dual beam acoustic lens.	105
	16. PRICE CODE

17. SECURITY CLASSIFICATION OF REPORT	18. SECURITY CLASSIFICATION OF THIS PAGE	19. SECURITY CLASSIFICATION OF ABSTRACT	20. LIMITATION OF ABSTRACT
Unclassified	Unclassified		